Spring 2015

Evaluation of millimeter-sized preformed particle gel for conformance control treatments using simple models

Ali Abdulmohsen Al Brahim

Department:

Evaluation of Millimeter-Sized Preformed Particle Gel for Conformance Control Treatments Using Simple Models

by

ALI ABDULMOHSEN AL BRAHIM

A THESIS

Presented to the Faculty of the Graduate School of the

MISSOURI UNIVERSITY OF SCIENCE AND TECHNOLOGY

In Partial Fulfillment of the Requirements for the Degree

MASTER OF SCIENCE IN PETROLEUM ENGINEERING

2015

Approved by:

Baojun Bai, Advisor
Ralph E. Flori
Mingzhen Wei

ABSTRACT

Millimeter-sized preformed particle gels (PPGs) have been successfully used to tackle the high-permeable zones, fractures and channels in mature oilfields for conformance control improvement. PPGs can significantly reduce the permeability of abnormal fractures and divert injected water to the low permeable zones where hydrocarbon was not swept by previous water flooding. Due to the irregularity of PPGs in shapes after swollen, their strength cannot be easily measured using the conventional methods. Therefore, the open hole screen plate models with various hole diameters and density were designed to establish a simple technique that can be used to measure the strength of PPGs quantitatively in laboratory as well as on site during gel treatments. The open fracture plates with various fractures widths were also designed to understand the PPGs propagation and extrusion behavior through fracture and fracture-like channels. The results show that the PPGs threshold pressure is correlated linearly with the elastic modulus (G'). The results from the fracture model indicate that the fracture width has the prominent effect on PPGs extrusion pressure and injectivity. Also, the experimental results show that the resistance factor increases as the fracture size increase which is consistent with the previous findings in PPGs transportation through the porous media. Furthermore, the use of the screening model enables a direct observation of the extruded gel particles from the models, and based on the initial and the extruded PPGs particle size distribution, extrusion patterns of PPGs were determined.

ACKNOWLEDGMENTS

I would like to express my sincere appreciation and gratitude to my advisor, Dr. Baojun Bai, for his valuable advice, encouragement, assistance and patience throughout the duration of my study.

I would like to thank my advisory committee, Dr. Ralph E. Flori and Dr. Mingzhen Wei for their support, comments and their useful suggestions on the thesis.

Appreciation is also extended to my family for their support, love and encouragements during my study.

Special thanks go to the Saudi Ministry of Higher Education for the scholarship and their valuable advice.

Funding for this research was provided by the Research Partnership to Secure Energy for America (RPSEA) through the small producer program authorized by the U.S. Energy Policy Act of 2005. Blue Top Energy LLC and Colt Energy, Inc. are acknowledged for their collaboration in this research.

TABLE OF CONTENTS

Page

LIST OF ILLUSTRATIONS

Page

LIST OF TABLES

Page

1. INTRODUCTION

After reservoirs get withdrawn from their primary resources of natural energy drive such as, water influx, solution-gas drive and gravity drainage, the need for an external means of force usually expressed as in term of pressure becomes inevitable. Water flooding as a Secondary oil recovery has been often used to maintain reservoir pressure and displace oil. A reservoir will be producing hydrocarbon under the water flooding process until it is no longer economical. In other words, the water-oil ratio becomes unfavorable. Commonly, only 10 percent of a reservoir's original oil in place can be produced during the primary recovery. Whereas, the secondary recovery resulting in the recovery of 20 to 40 percent of the original oil in place (U.S. DOE, Reference 2). In the United States, two-thirds of the oil (377 billion barrels) cannot be recovered using the conventional primary and secondary methods.

Enhanced oil recovery or tertiary recovery is often implemented in the reservoir to produce additional hydrocarbon after secondary oil recovery. EOR processes can be classified into four major categories: thermal processes, chemical processes, gas flooding and microbial processes (Roger et al., 2003). These processes are intended to improve the sweep efficiency, reduce the residual oil saturation and thus increase the incremental oil production. According to the USA Department of Energy, there is a potential of producing 688 Billion Barrels from enhanced oil recovery by 2030.

Conformance can be defined as the management and alteration of water and gas flows using the appropriate reservoir understanding to optimize hydrocarbon production (Soliman et al., 1999). In other words, it is a measure of the uniformity of the flood front

of the injected drive fluid during an oil recovery flooding operation. Conformance control can be defined as any action that is taken to enhance the injection or production profile of a well. It includes procedures that improve both recovery efficiency and wellbore/ casting integrity and stratify environmental regulations (Azari et al., 1996). Generally speaking, the conformance control can be divided into two main categories: treatments to improve volumetric sweep efficiency during oil-recovery operations and treatment to reduce excessive water.

Gel treatments are a proven cost-effective method that can assist in reducing the excessive water production and correct reservoir heterogeneity (Seright and Liang, 1995). The major objective of the gel treatments in injection wells is to reduce water flow through fractures, channels and conduit and divert the injected fluids toward the low permeable or hydrocarbon bearing zones. Whereas, in the production wells, the objective of the gel treatments is to reduce water production without impairing oil production.

Generally, there are two types of gels that have been used for conformance control: In-situ gels, where a mixture of polymer and crosslinker usually referred to as gelant is injected into a target formation to form gel under the reservoir condition that fully or partially seals the formation. The other type is using preformed particle gels (PPGs), which has become a new trend for gel treatment application for conformance improvement. PPGs can overcome some drawbacks inherent in an in-situ gelation system, such as lack of gelation time control and dilution by formation water (Bai et al. 2007a and 2007b; Chauveteau et al., 2003). PPGs come in various sizes that are ranged from micro-to millimeter-sized PPGs. Selecting the right size and the strength of PPGs are important to their performance as a plugging agent. Furthermore, it is crucial to

understand PPGs extrusion behavior through fractures, fracture-like channels and high-permeable zones to optimize PPGs treatments.

Conventional gel strength has always been measured by applying load to single, isolated sample with certain geometry. However, determining the strength of sugar-like PPGs with irregular shapes is a challenging task. Previous publications have proposed different methods to evaluate gel strength. However, those methods are not suitable for fast quantitative evaluation of PPGs.

The thesis presents a comprehensive evaluation of the millimeter-sized PPGs through the use of open hole screen plate and open fracture plate models. These models were designed to simulate the fractures and channels that exist in a reservoir. Compared to the core flooding and sandpack experiments, the evaluation of PPGs using these models are inexpensive and time -efficient.

The objective of using the open hole screen plate model is to develop a simple technique that can assist in evaluating the strength of the millimeter-sized PPGs both in the laboratory and on site during the PPGs treatment. This technique can be used to adjust the strength of PPGs based on the real-time PPG injection pressure response.

The objective of using the open fracture plate model is to examine the PPGs extrusion behavior through fractures and to determine the most influential factors on the PPGs injection pressure, injectivity and resistance factor.

The thesis also presents a study of the particle size distribution of the PPGs before and after extrusion through the proposed models. The purpose of this study is to identify the extrusion pattern of PPGs which can be useful in improving and optimizing the PPGs treatment. Some

The thesis also presents some work that was conducted using the simple experimental apparatus to run a filtration test. Viscous gels with different concentrations were used in this study to examine their plugging efficiency. Porous ceramic disks were deployed in this study to simulate the porous media.

2. LITERATURE REVIEW

2.1 PROBLEMS OF EXCESSIVE WATER PRODUCTION IN OIL FIELDS

Because of the long term water flooding, the excessive water production has become a major problem for oil fields operators as more and more reservoirs mature (Bai et al., 2008). Oil companies produce an average of three barrels of water for each barrel of oil. In addition, around 40 billion dollars are spent yearly in resolving the problems that are related with unwanted water (Bailey et al., 2000).

The excessive water production leads to a serious environmental hazard due to water disposal. Additionally, the production of large amounts of water increases the demand for more complex water-oil separation techniques, a fast corrosion of well equipment, a rapid decline of hydrocarbon production and eventually, a premature abandonment of the well. The technical problems arising from high water production maybe exaggerated by the production of sand together with the water.

In the United States, more than seven barrels of water on average are produced for each barrel of oil (Seright, 2001). One out of every six barrels of crude oil produced comes from stripper wells. These wells produce oil and gas at rates lower than 10 barrels of oil per day or 60,000 cubic feet of natural gas per day, numbers that represent typical operations for many small producers in the United States. According to the U.S. Department of Energy, about 80 percent of oil wells are now categorized as marginal wells. Tapping into additional oil and gas supplies from the nation's stripper wells could lead to a significant contribution to US energy security (U.S. DOE, Reference 1). According to Weidman (1996), for crude oil wells approaching the end of their production lives, the produced water can be as much as 98% of the material brought to

the surface. For production wells of a mature water flood reservoir, the amount of water produced can be between 10 to 20 barrel for each barrel of crude oil produced (Veil, 2004). According to the United States Department of Energy, if just 1% of the total 377 billion barrels of oil bypassed by water flooding in the United States could be recovered using enhanced oil recovery technologies, then domestic reserves could be increased by as much as 3.7 billion barrels.

2.2 GEL TREATMENT FOR CONFORMANCE CONTROL

Gel treatment has been proved to be cost-effective chemical conformance controls that help to block or reduce water or gas production that is resulted from high-permeability zones, channels, fractures and fractures- like channels. The gel treatment as a conformance control can be deployed for both injection and production wells. Gel treatment for conformance control can be classified into three categories, including water-shut-off, profile control and in-depth fluid diversion.

2.2.1 Water Shut-off. Water shut-off technology includes two types, selective and unselective. This technology is mainly implemented in the early stages of a reservoir. In selective water-shut-off treatment, plugging agents are injected through production wells to reduce permeability to water much more than to oil, it sometimes referred to as disproportionate permeability reduction (DPR) (Liang and Seright, 2000). These plugging agents are injected to control water from multiple layers in which they set and harden when they get in contact with water leading to sealing the water zone.

In unselective water shut-off treatment, one entire isolated zone that is producing large amounts of water is plugged or abandoned through the injection of the plugging agents. As a result, oil can be produced from other zones. The main objective of this

treatment is to correct reservoir heterogeneity among isolated layers. Moreover, this treatment targets the zones that have high water cut separated from other oil production zones.

2.2.2 Profile Control. Injecting a plugging agent through an injector well to partially or fully block high-permeability zones and allow the injected fluids to be diverted to the low-permeability zones. Thus, improving the injection profile of an injection well, improves the sweep efficiency and reduces excessive water production of the reservoir. This technology is implemented in the middle water cut stage of a reservoir. Acrylamide based strong gels, silicate gels and polymer gels are the typical plugging agents that are used as plugging agents for profile control.

2.2.3 In-Depth Fluid Diversion. Large volume of plugging agents are injected that can be transported deeply into the reservoir. This treatment is mostly deployed in mature oilfields that have little oil remaining near the wellbore. Some chemicals that can be used in this treatment include nanogels, colloidal dispersion gels (CDG) and weak gel.

2.3 TYPES OF GELS

Traditionally, in-situ gels have been widely used for conformance control. The mixture of polymer and crosslinker called gelant is injected into target formation, while the reaction occurs in the reservoir to form gel that can fully or partially seal the formation at reservoir temperature (Sydansk and Moore, 1992). A newer trend in gel treatment is applying preformed particle gels (PPGs) that can be formed at surface facilities prior to their injection into the reservoirs.

PPGs can overcome some drawbacks inherent in in-situ gelation systems, such as lack of gelation time control, uncertainty of gelling due to shear degradation, change of

gelant compositions and dilution by formation water. There are different commercially available PPGs, such as performed bulk gels (Seright, 2004), partially performed gels (Sydansk et al., 2004), pH-sensitive cross linked polymer (Al-Anazi et al., 2002; Huh et al., 2005), microgels (Chauveteau et al., 2000, 2001; Rousseau et al., 2005; Zaitoun et al., 2007), swelling micron-sized polymers such as Bright Water® (Pritchett et al., 2003; Frampton et al., 2004) and micrometer –to- millimeter-sized PPGs (Coste et al., 2000; Bai et al., 2007a, 2007b). The main differences among these types of particle gels lie in their particle size. Swelling ratio and swelling time.

Published documents show that microgels and submicron-sized polymers PPGs have been applied economically to reduce water production and improve oil recovery in mature oil fields. Microgels have been applied to approximately 10 gas storage wells to reduce water production (Zaitoun et al., 2007). Submicron-sized particles have been applied to more than 60 wells (Cheung et al., 2007; Mustoni et al., 2010). Additionally, swelling gels were successfully implemented to control CO_2 breakthrough in CO_2 enhanced oil recovery project (Wu and Bai, 2008).

Millimeter-Sized PPGs have been applied to over 5000 wells in water floods and polymer floods in china (Bai et al., 2013). Millimeter-sized PPGs are used mainly for reservoirs with fractures or fracture-like channels that have a permeability of more than a few Darcies. Therefore, millimeter-sized PPGs cannot penetrate into conventional porous media without fractures and voids, but they can plug fractures or high-permeability streaks/ channels in mature oilfields which cannot be accomplished by in-situ gels, microgels and sub-micro gels (Bai et al., 2013).

2.4 ADVANTAGES OF MILLIMETER-SIZED PPGS

PPGs have been proven to be a cost-effective method for oilfield conformance control improvements due to their unique advantages over the traditional in-situ gels. These advantages can be summarized in the following point:

- PPGs are both strength and size controlled, environmentally friendly, and their stability is not sensitive to reservoir minerals and the salinity of the formation water.
- PPGs can resist temperature up to 120^{o}C (250^{o}F) (Bai et al., 2013).
- PPGs can preferentially enter into fractures or fracture-feature channels while minimizing gel penetration into low permeability hydrocarbons zones/ matrixes.
- PPGs can significantly reduce the operation and labor costs at the surface facilities since they only have one component during injection.
- PPGs can be prepared with produced water without influencing their stability. Whereas, traditional in situ gels are often very sensitive to salinity, multivalent cations and H_2S in produced water (Chauveteau et al. 2003; Bai et al. 2007a & 2007b).
- Real-time monitoring data can be used to adjust the design of PPGs for better results.

2.5 METHODS FOR GEL STRENGTH EVAULATION

There have been several attempts to develop a technique for quantitatively determine the strength of in-situ gelation systems and preformed bulk gels (Riccardo, 1994; Perera et al., 1996; Sayil et al., 2001; Francesca et al., 2003). However, few studies

have focused on the determination of the strength of the performed particle gels especially for their application as conformance control plugging agents.

Gardner (1983) designed a closed-loop, high temperature pipe viscometer to evaluate the effects of shear intensity, shear duration, temperature and time on the apparent viscosity of the cross-linked fracturing fluids. The model was intended to evaluate the rheological properties of the gels that were used as fracturing fluids in the hydraulic fracture practice. Gardner used rheometer to study the rheology of relatively weak gels and polymers to examine their interaction in the in-situ gel generation in the fracture. He found out that the model was a useful tool to generate gels and rheologically characterize them under conditions that mimic the actual fracturing applications.

Meister (1985) designed a screen extrusion model to test and quantitatively compare the strength of various compositions of strong bulk gels used for conformance improvement for near-wellbore treatments. He operated the model using compressed air that supplied different constant pressures to extrude the bulk gels through 30 mesh stainless steel screen that had 1-7/8 inch diameter and 0.012 inch wire diameter. He examined the increase in gel strength with respect to gelation time, salinity, polymer concentration, intrinsic viscosity and the anionic character of the matured gel. He found out that the bulk gel strength increased as both the gelation time and the brine concentration increased.

Smith (1989) designed an apparatus for a fast quantification of large numbers of gel systems strength called the Transition Gel Unit (TGU) apparatus. The method was used to determine the right crosslinking system for the polyacrylamide crosslinked gels. The apparatus had a sample tube that was connected to the pressure source load and

screen pack that consisted of five 100-mesh screens. To affirm the consistency of the packs permeability, he assembled the pack at a 45 degree angle to the screen underneath it. He found out that the gel had two ways of responding depending on the range of the applied pressure. In the low range pressure, the gel inclined to squeeze through the screens rather than flow continuously due to the fact that the gel molecules were expanding and therefore plugging the pores. However, in the high range pressure, he found out that the gel molecules were stretching out and continuous flow was obtained. He concluded that all gels had a distinct pressure at which they undergo the transition from squeeze to flow range. As a result, he used this pressure as the transition pressure for the purpose of comparing the strength of different gel systems. His results revealed a proportional relation between the transition pressure and the gel strength, the higher the transition pressure the higher the gel strength.

Smith (1995) utilized the same transition pressure model to evaluate the strength of colloidal dispersion gels that are made up of low concentrations of polymer and aluminum citrate in water. Performance of the colloidal dispersion gel depends primarily on the type and the quality of the polymer used. He examined the performance of 18 different polymers in the colloidal dispersion gels. The main purpose of his study was to learn what types of polymers perform best in these gels, and what properties determine whether or not a polymer will form unstable colloidal dispersion gels. The second objective of his study was to investigate the effects of low concentrations of salt and polymer to aluminum ratio on gel formation. Six types of polymers that are commonly used in the oilfield have been used that are ranged in their average molecular weight and their degree of hydrolysis. His results revealed that the gel strength was proportional to

the transition pressure values. However, he categorized the strength of the formed gel based in a small variation in pressure range. That can be related to the use of the mesh size. Based on the PPGs screening model results, different mesh sizes are necessary to correlate and compare the strength of different gel systems.

Sydansk (1988) developed semi-quantitative criteria to measure the gelation rate and the gel strength referred to as the bottle testing method. He used this method to screen gel formulations over a wide range chemical compositions, brine compositions and temperatures. In the bottle test method, he assigned a letter code of A through J as defined by the gel strength code in Table 2-1. The codes for the gel strength range from highly flowing gels with barely any gel structure visibly detectable to rigid rubbery gels. To conduct the gel strength measurement applying this method, the pre-gel solutions were firstly formulated and placed in the bottle. Then, gel strength was monitored as a function of time. Then, bottles were inverted during each reading to determine the gel's flow characteristics under the influence of gravity. As a result, a gel-strength code was assigned as indicated in Table 2-1.

Table 2-1. Sydansk gel-strength codes.

Gel Strength Code	Fluid Description	Criteria of the fluid
A	No detectable gel formed	The gel appears to have same fluidity as the original polymer.
B	Highly flowing gel	The gel appears to be only slightly more viscous than the initial polymer solution.
C	Flowing gel	Most of the obviously detectable gel flows upon inversion.
D	Moderately flowing gel	A small portion (5 to 15%) of the gel does not flow readily upon inversion.
E	Barely flowing gel	The gel slowly flows to the bottle cap and/or a significant portion (>15 %) of the gel does not flow upon inversion.
F	Highly deformable nonflowing gel	The gel does not flow to the bottle cap upon inversion.
G	Moderately deformable nonflowing gel	The gel flows about halfway down the bottle upon inversion.
H	Slightly deformable nonflowing gel	Only the gel surface deforms slightly upon inversion.
I	Rigid gel	There is no gel surface deformation upon inversion.
J	Ringing rigid gel	A tuning-fork-like mechanical vibration can be felt after the bottle is tapped.

Kakadjian (1999) used the dynamic rheology as a developing method for rheological characterization to evaluate the gel strength of the polymeric systems quantitatively in order to replace the qualitative letter code that is generally used to classify the gel strength. The method enables the study of the general consistency of gelling systems (G*) which represents the total resistance of a substance against the maximum applied strain, the elastic behavior of the consistency (G'), the viscous component of the consistency (G") and the relationship between the two modulus (Tan δ). He conducted the rheological measurements using the dynamic rheology that was fixed with plate-plate sensor in which the gelling systems were characterized by imposing a

defined oscillatory strain at a fixed strain rate. He applied some modifications to permit gelling the system under study by changing the sweep of deformation and the sweep of frequency and by evaluating the gelling system under various temperatures. His research results revealed that the behavior of elastic and the loss component was not only dependent of the gelling time and the final consistency, but also depends on the frequency under study. This behavior could influence the changes in the residual resistance factor at different flow rates. Additionally, his results showed that the addition of the sodium acetate to the commercial polyacrylamide/Cr (III) systems making them weaker and more viscous. This work established a dynamic rheological characterization as an effective tool to determine quantitatively the consistency of gelling systems.

Awang et al., (2003) studied the correlation between the gel strength codes obtained from the bottle testing method that was developed by Sydansk (1988) and the reduction in the permeability of the porous media after the injection of the pre-gel polymer using the sand pack. In his study, the displacement of gel solution in sandpack and the bottle testing observations were run at the same time. Firstly, he placed the gel solution in bottle to achieve a certain gel code from the bottle testing method. Then, he injected two pore volumes of the gel into the sandpack to displace the gel and the breakthrough pressure was measured. Later, he injected brine water into the sandpack to determine the final permeability. His results indicated that when the gel strength code H was observed i.e. the gel surface deformed slightly upon inversion, the permeability reduction in the sandpack was 100%. Therefore the alphabetic code can be used to estimate total blocking. Moreover, his results showed that when the same polymer and crosslinker were used, clear trends were observed between the alphabetic code and the

sand pack permeability. However, his laboratory results showed that a linear correlation of permeability reduction was unable to be established with gel strength code

Sydansk (1990) studied the use of the Chromium (III) gel technology in the conformance control treatments. In fact, this type of gel is designed to treat fracture conformance problems in naturally fractured reservoirs. The laboratory studies revealed the dependence of the gelation rate and the gel strength on (1), the concentration, molecular weight, and the hydrolysis level of the polymer; (2) the polymer to Cr (III) ratio; (3) temperature; (4) polymer solution pH and finally the salinity. The gels of this technology contains a single-fluid system and do not involve sequentially injected fluids. Gels are produced by basically adding a single aqueous crosslinking-agent solution to the aqueous polymer solution. An entire family of gels ranging from the highly flowing to rigid, rubbery gels can be produced by varying the formulation of the same chemical set. As a result, this gel technology is applicable to a wide range of oilfield problems and uses. The gels formulated with polyacrylamide (PA) and partially hydrolyzed polyacrylamide (PHPA) with crosslinking agent chromic acetate is used in the paper.

Zeron et al., (2008) evaluated the use of the low-field nuclear magnetic resonance (NMR) as a nonintrusive technique to monitor gelation rates and to characterize gel strength of polyacrylamide/ chromium acetate gel. The low-field (NMR) detects the response of the hydrogen protons in magnetic fields which can be utilized to measure the fluid bulk relaxation rate which is directly proportional to the viscosity of the material. He examined the effect of the polymer concentration, Cr (III) acetate concentration and salinity of the polymer gel forming solution on the crosslinking reaction and compared his findings with the bottle test and the rheological measurements using the rheometer.

His results showed that (NMR) was capable of observing the alterations of gel properties as a result of changes in polymer and crosslinker concentration and the salinity of the polymer solutions. Furthermore, he concluded that (NMR) was a reliable tool in detecting the liquid/ solid transition and the estimation of the gel point which could be used in the porous media to monitor the gelation process after placing the gel in the target zone since the Low-field (NMR) does not disrupt or influence the gelation process in any way.

Ramazani et al., (2005) realized the demand for a practical method to measure the swollen gel strength of superabsorbent polymer (SAPs) hydrogels. Because the hydrogels are mostly sugar-like particles with irregular shapes, using the conventional testing of the swollen state of the gels is impossible. He measured the swollen gel strength of a typical SAP sample by determining the absorbency under load (AUL) and then the mechanical strength of the swollen sample was measured using the oscillatory rheometer. To calculate the (AUL), he used a macro-porous sintered glass filter plate that was placed in a Petri dish. Then , he placed the dried SAP on the surface of a polyester gauze located on the sintered glass where the cylindrical solid weight Teflon was used to apply the desired load pressure 0.3, 0.6 or 0.9 psi to the dry SAP particles. After that, 0.9% saline solution was added to the sample, and after 60 minutes, the swollen particles were weighted again and (AUL) was calculated. Then, he used the same samples to conduct the rheological measurement. Based on his experimental results, he concluded that (AUL) decreased with the increase in the loading pressure. This method gives more sense of practicality for measuring the strength of the hydrogels; however, the maximum applied pressure in his work was 0.9 psi which is not sufficient for the PPGs treatments in the oil industry.

Additionally, the elastic modulus of the different samples did not demonstrate any significant difference.

Most of gel strength methods that have been proposed in the literature focus primarily on the properties of in-situ gels. These methods are not reliable to be used for determination of the gel strength for preformed particle gel. Therefore, there is a need for a simple and practical method that can assist in evaluating preformed particle gel strength quantitatively in the laboratory and on site during a PPG treatment process.

2.6 GEL TRANSPORTATION THROUGH FRACTURES

The main objective of gel treatments is to reduce water flow through high-permeability channels or fractures without damaging the hydrocarbon bearing zones. The gel treatments are most likely to be successful when are being implemented to treat fractures or fractures-like features that cause channeling in reservoirs (Liang and Seright, 1993; Seright, 1988). The ability of gels to be extruded through fractures or fracture-like features is a key factor for successful treatments (Seright, 1999). Therefore, understanding the behavior of the gels when they extrude through fractures and high-permeability is a fundamental aspect for a successful conformance control treatment. Seright (1997) investigated comprehensively the extrusion behavior of in-situ and preformed bulk gels through fractures and tubes. He examined the effect of fracture conductivity and tube diameter on the gel extrusion behavior. Seright (1999) investigated the dehydration of polymer gels during extrusion through fractures. Liu and Seright (2000) identified a correlation between the extrusion properties of gels in fractures and gel rheology. Seright (2001) also studied the effect of the superficial velocity on both gel resistance factor and pressure gradients and his conclusion was that, at high superficial

velocities, the gel extrusion pressure gradients were insensitive to injection flow rate. Ganguly et al., (2000) studied the effects of fluid leakoff on gel strength when placed in fractures. Sydansk et al., (2005) characterized water-shutoff polymers gels in the partially formed state that were injected into fractures which are connected to production wells. Wang and Seright (2006) investigated whether using rheology measurements to evaluate gel properties could be a good substitute for the extrusion experiments. Bai et al., (2007a, 2007b) studied the transportation of swollen particle gel through porous media using both micromodels and sandpack. McCool et al., (2009) studied the flow of Polyacrylamide/Chromium acetate system in a long conduit. Zhang and Bai (2011) investigated the effect of PPGs extrusion through fractures on the injectivity and plugging efficiency. Imqam et al., (2014) studied PPGs extrusion behavior through open conduits.

In this study, the PPGs transportation and extrusion behavior have been examined through the use of simple models, where plates of various open hole sizes and fracture widths are implemented to simulate the fractures and fractures- like channels. This method is inexpensive, time efficient and allows a direct observation of the extruded gel particles. The later can assist in understanding the extrusion patterns of PPGs through fractures.

3. OPEN HOLE SCREEN PLATE MODEL

3.1 SUMMARY

This research includes a series of experiments that were conducted using a simple hole screen plate model in order to evaluate the strength of PPGs. In this study, the threshold pressure of PPGs was considered as a method to provide a quantitative indication of the PPGs gel strength. The effect of hole size, brine concentration and holes density on the threshold pressure have been examined. The results show that using the simple hole screen plate model can be an effective tool to measure the PPGs strength and rheological properties in the laboratory as well as on site during gel treatment. Additionally, a correlation between the PPGs elastic modulus and the threshold pressure has been established in which can assist in estimating the PPGs strength for a better conformance control treatment.

3.2 INTRODUCTION

PPGs strength is an essential parameter for designing gel treatment for conformance improvement operations. Conventionally, there are several different measurements of gel strength (Sydansk, 1990). One such measurement is elastic strength which relates to the resistance to physical deformation that a gel will exhibit while extruding through a restriction in a fracture in its flow path.

Another measurement is the yield strength; when this strength is exceeded, portions of the chemical structure of the gel will break. This gel strength is measured by placing a gel sample in a large container having a small orifice and then increasing the pressure in the container until the gel flows through the orifice. The yield strength of a

gel is often mush larger that its elastic strength (Sydansk, 1990). The method that used in this study is similar in principal to the measurement of the yield strength.

Researchers have developed several methods to measure bulk gel strength. Gardner (1983) used rheometer to study the rheology of relatively weak gels. Meister (1985) designed a simple gel strength tester to quantitatively compare strong bulk gels. Sydansk (1990) proposed bottle-test gel strength codes that can quantitatively evaluate gel strength using letter codes from A for high flowing gel to J for rigid rubbery gels.

Another proposed method for quantifying the gel strength of PPGs include using a dynamic oscillatory rheometer in order to measure the elastic or storage modulus (G') and the viscous or loss modulus (G''), which represent the PPG's elastic energy and viscous energy, respectively. The measurement is conducted using parallel plate geometry with a plate and sensor. The gap between the plate and sensor is selected according to the particle size. However, the gap height selection significantly impacts the measured gel strength value. In fields and laboratories, the strength of swollen PPGs has been roughly evaluated through observation and touch by pressurizing the particles between fingers

Most of these methods focus primarily on the evaluation of the conventional bulk gel strength. They are costly, requiring a great deal of time and efforts to operate and inaccurate to some extent to be used with PPGs. For conformance control in oilfields, there is a demand for a fast and effective method that can be used to quantitatively evaluate the strength of PPGs. In many cases, the design of the PPGs treatment can change on the fly based on the injection pressure response. This requires a fast method by which to evaluate the PPGs strength so that it can be increased or decreased.

In this study, a simple model for experimental evaluation of PPGs strength is presented. The main advantage of using this technique is that it provides a simple, fast, and practical technique to quantitatively evaluate PPGs strength in laboratory as well as on site during PPGs treatment process. The first part of this chapter presents some definitions of terms and the experimental apparatus set up. The second part summarizes the experimental procedures and results and presents interpretation and discussion of the experimental findings. The final part will be summery of the conclusion drawn from the experiments.

3.3 DEFINITION OF TERMS

3.3.1 Threshold Pressure (Pt). PPGs are deformable and its particles can pass smaller size pore throats but they require a force to push them through these pore throats. This force is equivalent to the threshold pressure, which is defined as the minimum pressure required to force the PPGs to move through the pore throats.

3.3.2 Apparent Viscosity (μ_{app}). The apparent viscosity is the measure of PPG resistant to flow while extruded through pore throat or channels. It is known that PPGs are pseudoplastic materials that exhibit shear thinning properties and plotting apparent viscosity as a function of shear rate will assist in validation of the proposed method. The PPGs apparent viscosity in this study was determined using the following equation

$$\mu_{app} = \frac{\Delta p_{gel}}{\Delta p_{brine}} \tag{1}$$

Where Δp_{gel} is considered to be the stabilized pressure drop across the screen plate during PPGs extrusion as a function of flow rate under different screen plates and brine salinities.

Δp_{brine} is the pressure drop across the screen plate when brine is injected which can be calculated using Darcy's law.

3.3.3 Swelling Ratio (SW). In basic terms, the swelling ratio can be defined as the ability of gel particles to absorb the aqueous solution in which they are immersed in. It can be measured by a weight method, which depends on the knowledge of the initial weight of the dry gel particles (m_o) and on the weight of the swollen particles at the point of equilibrium (m_t).

$$SW = \frac{m_t - m_o}{m_o} \tag{2}$$

3.4 EXPERIMENTAL MATERIALS AND PROCEDURES

3.4.1 PPGs. A commercial superabsorbent polymer (SAP) LiquiBlockTM 40K, supplied by the Emerging Technologies, was selected as a PPG for these experiments. The main component of the product is Potassium salt of cross-linked polyacrylamide copolymer. The dry PPGs particles are white, sugar-like, granular power. Table 3-1 lists the typical characteristics of the PPGs used in the study. In aqueous solutions, PPGs can absorb a large amount of water because of its hydrophlicity which allows a hydrogen bond with the water molecules, although the swelling solution salinity affects its ability to absorb water. Figure 3-1 shows a comparison of dry gel particles and fully swollen particles in 1.0 wt. % sodium chloride (NaCl). Standard U.S. sieves were used to select (18/20) mesh size (0.85/1000 mm) of dry PPGs, which were used in all the experiments.

Table 3-1. Characteristics of PPGs used in the experiments.

Properties	Value
Absorption of De-ionized Water (g/g)	>200
Apparent Bulk Density (g/l)	540
Moisture Content (%)	5
pH Value	5.5-6.0 (+/- 0.5; 1% gel in 0.9% NaCl)

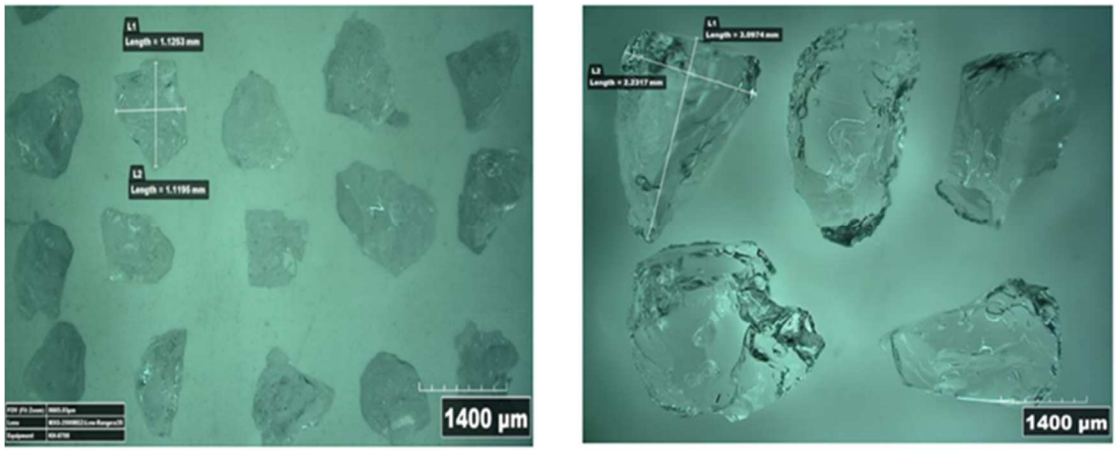

(a) (b)

Figure 3-1. Comparison of dry and swollen PPG: (a) dry granular PPGs with 18/20 mesh size, (b) fully swollen PPGs in 1.0 wt. % NaCl.

3.4.2 Swelling Ratio Evaluation. The swelling capacity of the PPGs is a function of brine concentration. The dry gel particles were placed in six different brine concentrations (0, 0.025, 0.25, 0.50, 1.0 and 5.0) wt. % NaCl for 24 hours to evaluate the swelling capacity of the PPGs. Then the excess water was separated from the swollen PPGs using the wire gauze and after that the weight method as stated above was used to calculate the SW. Figure 3-2 shows the swelling ratio of the PPGs in (g/g) as a function of brine salinity. It is evident that increasing the salinity nature of the aqueous solution

will lead to a decrease in the swelling ratio due to the osmotic pressure difference between the gel particle network and the solvent phase. This pressure difference creates a driving force to allow the diffusion of the solvent to the gel phase. Moreover, the osmotic pressure difference is decreased in the presence of the salt solutions, which leads to less swelling in contrast with distilled water.

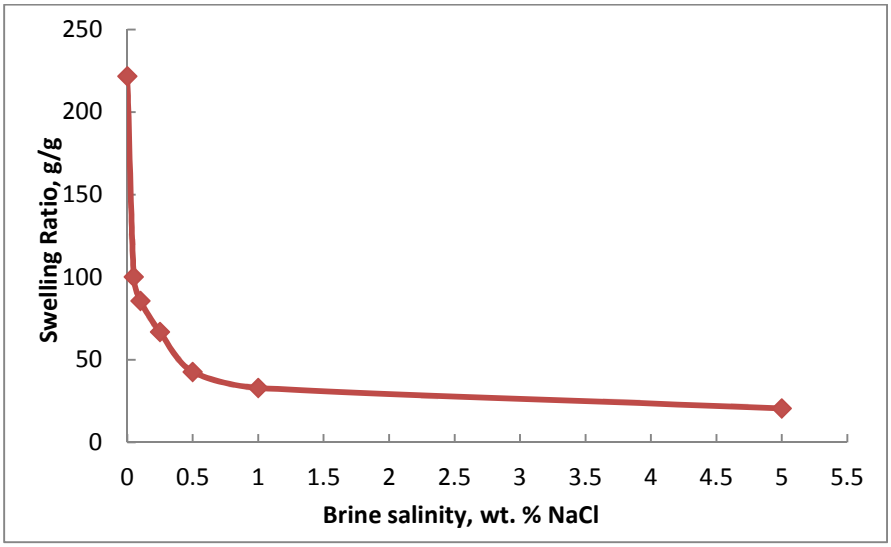

Figure 3-2. Effect of brine salinity on swelling ratio.

3.4.3 G' Measurements. The rheological properties of PPGs are usually evaluated by dynamic oscillatory measurements using parallel plate geometry with a plate and a senor. A defined geometry sample is normally placed between the plate and the sensor of the rheometer. However, commercial PPGs are irregular granule particles, which makes it hard to measure the G' because swollen particle tend to slide out of the gap when the sensor start pressing on them. In this experiment, three gap heights of 0.5, 1.0, and 1.5 mm were used between the sensor and the plate were the PPGs samples were placed. The oscillation time sweep curve model was selected for these measurements; it

represents the elastic modulus logarithmically in Pascal (Pa) as a function of time in seconds. The frequency was set at 1.00 Hz. For each sample, G' reading was taken every 30 seconds for 200 seconds. All experiments were conducted at ambient of 25 °C. Figure 3-3 displays the elastic modulus as a function of the gap height between the rheometer's plate and sensor. PPGs swollen in high salinity brine had smaller particles size that have stronger polymer network bond which cause the elastic modulus to be high.

While useful, this method requires attention to the preparation of the samples for measurement. The excess water solution must be blotted from these samples with care because if too little water is removed, the particles will move in the excess solution and the measured G' will be too small as a result of interparticle slippage. If too much water is removed, the PPG will not swell fully. Improper sample preparation leads to measurement discrepancies between analyses even with the same PPG sample.

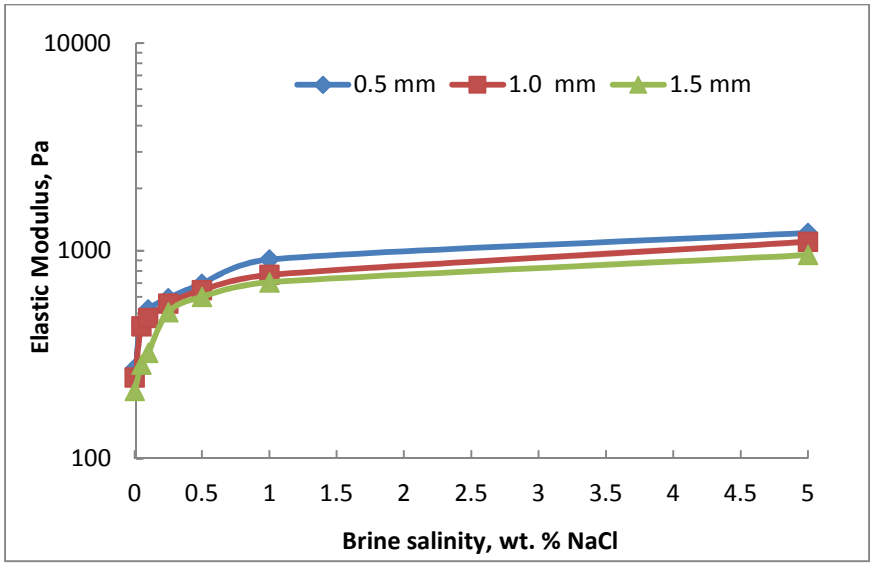

Figure 3-3. Effect of gap height on the elastic modulus of swollen PPGs.

3.4.4 Brine Solution. In order to have different PPG strengths available for evaluating the proposed model, six different brine (NaCl) weight concentrations (0.05, 0.1, 0.25, 0.5, 1.0, and 5.0 wt. %) and DI water were used, which yielded PPGs with various swelling ratios and strength , respectively.

3.4.5 Particle Size Distribution (PSD). Hirox Digital Microscope was used to determine the particle size distribution of PPGs that were initially swollen in different brine concentrations of (0.25, 0.50, 1.0 and 5.0 wt. % NaCl) and DI water. For each brine concentration PPG, 100 particles were selected randomly to be measured under the microscope. To reduce the potential for significant sampling errors, a randomization of the particles were conducted by mixing the particles that exist in a tube and then a small portion of particles from each side of the tube was selected and placed into a new tube for PSD measurements.

Because of the fact that the gel particles are irregular in shape, the equivalent diameter of each gel particles was measured under the microscope by considering the projected area of irregular particle in two dimensions. This is equivalent to the projected area of a circular particle with an equivalent diameter (Bai et al., 2007a). After conducting the measurements using the microscope, a test for normality using both numerical and graphical method was conducted using SAS software. This test was performed to ensure that the PSD of initial swollen PPGs at the chosen brine are representative and reliable. As a result, it can be utilized later to compare the initial and extruded gel particles through the different screen plates. The later can assist in developing an understanding of the extrusion pattern of PPGs.

Figure 3-4 shows the PSD of the PPGs that were fully swollen in different brine concentrations. It is clearly that PPG swollen in DI water had the highest average equivalent diameter of 5.858 mm, while the PPG swollen in brine with a salinity of 5.0 wt. % NaCl had the lowest average equivalent diameter of 3.125 mm. This observation is consistent with the swelling ratio measurement presented in Figure 3-2. Thus, the swelling ratio and particle size were affected greatly by the brine salinity

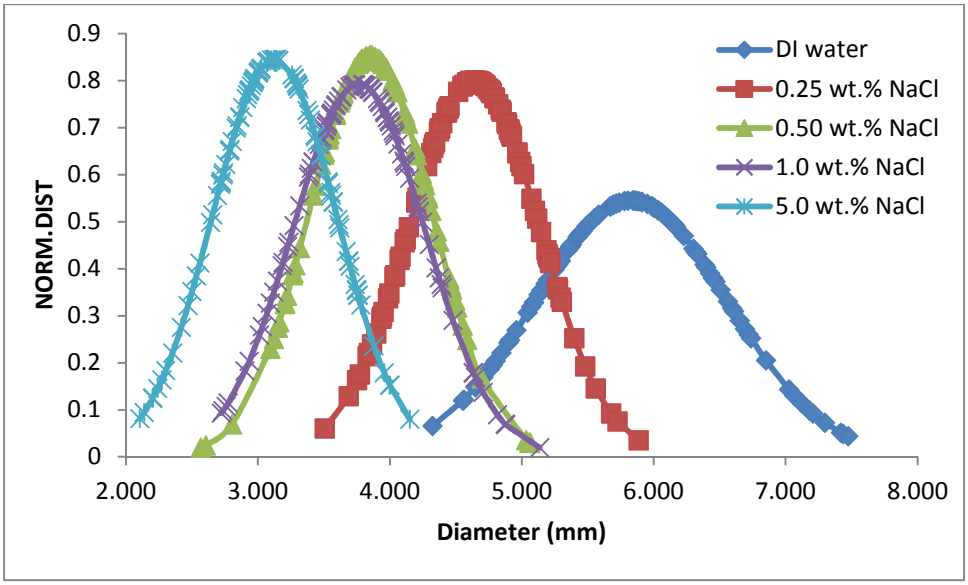

Figure 3-4. PSD of PPGs swollen in different brine concentration.

Figure 3-5 presents the Q-Q plot of the measured diameters of PPGs at the different brine concentrations. It is evident that the measured particles are not deviated from the fitted line which indicates that the measured diameters of PPGs are normally distributed.

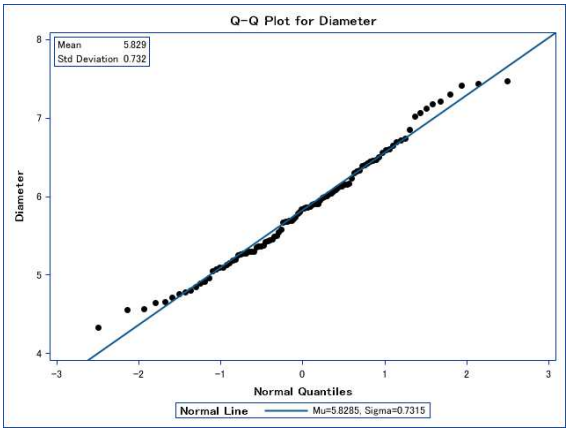

DI water

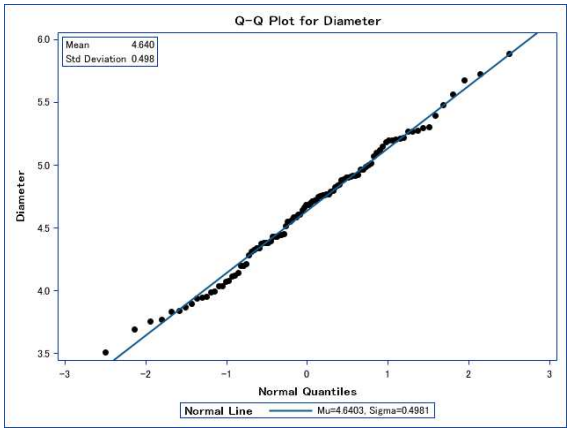

0.25 wt.% NaCl

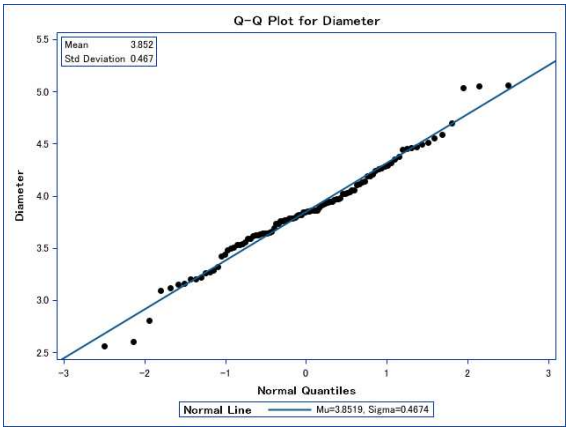

0.50 wt.% NaCl

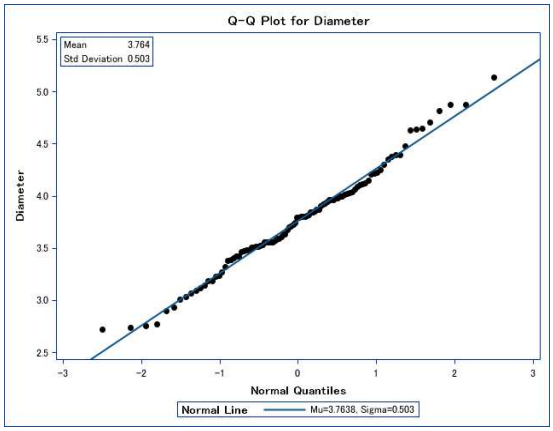

1.0 wt.% NaCl

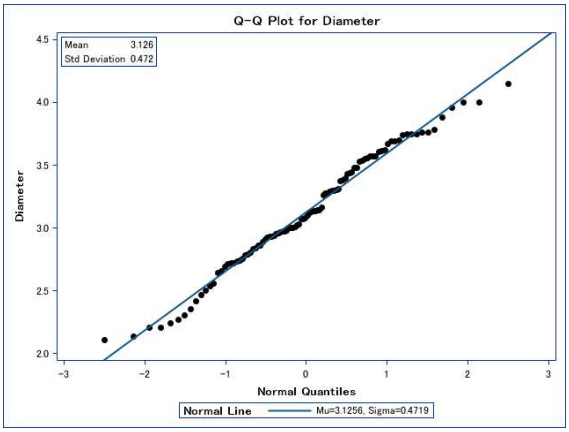

5.0 wt.% NaCl

Figure 3-5. Q-Q plot of PPG diameter swollen in different brine concentrations.

Table 3-2 summarizes the statistical information regarding the initial particle size distribution of PPGs swollen in different brine concentration. The table also shows the p-values of the normality test that was conducted using Shapiro-Wilk (W) test. The null-hypothesis of this test is that the data is normally distributed, and if the p-value is less than the chosen alpha value, then the null-hypothesis is rejected which implies that the data is not normally distributed.

Table 3-2. Statistical information of initial swollen PPGs PSD.

Brine Con	N	Mean (mm)	Std Deviation	Skewness	Kurtosis	Tests for Normality p-value
DI water	100	5.828	0.732	0.271	-0.456	0.2449
0.25 wt. %	100	4.640	0.498	0.033	-0.415	0.7978
0.50 wt.%	100	3.852	0.467	0.010	0.755	0.2331
1.0 wt.%	100	3.764	0.503	0.227	0.0683	0.4643
5.0 wt.%	100	3.126	0.472	-0.112	-0.563	0.2397

3.5 MODEL DESCRIPTION

The experimental apparatus, presented in Figure 3-6, is easy to assemble and use device. It is comprised of ISCO pump and a specially-designed steel screen piston accumulator. The top cap of the accumulator has a hole connected to a pump by tubing and fittings; the bottom cap is a stainless steel screen plate with. Two sets of screen plates were used in this study; their dimensions are presented in Table 3-3. Because the PPG sample is isolated by piston, any pressure source (i.e. air or liquid) can be used to push

the piston and force the gel particle to extrude through the screen plate. A pressure gauge is mounted in the lower part of the accumulator near the screen plate to record the threshold and extrusion pressure. The test accumulator is made of stainless steel material so it is easy to clean and will not wear easily.

Table 3-3. Dimension of the screen plates used in the experiments.

Screen plate #	**Hole size (D_{pt}), mm**	**Screen plate Thickness, mm**	**Number of holes per screen plate**	**Porosity (Φ), %**	**Permeability (K) Darcy**
1	1.5	7.5	40	1.66	1156.98
2	1.0	7.5	40	0.74	228.24
3	0.5	7.5	40	0.18	14.28
4	0.25	7.5	40	0.05	0.89
5	1.5	7.5	122	5.06	3528.78
6	1.0	7.5	122	2.25	697.04
7	0.5	7.5	122	0.56	43.57

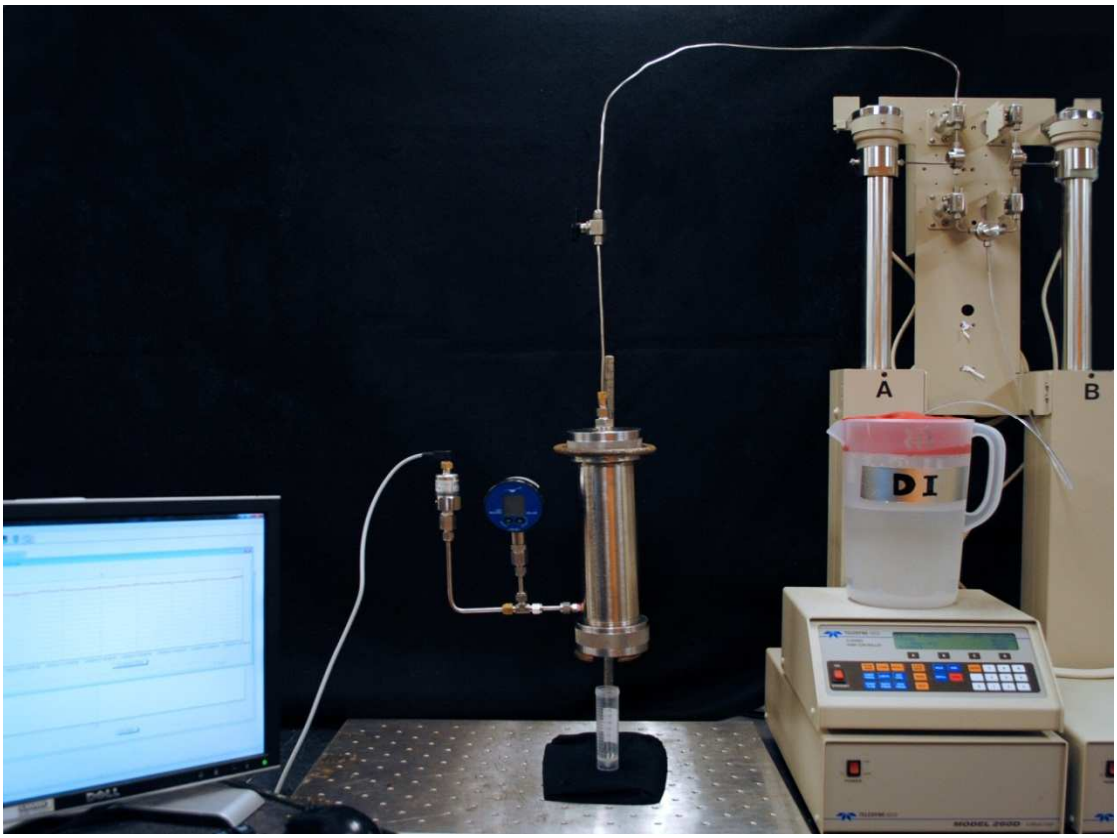

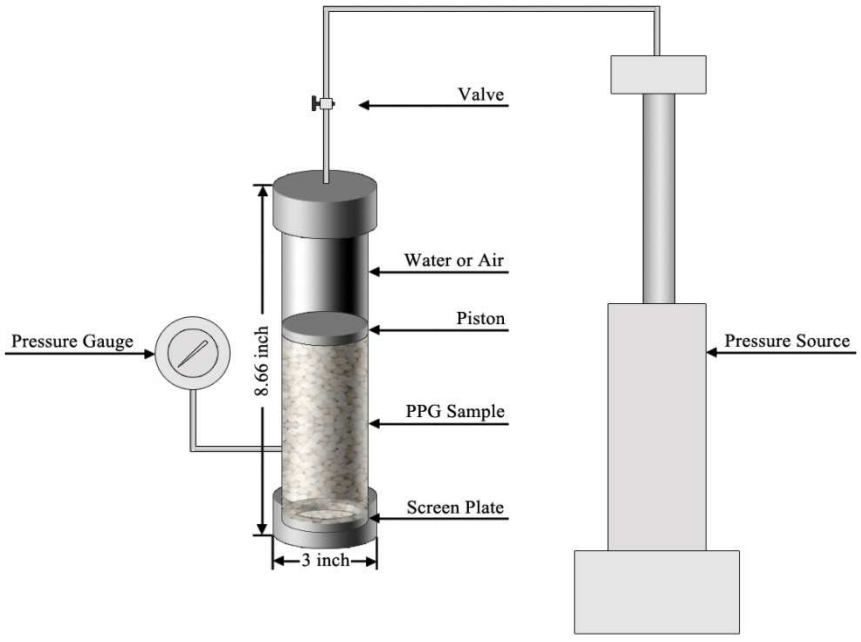

Figure 3-6. The experimental apparatus.

3.6 MODEL EXPERIMENT PROCEDURE

3.6.1 Sample Preparation and Loading.

- Depending on the brine salinity, 10 to 20 g of the dry PPGs was added slowly to the brine solution. The mixture then was stirred for 5 to 10 minutes and left for 24 hours until the PPG fully swollen.
- 500 ml of fully swollen and blotted from access water gel particles sample was loaded inside the sample container between the piston and a screen plate by putting the piston inside the container first then putting the gel sample and placing the screen plate on top of the sample and the caps were tightened, Figure 3-7 shows the sample loading procedures.
- During the experiment the container is turned upside down in vertical position where the screen plate would be in bottom.
- The gap between the top cap of the accumulator and the piston was filled with water to avoid any gas between them.

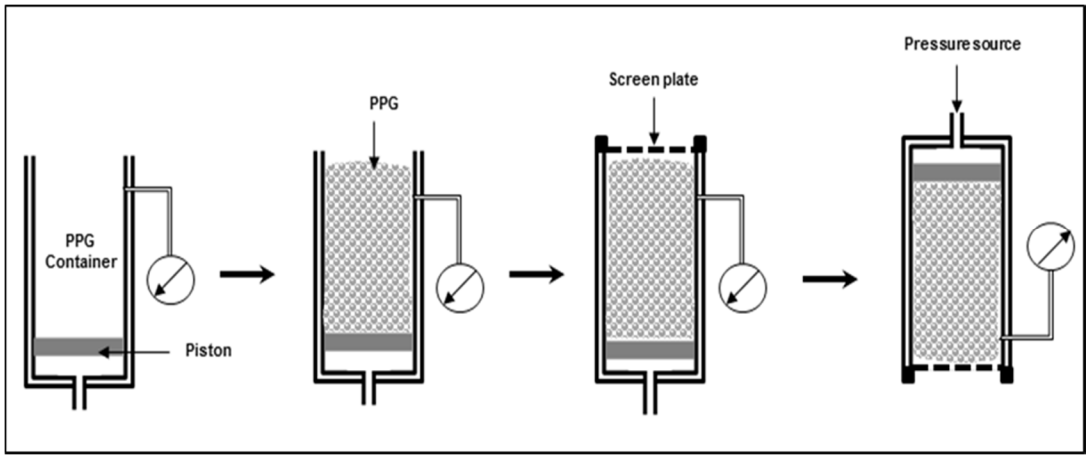

Figure 3-7. PPGs sample loading procedure.

3.6.2 Threshold Pressure Measurement.

- An ISCO pump was used to deliver constant pressure to push the PPG through the screen plate.
- The initial constant pressure was 10 psi, and then the pressure was increased gradually (2.0 psi at a time) until the PPG start extruding through the screen plate. The reading in the pressure gauge at the time of the first PPG extrusion is considered the threshold pressure.
- The procedures above was repeated for each combination of screen hole size and brine salinity; the threshold pressure was recorded each time.

3.6.3 Apparent Viscosity Determination. After obtaining the threshold pressure, the constant injection pressure that was provided from the ISCO pump kept increasing gradually until continuous discharges of gel particles from the effluent were obtained. The discharge flow rate was calculated by measuring the volume of gel collected over a specific period of time. Once the gel discharge flow rate was stable, the constant injection pressure increased to acquire PPGs extrusion pressure- flow rate relation which can assist in finding the apparent viscosity. The procedures were repeated for the different sizes screen plates and the different brine concentrations.

3.7 EXPERIMENTAL RESULTS

3.7.1 Threshold Pressure Evaluation. Several factors can affect the threshold pressure of PPGs. In this study, the following factors were investigated:

Effect of brine salinity. In this study, PPGs were swollen in brine concentrations ranging from DI water to 5.0 wt. % NaCl. Increasing the brine concentration cause the PPGs stiffness to increase, making it more difficult for PPGs to pass through the screen

plate. Figure 3-8 plots four curves of the threshold pressure of swollen PPG in different brine concentrations passing through different hole sizes. It is clear that the threshold pressure increased with increasing the brine concentration when the hole size is the same. This indicates that PPG is prone to stiffen when the swelling media has higher salinity. The figure also show a comparison of four hole sizes, the threshold pressure values are the highest with small hole size (0.25 mm).

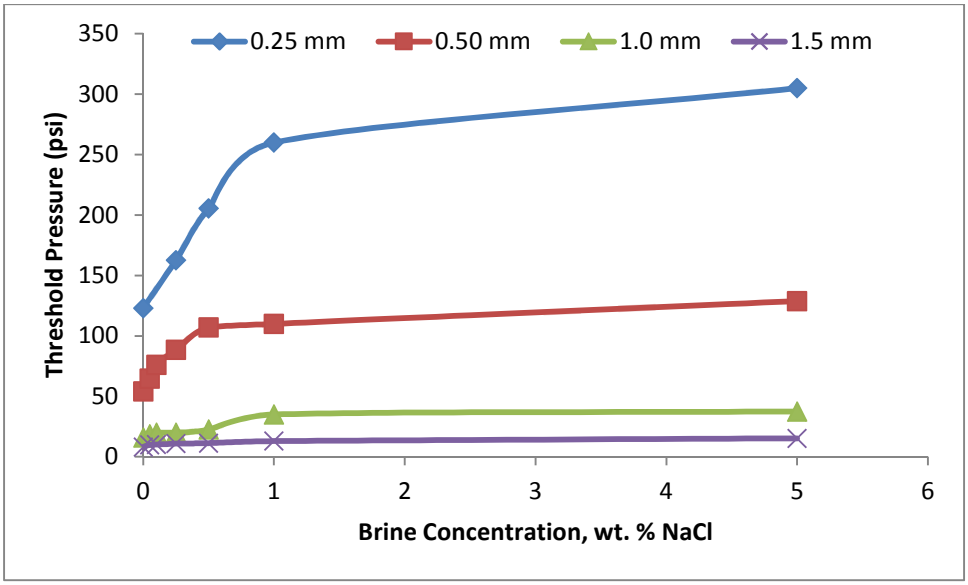

Figure 3-8. Effect of brine concentration on the threshold pressure of PPGs using four different screen plate hole sizes.

Ratio of swollen PPG size (D_p) to hole size (D_{pt}). Figure 3-9 shows the prominent effect of the ratio of D_p to D_{pt} on the threshold pressure. The threshold pressure significantly increases with brine salinity when the ratio is the same. The gel particles that were prepared by high concentration brine have higher strength than the one that

were prepared in low concentration brine. Therefore, the result indicates strong particles need higher pressure to push them through holes than weak particles.

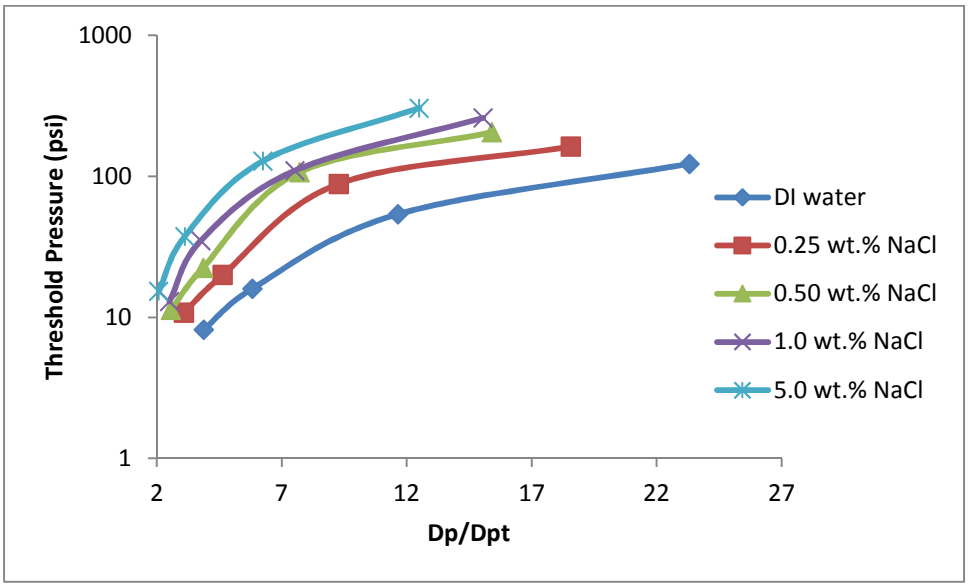

Figure 3-9. Effect of the ratio of swollen PPGs D_p to D_{pt} on threshold pressure.

Holes density. The effect of the number of holes (density) per screen plate on the threshold pressure was examined. Three additional screen plates were designed with hole sizes (0.5, 1.0 and 5.0 mm), but with 122 holes per screen plate. The evaluation of this parameter is important because it relates to the porosity and permeability of the porous media and can be used as a criterion in PPGs treatment design. Figure 3-10a through g present the threshold pressure values using 40 holes per screen plates compared to the threshold pressure values using 122 holes per screen plates. All seven figures demonstrate an identical trend; the difference between the threshold pressure values was moderate for the 1.0 and 1.5 mm screen plate. However, a huge difference occurred in the threshold pressure values when using 0.5 hole size.

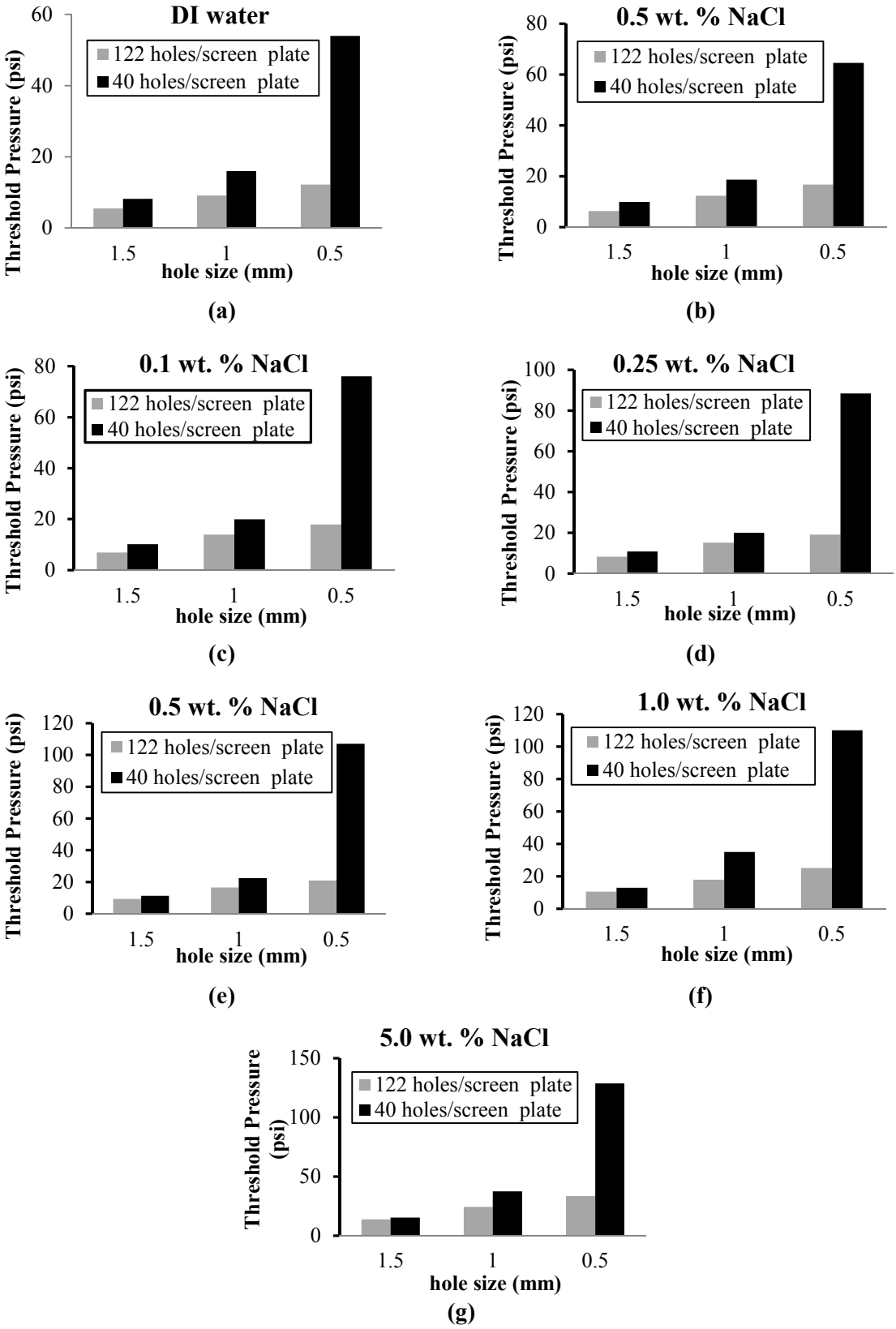

Figure 3-10. Comparison of threshold pressure using different screen plate hole densities.

3.7.2 Apparent Viscosity Determination. The proposed model can be utilized to determine the apparent viscosity of PPGs, this is an important parameter in evaluating their rheological behavior. After acquiring the PPGs injection flow rate relation with respect to the constant injection pressure, the apparent viscosity was calculated using Eq. 1 where Δp_{brine} was calculated using Darcy's equation, where K is the permeability of the screen in Darcy calculated using Eq. 3, where d is the screen hole diameter in inch and ϕ is the porosity of the screen plate obtained from Table 3-3.

$$K = 20 \times 10^6 \times d^2 \times \phi \tag{3}$$

The length term in Darcy's equation was considered to be the thickness of the plate, and the area was calculated using the diameter of the screen plate. The flow rate was the discharge flow rate what was measured at a certain constant injection pressure.

The apparent viscosity was plotted against the shear rate. The shear rate was calculated by converting the flow rate to a superficial velocity and then using equation Eq. 4, where v is the superficial velocity in mm/sec, and d is the diameter of the hole in the screen plate in mm.

$$\gamma = 4v / d \tag{4}$$

Figure 3-11 shows the relationship between the apparent viscosity and the shear rates. It was found out that the apparent viscosity values from the experimental results in different size of the holes almost follow the same line in log-log scale when the brine

concentration is the same. This fact indicate that the hole size does not affect the apparent viscosity. Furthermore, form the same figure. It is clear that the apparent viscosity values decreased as the shear rate increased indicating that all the swollen PPGs were shear-thinning materials.

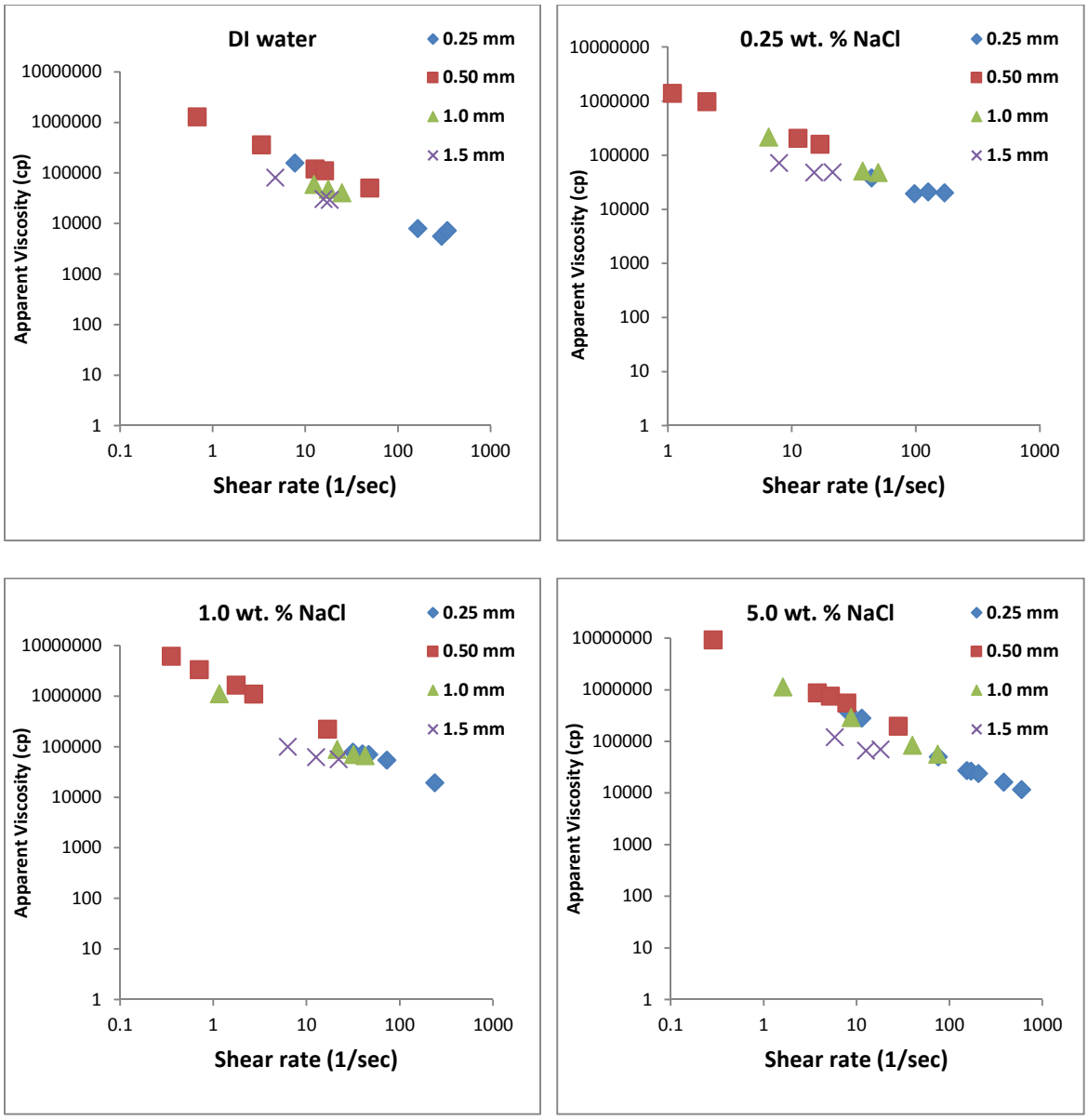

Figure 3-11. Shear rate effect on apparent viscosity as a function of brine concentration and hole size.

3.7.3 Correlation between Threshold Pressure and PPGs Elastic Modulus. To validate the results, the threshold pressure was plotted against the elastic modulus values. Figure 3-12 demonstrates the relation between the threshold pressure and the elastic modulus of the swollen PPGs under different numbers of screen plate holes and different gap heights. A linear relationship was attained when both parameters were plotted for the PPGs swollen in the various brine concentrations. Eq. 5 can be used to quantify the elastic modulus when the threshold pressure is measured using the proposed model.

$$P_t = K \times G' + C \tag{5}$$

Where P_t is the threshold pressure in Pa, K and C are constants that are dependent on the brine concentration, hole size and density per screen plate, and G' is the elastic modulus in Pa. Table 3-4 summarizes the values of K and C obtained from fitting Eq. 5. The constants K and C are a function of the parameters impacting the threshold pressure. More research is needed to examine the nature of these constants.

Table 3-4. Fitting equations for P_t to the G' of PPGs.

Screen Plate #	Numbers of holes per screen plate	Hole size (D_{pt}), mm	Constant K	Constant C	R^2
1	40	1.5	59.006	47134	0.9531
2		1.0	195.87	48669	0.8581
3		0.5	563.66	244201	0.9168
4	122	1.5	74.726	21389	0.9914
5		1.0	118.37	35817	0.9925
6		0.5	149.91	43609	0.9921

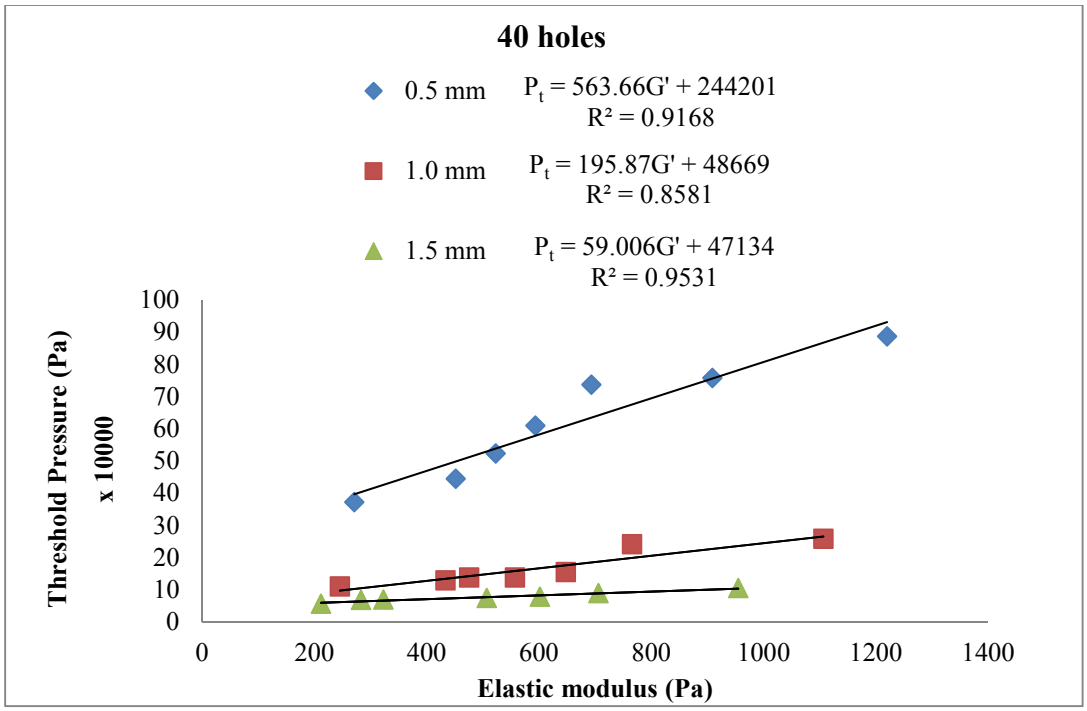

(a)

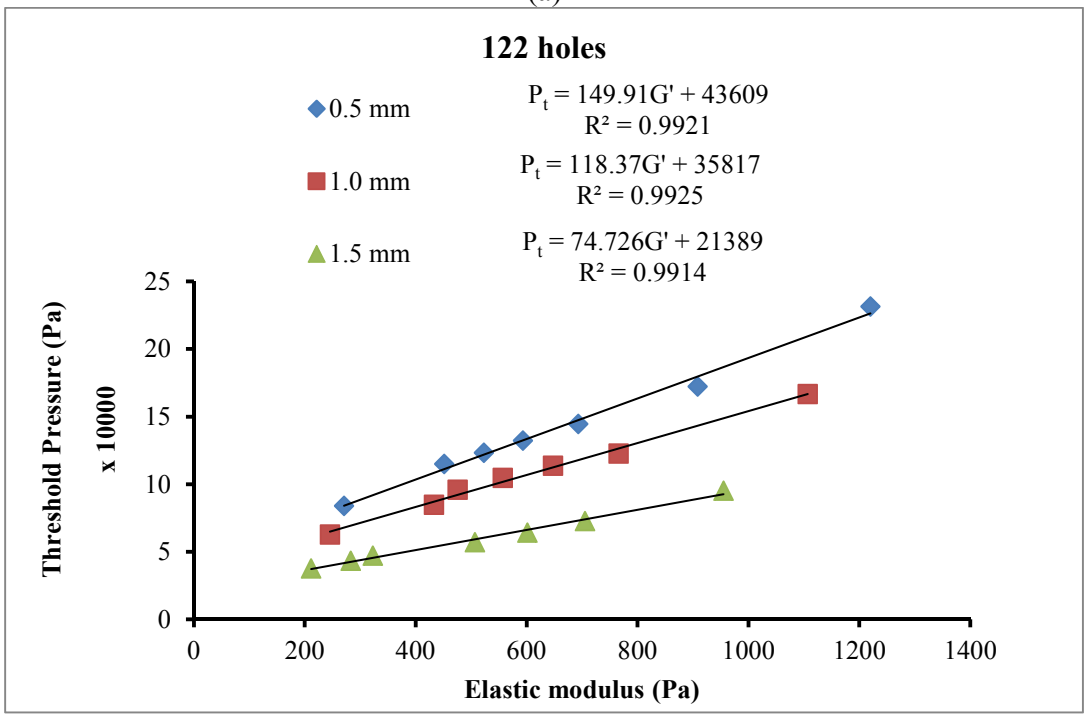

(b)

Figure 3-12. The correlation of threshold pressure to the elastic modulus for PPG swollen in 0 to 5.0 wt. % NaCI solutions at different hole sizes and gap heights: (a) correlation with 40 hole per screen plate, (b) correlation of 122 holes per screen plate.

3.7.4 Mesh Size Effect. Three experiments were performed to examine the effect of changing the mesh size of the dry PPGs on the PPGs threshold pressure. (18/20), (30/40) and (60/70) mesh sizes dry PPGs were used in the study. The PPGs were swollen in 1.0 wt. % NaCl and 1.5 mm hole screen plate was used. The same experimental procedure was followed to obtain the threshold pressure.

Figure 3-13 shows the threshold pressure values for the different PPGs mesh size. It is noticeable that threshold pressure or the strength of PPGs increases in accordance with increasing the dry mesh size. For example, the 1.0 wt. % NaCl PPGs with mesh size of (60/70) had a threshold pressure of 0.3 psi. This is because the swollen solution tended to be more viscous and easily flowing. Thus, a small exerting force is required to extrude this solution through the hole screen plate.

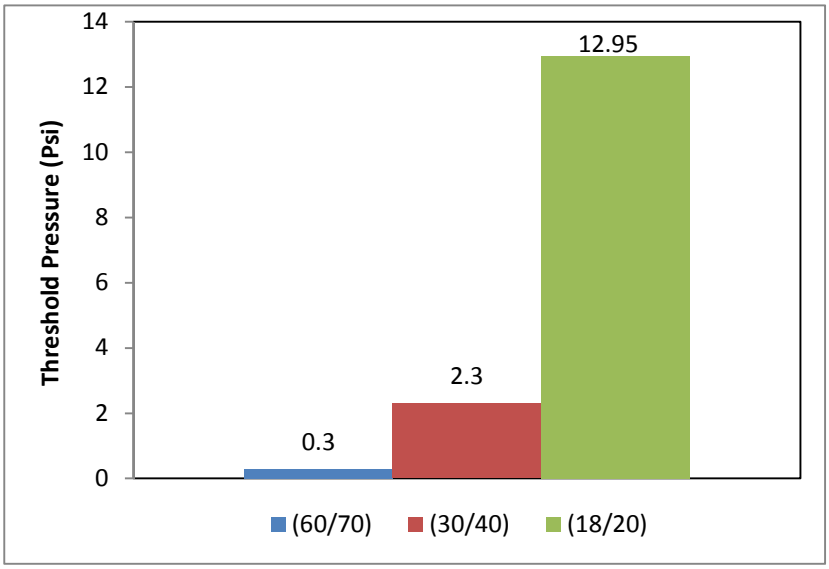

Figure 3-13. Mesh size effect on PPGs threshold pressure.

3.7.5 Particle Size Distribution of the Extruded PPGs. The use of the screening model enables a direct observation of the gel particles transport through the open hole screen plates model. That can be advantageous in determining the controlling mechanism of the gel particles transportation. In this study, the dry gel particles were swollen in DI water and three different brine concentrations of (0.25, 1.0 and 5.0 wt. % NaCl) that resulted in obtaining four different swollen PPGs that have four equivalent diameters of (5.828, 4.640, 3.764 and 3.126 mm , respectively). The strength of these particles is inversely proportional to their equivalent swollen diameters. Then, each of these particles was injected through the four hole screen plate with hole diameters of 1.5, 1.0, 0.5 and 0.25 mm, respectively.

After the threshold pressure was obtained, analysis of the particle size distribution of the extruded particles where 100 particles were chosen randomly from the effluent to measure their equivalent diameter using the microscope, frequency distribution where the particles were grouped based on their diameters and the visual observation of the particles in the effluent were obtained. As a result, particles evaluation index can be found, the later can be defined as the ratio of the equivalent diameter of the extruded gel particles to the ratio of the initial swollen gel particles at the same medium of brine concentration and fracture size. The evaluation index can be an indication of which pattern or transportation mechanism did the gel particles undergo to pass through the open hole screen plates.

Generally, the PPG transportation through the porous media can be classified into three patters: pass, broken into pieces and pass and plug (Bai et al, 2007a). However, no plugging pattern was observed in this study and this is attributed to the deformability

nature of the gel particles. Consequently the extrusion pattern of the extruded gel particles were only limited to the pass, and broken into pieces and pass patterns. In the pass pattern, the gel particle will deform and then be extruded through the open hole screen plate maintaining almost their initial equivalent diameter. The broken and pass pattern, on the other hand, the gel particles will be broken into pieces and then extruded through the various open hole screen plates.

3.7.5.1 Extruded PPGs through 1.5 and 1.0 mm hole size screen plate.

Figures 3-14 through 3-17 show the frequency and the particle size distribution of the initial and the extruded PPGs that were swollen in different brine concentration and extruded through 1.0 and 1.5 mm hole screen plate. It is clear from these figures along with the visual observation of the extruded gel particles in Figures 3-18 through 3-21 that most of these particles follow the broken and pass pattern. For example, when the DI water PPG extruded through the 1.5 and 1.0 mm hole screen plates, their equivalent extruded diameters have been reduced from 5.828 to 1.808 mm (69.01 %) reduction and from 5.828 to 1.663 mm (71.5 %) reduction, which yielded a particle evaluation index of 0.310 and 0.285, respectively.

However, for the PPG that was swollen in 5.0 wt. % NaCl, and extruded through 1.5 mm hole screen plate as it is seen in Figure 3-17, it is obvious that most of the extruded particles fall in the same range as the initial particle size distribution. In fact, the equivalent extruded diameter was only reduced from 3.126 to 3.093 mm (1.1 %) which is equivalent to a particle evaluation index of 0.989. This information along with the image analysis in Figure 3-21, a conclusion can be drawn that the 5.0 wt. % NaCl PPG followed the pass pattern when it was extruded through 1.5 mm hole screen plate.

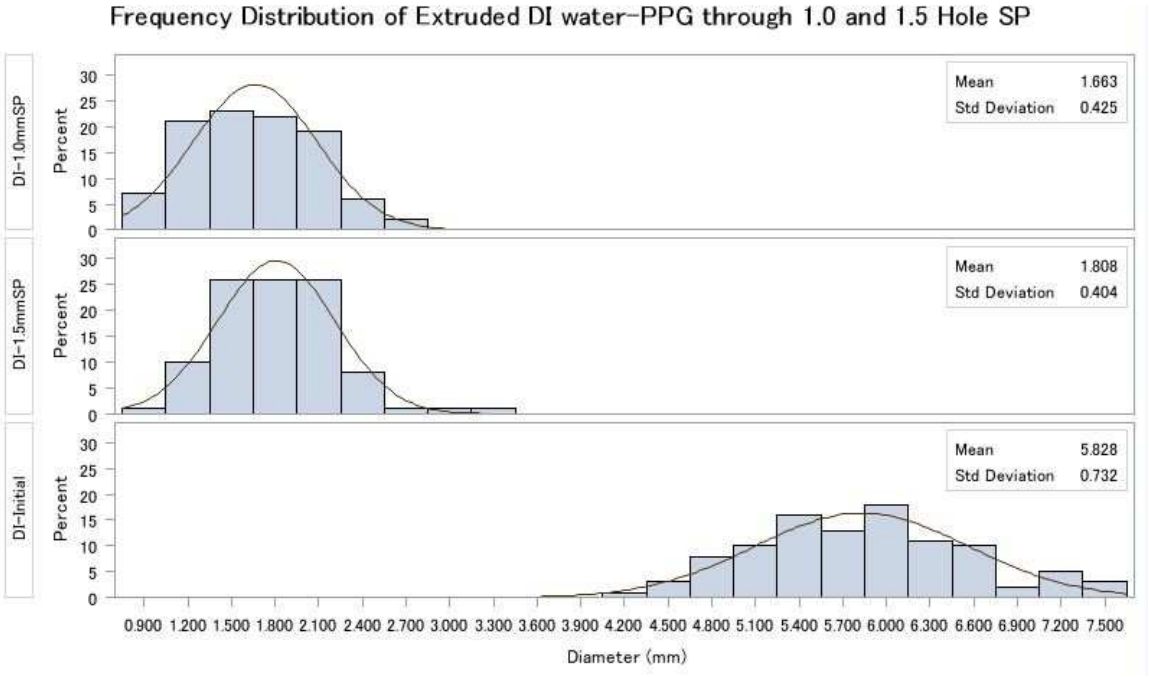

(a)

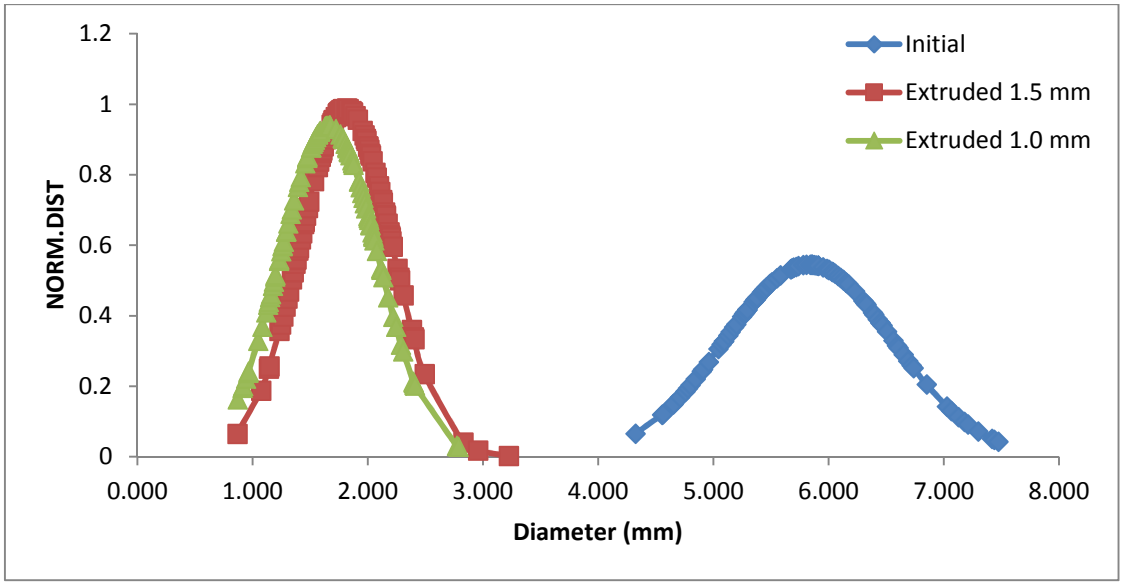

(b)

Figure 3-14. Comparison between DI water PPG before and after extrusion through 1.5 and 1.0 mm hole screen plate (a) frequency distribution (b) PSD.

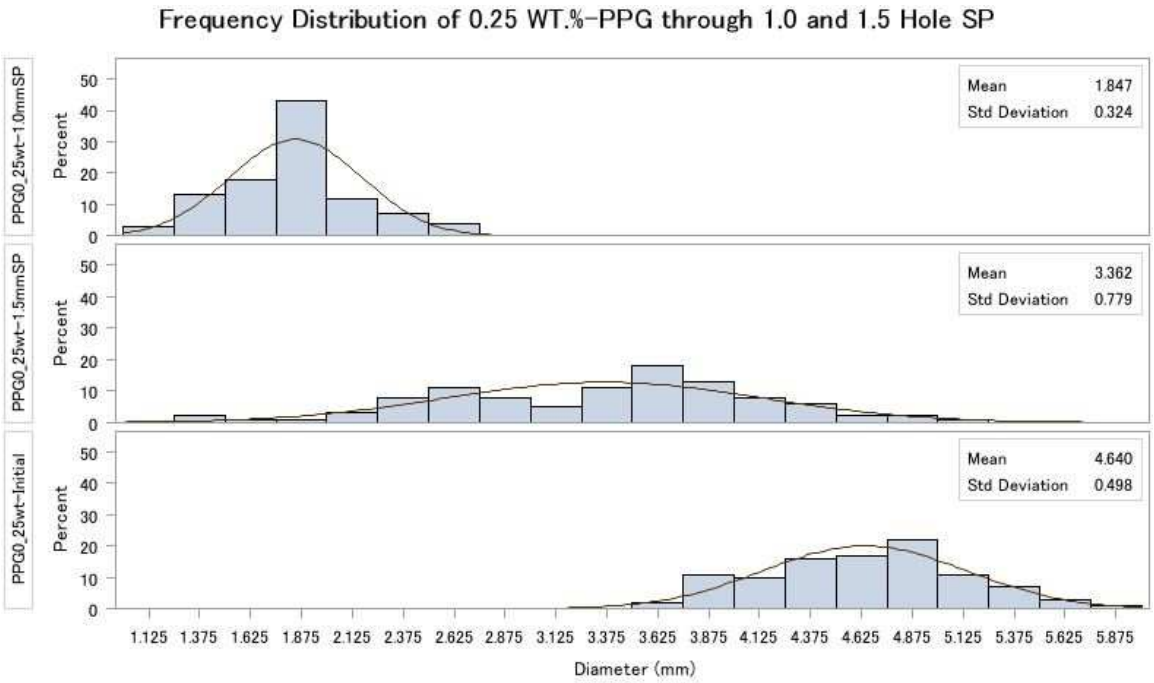

(a)

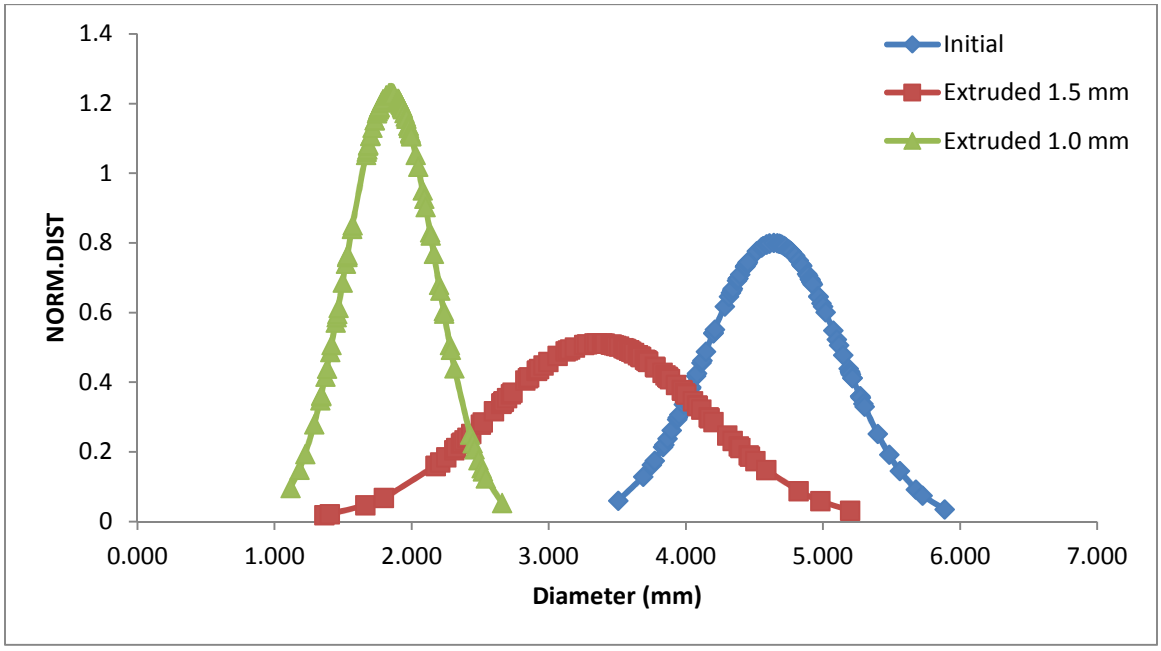

(b)

Figure 3-15. Comparison between 0.25 wt. % PPG before and after extrusion through 1.5 and 1.0 mm hole screen plate (a) frequency distribution (b) PSD.

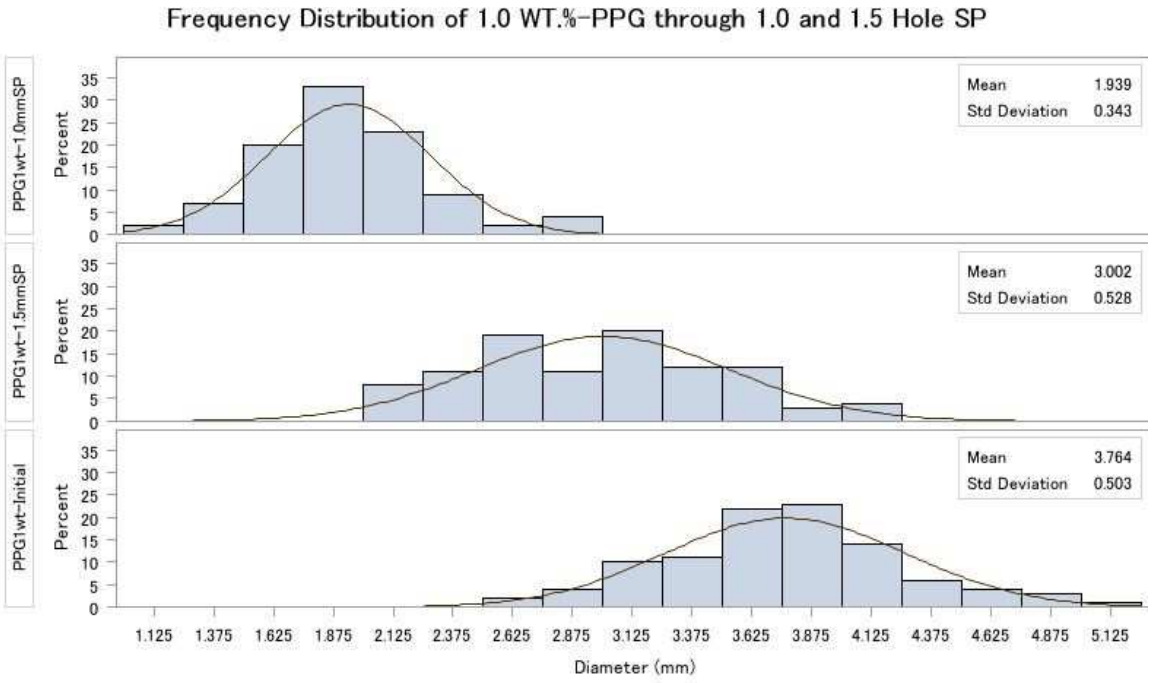

(a)

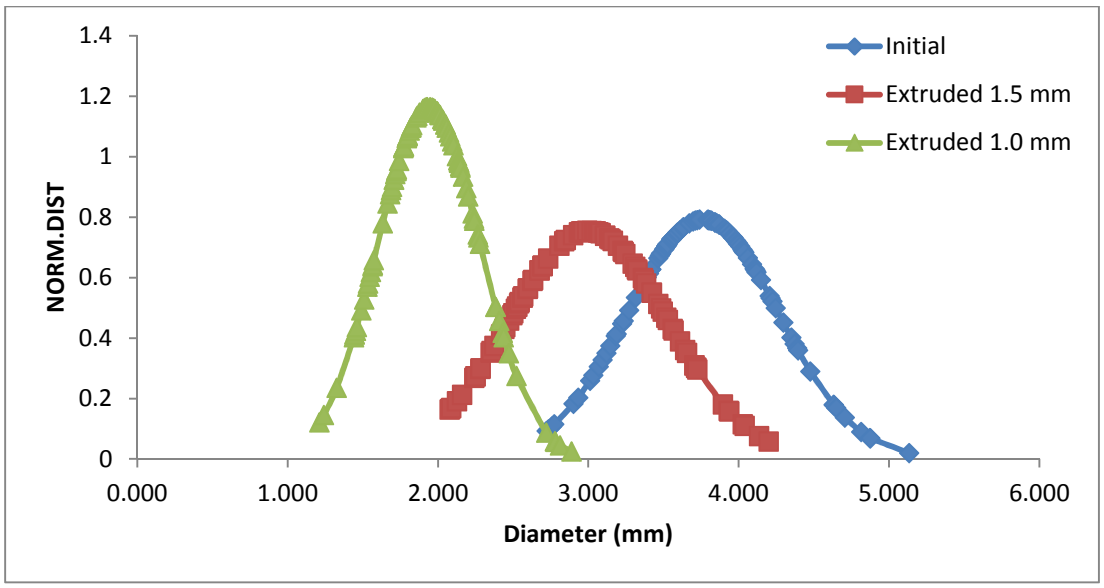

(b)

Figure 3-16. Comparison between 1.0 wt. % PPG before and after extrusion through 1.5 and 1.0 mm hole screen plate (a) frequency distribution (b) PSD.

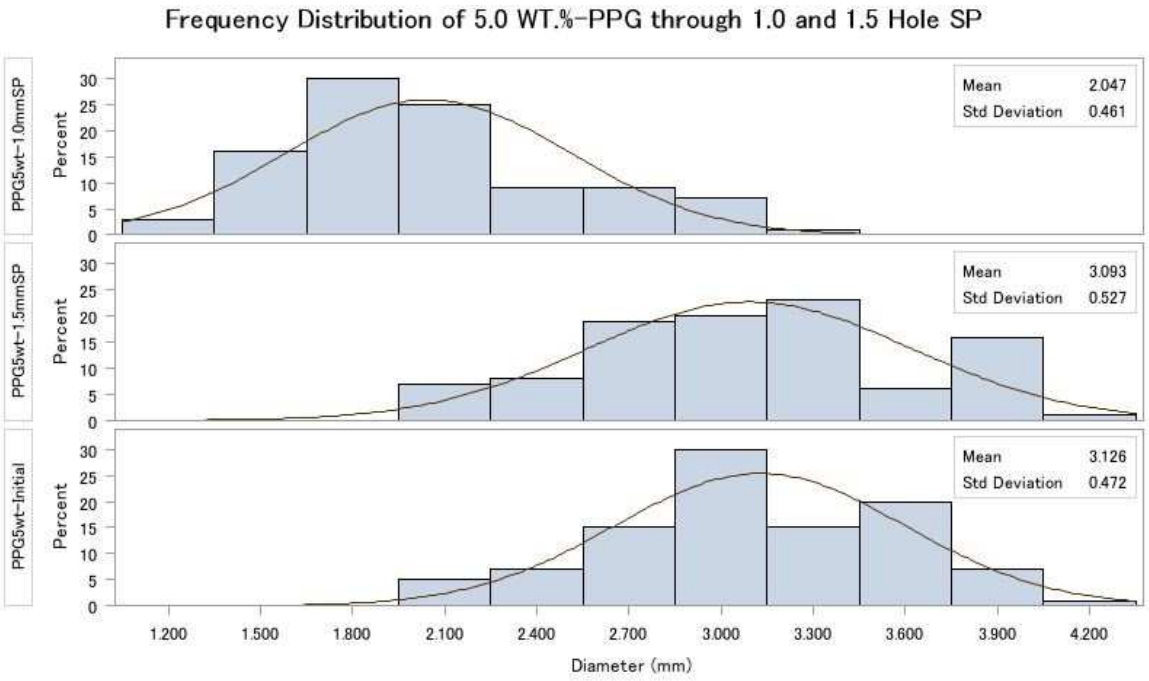

(a)

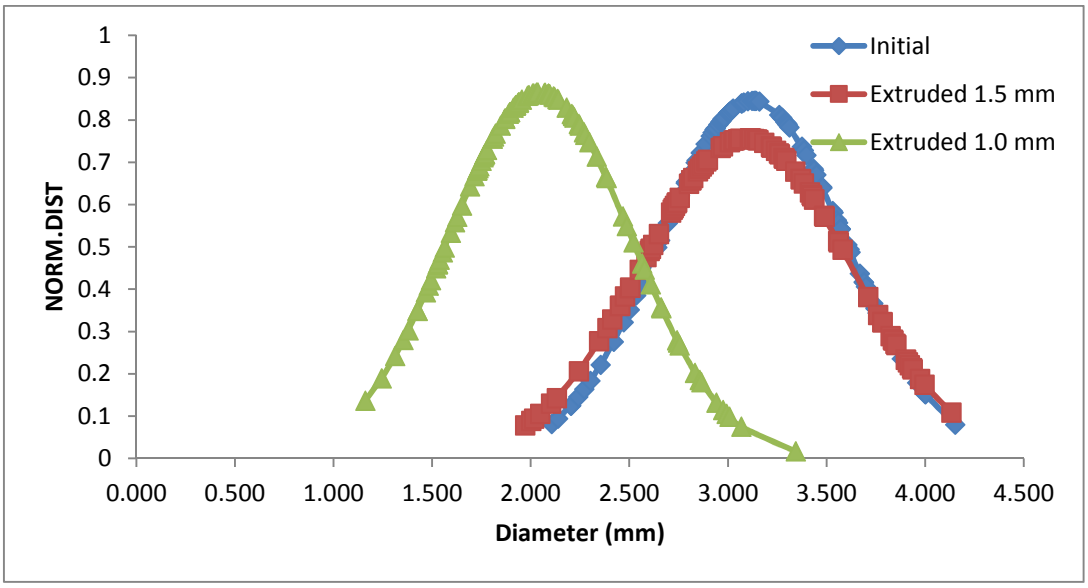

(b)

Figure 3-17. Comparison between 5.0 wt. % PPG before and after extrusion through 1.5 and 1.0 mm hole screen plate (a) frequency distribution (b) PSD.

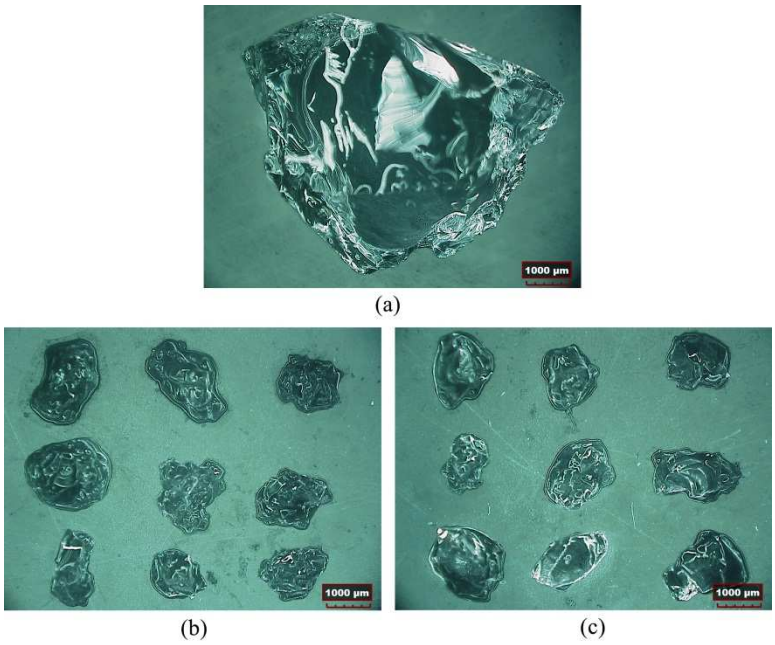

Figure 3-18. Comparison between initial and extruded DI water PPG (a) Initial (b) extruded through 1.0 mm hole screen plate (c) extruded through 1.5 mm hole screen plate.

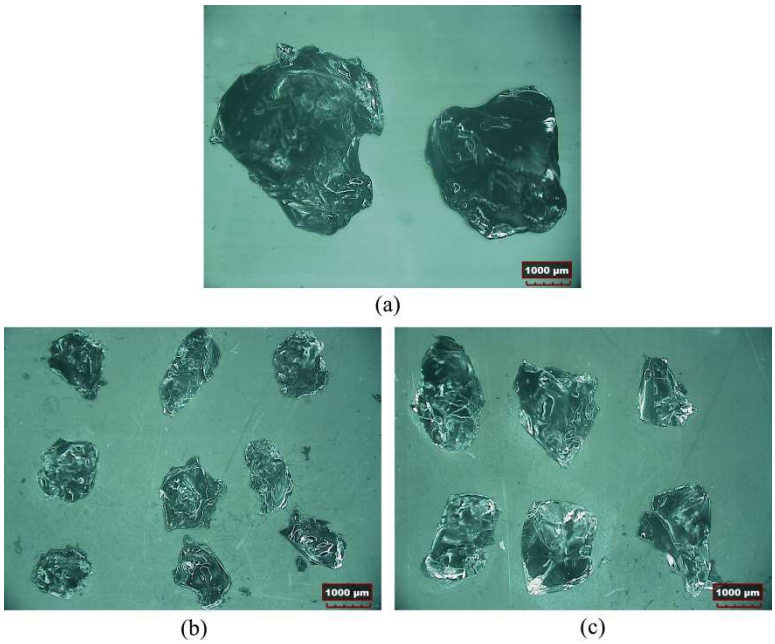

Figure 3-19. Comparison between initial and extruded 0.25 wt. % NaCl PPG (a) Initial (b) extruded through 1.0 mm hole screen plate (c) extruded through 1.5 mm hole screen plate.

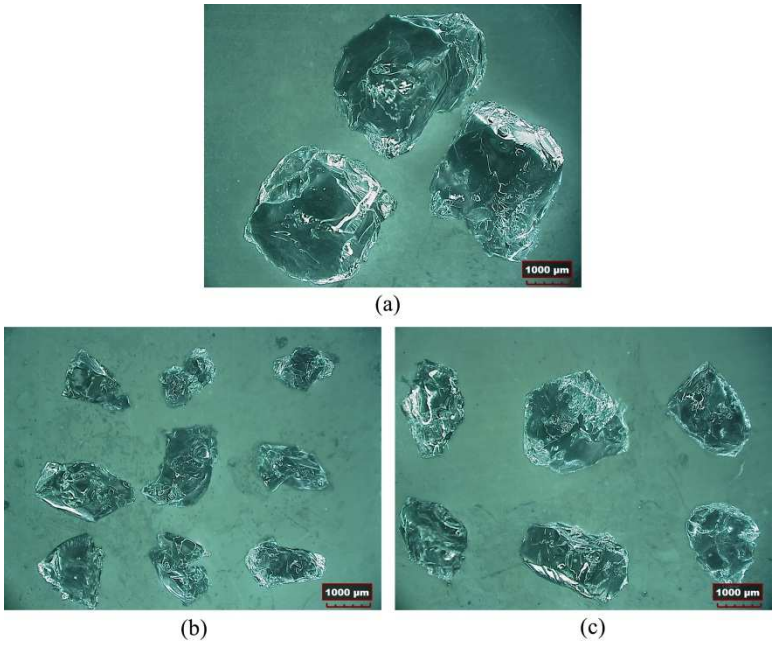

Figure 3-20. Comparison between initial and extruded 1.0 wt. % NaCl PPG (a) Initial (b) extruded through 1.0 mm hole screen plate (c) extruded through 1.5 mm hole screen plate.

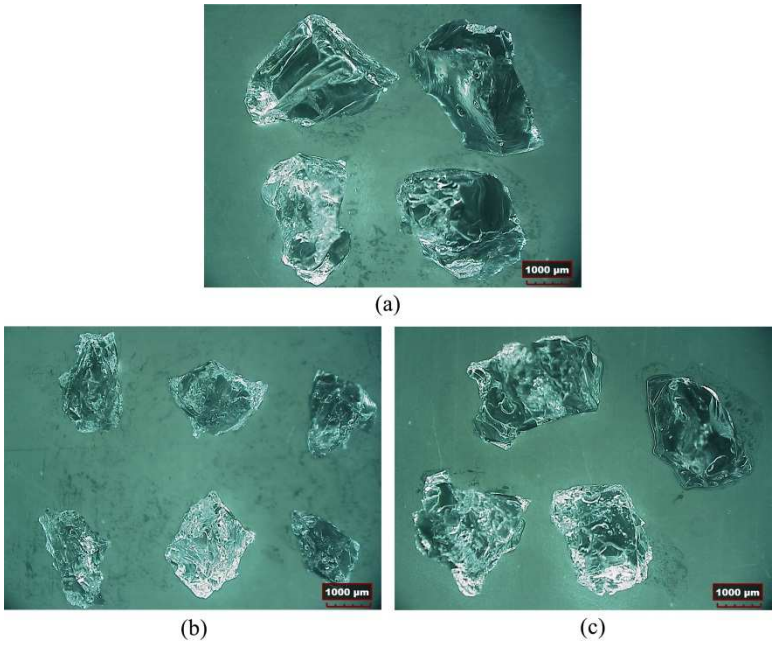

Figure 3-21. Comparison between initial and extruded 5.0 wt. % NaCl PPG (a) Initial (b) extruded through 1.0 mm hole screen plate (c) extruded through 1.5 mm hole screen plate.

3.7.5.2 Extruded PPGs through 0.5 and 0.25 mm hole size screen plate. The PPGs that were extruded through 0.50 and 0.25 hole size screen plate were not distinguishable to be measured using the microscope. Figure 3-22a and b demonstrates 1.0 wt. % NaCl PPG that was extruded through 0.50 and 0.25 mm hole size screen plate, respectively. It is clear that the particles were adhered to each other after extrusion. Such a trend was observed with the rest of the brine concentrations PPGs used in this study.

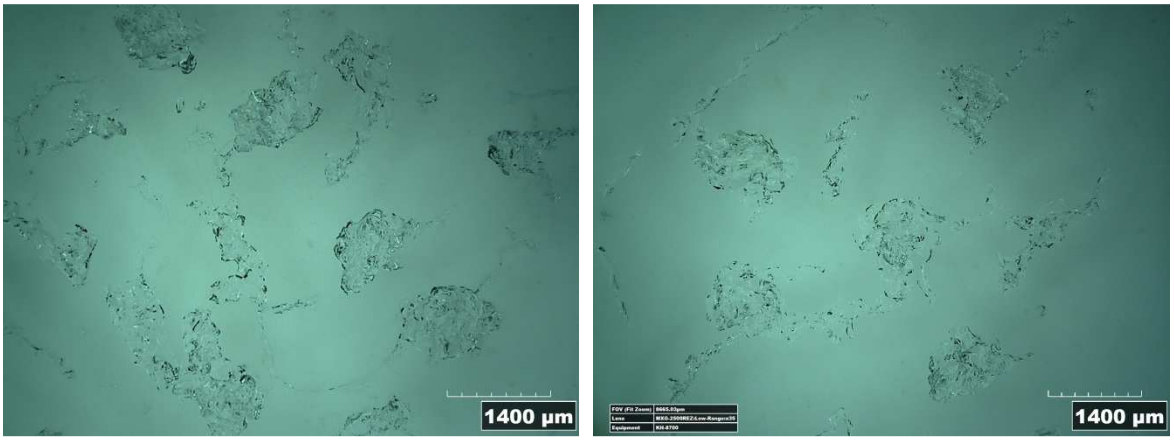

Figure 3-22. 1.0 wt. % NaCl PPG extruded through 0.50 and 0.25 mm hole screen plate (a) 0.50 mm screen plate (b) 0.25 mm screen plate.

During the extrusion experiment of PPGs through 0.50 and 0.25 mm screen plate, it was clear that the discharging flow rate was relatively small compared to the applied constant injection pressure. Figure 3-23 shows the constant injection pressure relationship with the discharging flow rate for 5.0 wt. % NaCl PPG through 0.25 mm hole size screen plate which has a permeability of 0.89 Darcy. The relatively small values of the discharging flow rate is mainly attributed to the dehydration and the broken of particles as they transported through the screen plate. Seright (1999) observed the same behavior in the polymer gels extrusion though small fracture widths. He explained the low flow

rates of gels propagation in small fracture widths was a result of gel dehydration and concentration during extrusion. Figure 3-24 presents a comparison between the initial 5.0 wt. % NaCl PPG and after extrusion through 0.25 mm hole size screen plate. Table 3-5 summarizes the particle evaluation index and the extrusion pattern for PPGs extruded through open hole screen plate model of various hole size diameters.

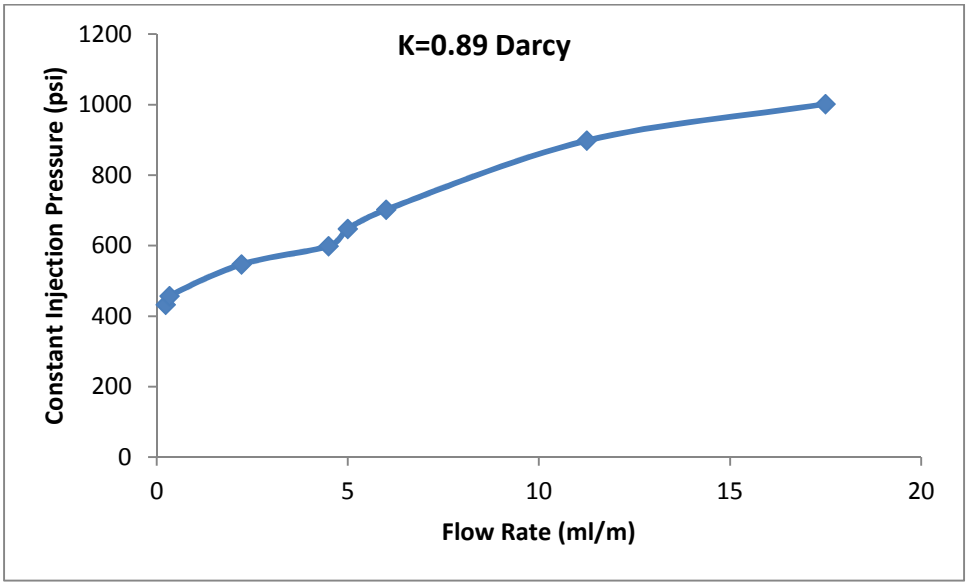

Figure 3-23. 5.0 wt. % NaCl PPG extrusion pressure as a function of flow rate.

Figure 3-24. Comparison between initial and extruded 5.0 wt. % NaCl through 0.25 mm screen plate (a) initial (b) after extrusion.

Table 3-5. Particle evaluation index and extrusion pattern for PPG transport through open hole screen plate model.

	Initial Equivalent Diameter (mm)	**Extruded through hole size (mm)**	**Equivalent Diameter After Extrusion (mm)**	**Particle Evaluation Index**	**Extrusion Pattern**
DI water PPG	5.828	1.5	1.808	0.310	Broken and Pass
		1.0	1.663	0.284	Broken and Pass
		0.5	-	-	Broken, Dehydration and Pass
		0.25	-	-	Broken, Dehydration and Pass
0.25 wt. % NaCl PPG	4.640	1.5	3.362	0.725	Broken and Pass
		1.0	1.847	0.398	Broken and Pass
		0.5	-	-	Broken, Dehydration and Pass
		0.25	-	-	Broken, Dehydration and Pass
1.0 wt. % NaCl PPG	3.764	1.5	3.002	0.798	Broken and Pass
		1.0	1.939	0.515	Broken and Pass
		0.5	-	-	Broken, Dehydration and Pass
		0.25	-	-	Broken, Dehydration and Pass
5.0 wt. % NaCl PPG	3.126	1.5	3.093	0.989	Pass
		1.0	2.047	0.655	Broken and Pass
		0.5	-	-	Broken, Dehydration and Pass
		0.25	-	-	Broken, Dehydration and Pass

3.8 CONCLUSION

In this study, experiments were conducted to evaluate the strength of PPGs that were swollen in different brine concentration using a simple open hole screen plate model. The major findings of this study can be summarized in the following points:

- A simple technique was established that can provide a fast and practical method to quantitatively evaluate the strength of the millimeter-sized PPGs in the laboratory and on site during PPGs treatment process.
- Two parameters of PPGs characterizations, the threshold pressure and apparent viscosity, can be quantitatively determined using this method.
- PPGs swollen in higher brine concentrations are more stiffen and thus requiring a higher threshold pressure.
- The relation between the hole density of the screen plate and the threshold pressure is presented which can be related to the porosity and the permeability of the porous media and can be used as a criterion in PPGs treatment design.
- The proposed model can be used to examine the strength of different PPGs products provided that using one specific screen plate and brine concentration.
- The PPGs threshold pressure correlates lineally with the elastic modulus which shows the validation of the proposed method.
- The PPGs extruded through 0.25 and 0.50 mm hole size exhibit broken, dehydration and pass pattern; whereas, the PPGs extruded through 1.0 and 1.5 mm hole size exhibit broken and pass pattern.

4. OPEN FRACTURE PLATES MODEL

4.1 SUMMARY

This chapter presents the experiments that were conducted to examine the PPGs extrusion and propagation behavior through various widths open fracture plates. Several factors that impact the PPGs extrusion behavior were considered in this study. Those include the effect of brine concentration, flow rate, and size of the fracture. Additionally, this chapter presents the particle size distribution of the gel particles before and after PPGs extrusion through the various fractures and a full-design factorial analysis was conducted to have an understanding of which factor can influence the PPGs injection pressure, resistance factor and injectivity. The experimental results have shown that for a certain fracture width, the brine concentration or the swelling ratio would not influence the PPGs injection pressure greatly compared to the size of the fracture width, which is totally different from the previous results regarding PPGs transportation through open fracture. Additionally, the results have shown that the PPGs resistance factor increases as fracture width increases.

A total of twelve experiments were performed to examine the PPGs transportation behavior through the open fracture plate model. Figure 4-1 presents the major outcomes of the experiments. As shown in Figure 4-1, DI water and three different brine concentrations (0.25, 1.0 and 5.0 wt. % NaCl) were used in this study to obtain different swollen PPGs of different gel strength and swelling ratio, accordingly. Three open fracture screen plates with different fracture width (0.25, 0.50 and 1.0 mm) were used to examine how the fracture width size can be related to the PPGs injection pressure, resistance factor and injectivity). Moreover, an analysis of the particles size distribution

of PPGs before and after extrusion was conducted to obtain particle evaluation index to assist in understanding the extrusion pattern of PPGs through the fracture plates. A full-factorial design was developed to examine the most influential parameters on injection pressure, resistance factor and PPGs injectivity.

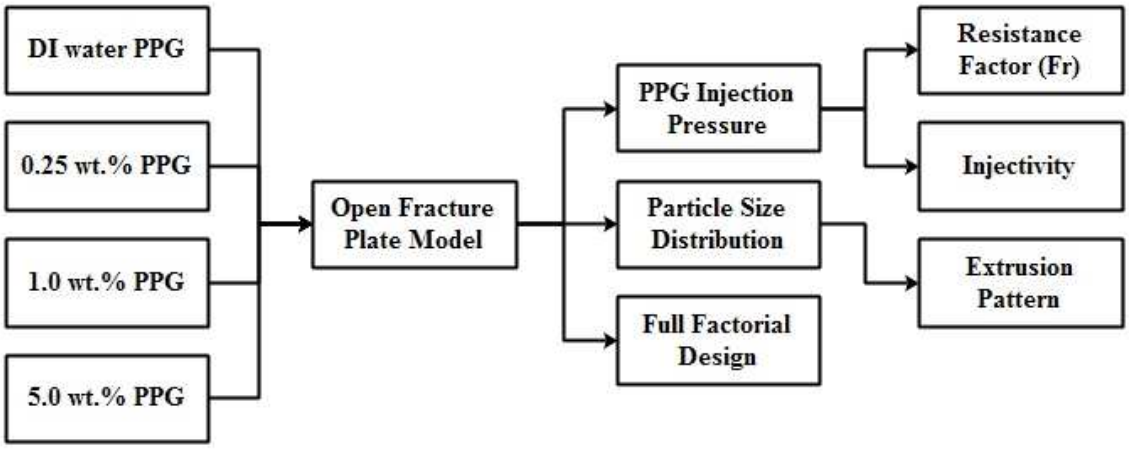

Figure 4-1. The outcomes of the experiment.

4.2 INTRODUCTION

Gel is considered to be a fluid diverting agent that is being used in mature reservoirs to reduce channeling fluids through high permeable and streak zones. The gel particles are fracture filling materials that have the ability to form concentrated gel packs in open fracture (Al Ibadi et al, 2012). Therefore, the gel's extrusion ability is a main factor for a successful gel treatment (Seright, 1999). Many studies were conducted to understand to the mechanism of gel behavior through fractures. Seright (1995, 1997, 1998, 1999 and 2001) conducted intense studies to examine the in-situ bulk gel behavior through fractures. Zhang and Bai (2011) studied the PPGs propagation through open fractures. Imqam et al., (2014) studied the PPGs extrusion behavior through open conduits during conformance-control treatments. Muhammed et al., (2014) studied the interaction between the surfactant flooding with the PPGs through the facture model. The results revealed that the PPGs can be effective in treating the fractures and the fractures-like channels in the mature reservoirs.

This chapter presents the experimental studies that were performed to understand the PPGs propagation through the open fracture screen plate model. The open fracture plate model was used to mimic the fractures and the fractures-like channels that exist in the mature reservoirs. Injecting the PPGs through the open fracture screen plates can facilitate in determining the major parameters that can be utilized to yield an efficient gel treatments through fractures for a better conformance control treatments.

4.3 OPEN FRACTURE PLATES

Figure 4-2 shows the three different stainless steel open fracture plates of various widths that were used in this study. The fractures were designed to be in the center of the

plates to be easily fit in the experimental model. The open fracture plates have a total diameter of 63.5 mm and a thickness and a total length of 7.5 and 66 mm, respectively. The equivalent permeability of each open fracture plate was calculated using Eq. 6, where k is the permeability in (md) and b is the fracture width in (inches).

$$k = 5.4476 \times 10^{10}\, b^2 \tag{6}$$

This equation can be used to estimate the permeability of open, smooth-walled fractures, with parallel faces, where the permeability is dependent on the fracture width. (Witherspoon et al, 1980). Table 4-1 summarizes the dimensions of the open fracture plates and the equivalent permeability calculations. The high values of the equivalent permeability calculations are due to the fact that the fractures have a significant effect on fluid flow through fractures since they are isolated.

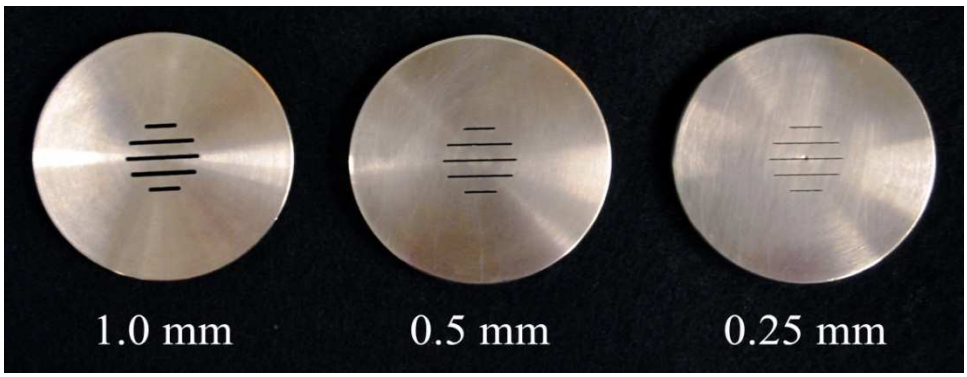

Figure 4-2. The open fracture plate of various fracture widths.

Table 4-1. The dimensions of the open fracture plate and the equivalent permeability calculations.

Fracture width (mm)	Thickness (mm)	Total fracture length (mm)	Diameter (mm)	Permeability (Darcy)
0.25	7.8	66	63.5	5277
0.50	7.8	66	63.5	21109
1.0	7.8	66	63.5	84438

4.4 EXPERIMENTAL SETUP AND PROCEDURE

4.4.1 Experimental Setup. The same screening apparatus Figure 3-16 has been used in this study to evaluate PPGs extrusion through the open fracture plates. The plate of different fracture widths were placed between the swollen PPGs particles and the bottom of the accumulator. The threshold pressure and the PPGs injection pressure were measured through the pressure gauge that was mounted in the lower part of the accumulator.

4.4.2 Experimental Procedure. The following experimental procedure was performed:

- Initially, 10 to 20 g of dry PPGs with a mesh size of (18/20) were added to the desired brine solution, where the mixture left for 24 hours to allow the PPGs to be fully swollen.
- Then, 500 ml of fully swollen gel particles from which excess water has been blotted were put in the accumulator and the open fracture plate was attached to it.
- Gas between the piston and the top cap was released, and the gap was filled with distilled water to avoid a two phase medium.

- The ISCO pump was initially run at constant pressure starting at 10 psi and then the pressure increased gradually to get the threshold pressure.
- Then the pump was run using constant flow rates (1.0, 2.0 3.0, 4.0 and 5.0 ml/min) and the stabilized pressure was recorded for each flow rate.

4.5 RESULTS AND DISCUSSIONS

4.5.1 PPGs Threshold Pressure Measurements. The threshold pressure can be defined as the minimum pressure that is required for the PPGs to be extruded through the open fracture plate. The threshold pressure was measured in the experiment by applying a constant pressure of 10 psi, which is the minimum pressure that can be obtained from the ISCO pump, and then the pressure increased gradually until the PPG was observed in the effluent.

Figure 4-3a through c show the effect of brine concentration and the fracture width on the threshold pressure. The results indicate that for a certain brine concentration, the threshold pressure increased as the width of the fracture plate decreased. For example, the threshold pressure for 1.0 wt. % PPG through 1.0, 0.50 and 0.25 mm fractures were 9.7, 5.2 and 0.68 psi, respectively. Moreover, it is evident form the figure that for a certain fracture width, increasing the brine concentration will result in an increase in the threshold pressure. For instance, at 0.25 mm fracture, the threshold pressure for DI water and 0.25, 1.0 and 5.0 wt. % PPGs were 10.9, 9.7, 8.3 and 7.9 psi, respectively. However, the effect of brine concentration is less prominent compared to the fracture size, and that is due to the high fluid conductivity within the fractures.

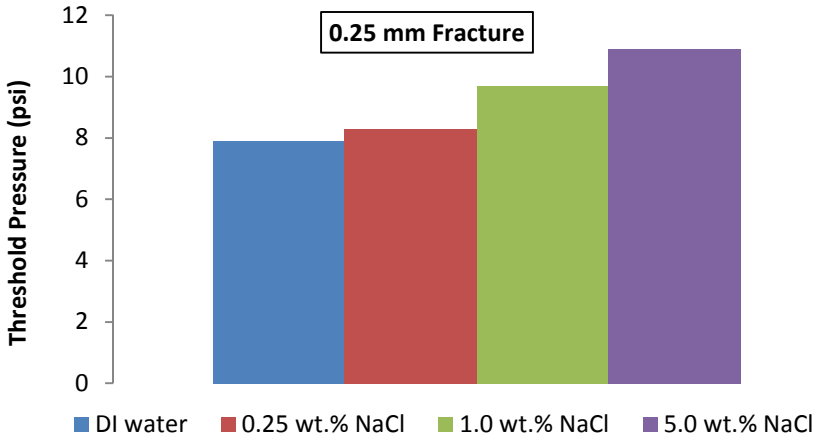

(a)

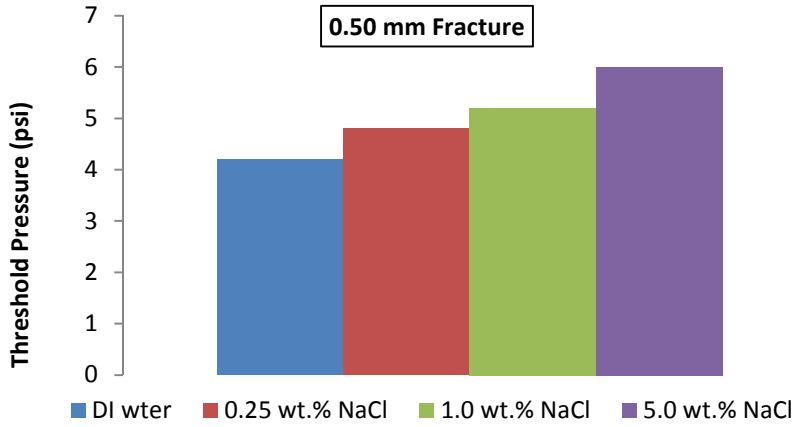

(b)

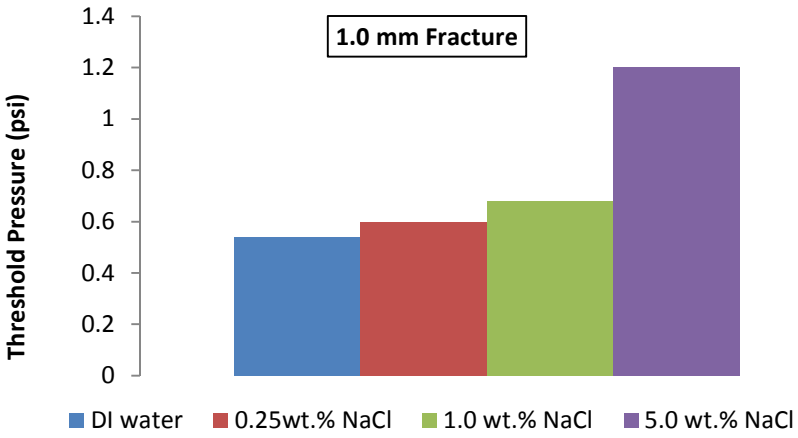

(c)

Figure 4-3. The effect of brine concentration and fracture width on PPGs threshold pressure.

4.5.2 PPGs Injection Pressure Trend. After obtaining the threshold pressure, the experiments were run using constant flow rate that was supplied from the ISCO Pump. Erratic PPGs injection pressure response that was fluctuating in a certain range was noticed. Figure 4-4 and Figure 4-5 show two examples of the PPGs injection pressure response that was occurred during the PPGs injection. It is obvious that there is a fluctuation trend in the injection pressure regardless the fracture width and the brine concentration of the swollen PPG that was used, respectively. To understand the reason for why such a response occurs, the possible causes in the experiment that might lead to such detrended response in the pressure were examined. It was found out that there are two possible reasons that account for such a response. It is either the orientation of the fracture plate or the heterogeneity of the swollen PPGs particles. Since the fractures plate was designed and manufactured upon standards, the scope of investigations directed to the second possible factor which is the heterogeneity of the swollen PPGs particles.

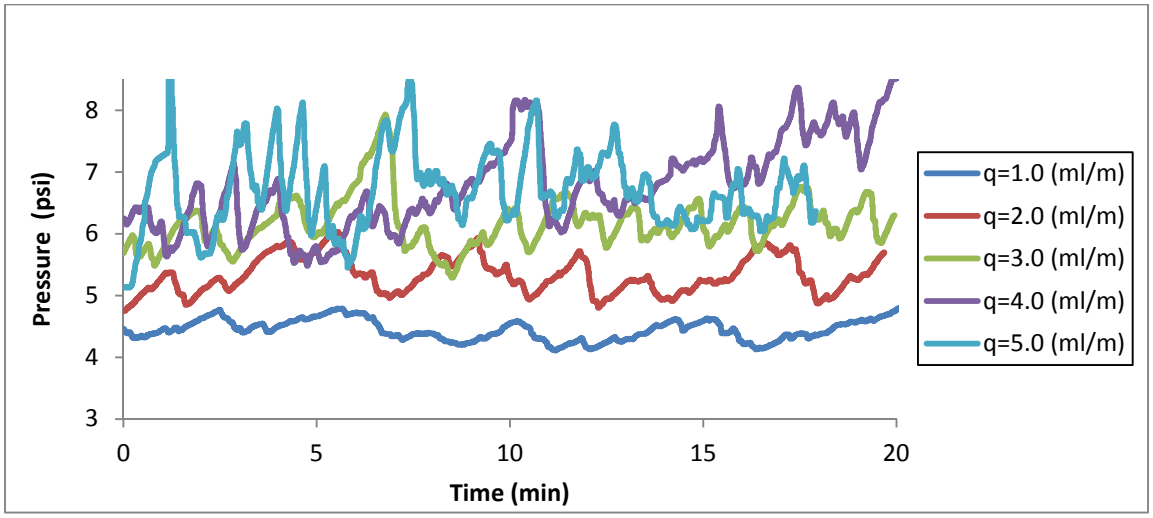

Figure 4-4. DI PPG injection pressure through 0.50 mm fracture as a function of time and flow rate.

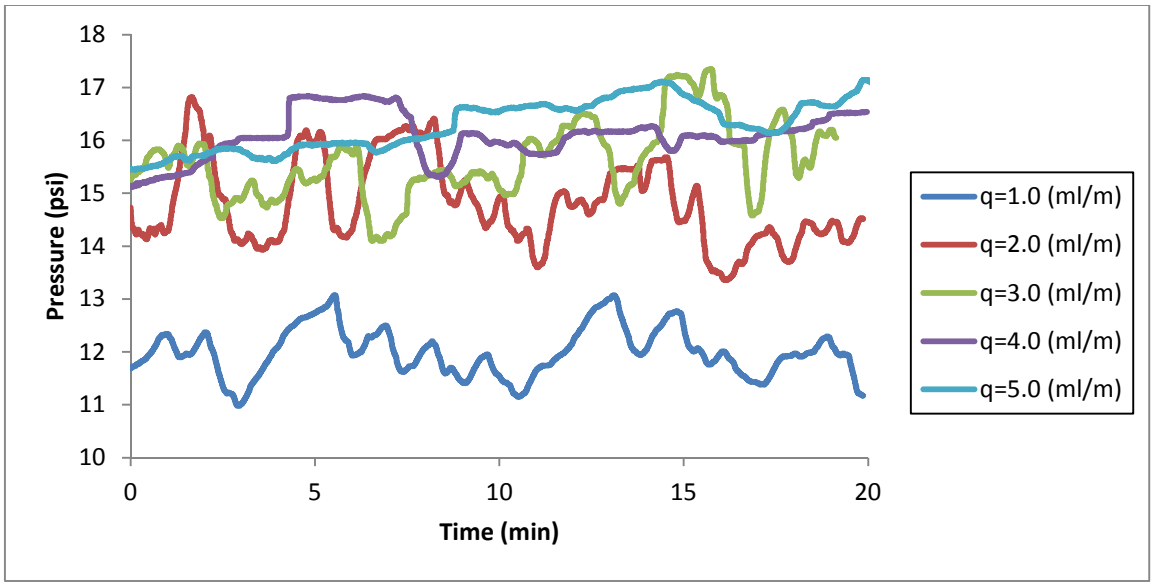

Figure 4-5. 5.0 wt. % NaCl PPG injection pressure through 0.25 mm fracture as a function of time and flow rate.

4.5.2.1 Injecting uniform sphere gel particles. Sphere gel particles of uniform swollen size were injected through the open fracture screen plates to examine how the injection pressure respond to the injection of homogenous swollen gel particles. Similar to the PPGs, these sphere particles have the tendency to absorb a large amount of water when they get interacted with the different brine concentrations forming a three-dimensional structure of uniform gel. Figure 4-6a and b shows the swelling ratio and the uniform sphere gel particles that were swollen in different brine concentration. It is evident that the particles will be uniform after they get fully swollen. The swollen sphere particles were then injected in the model using 0.50 mm fracture width and two medium of brine concentrations of DI water and 5.0 wt. % NaCl. Unlike the 40-K PPG, stabilized injection pressure was observed as it is seen Figures 4.6 and 4.7 during the injection, indicating that the heterogeneity of the PPGs particles caused the fluctuations in the

pressure response. However, the sphere particles might look strong and quiet elastic, but these particles were totally smashed and broken into fine pieces as they were extruded from the fracture due to their lack of strength and deformability.

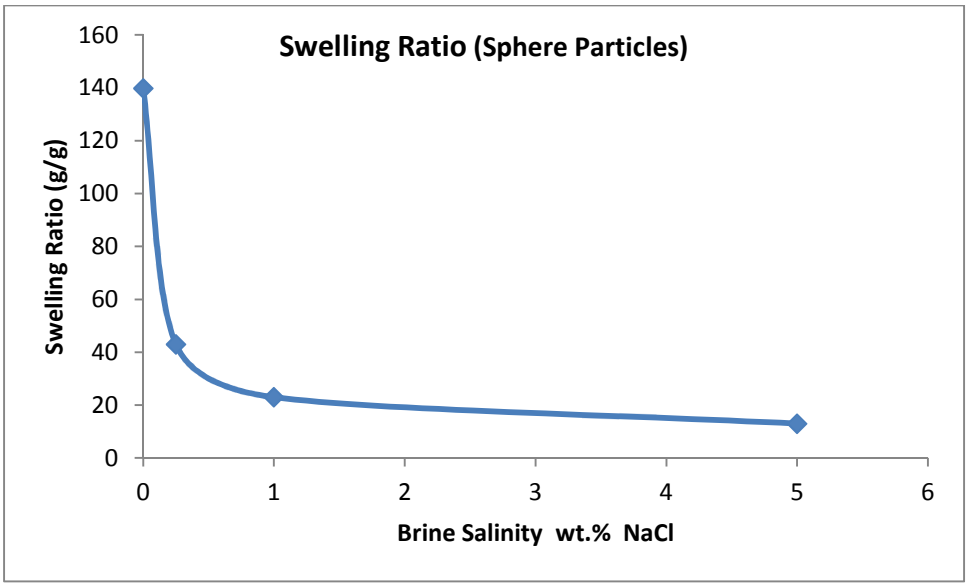

(a)

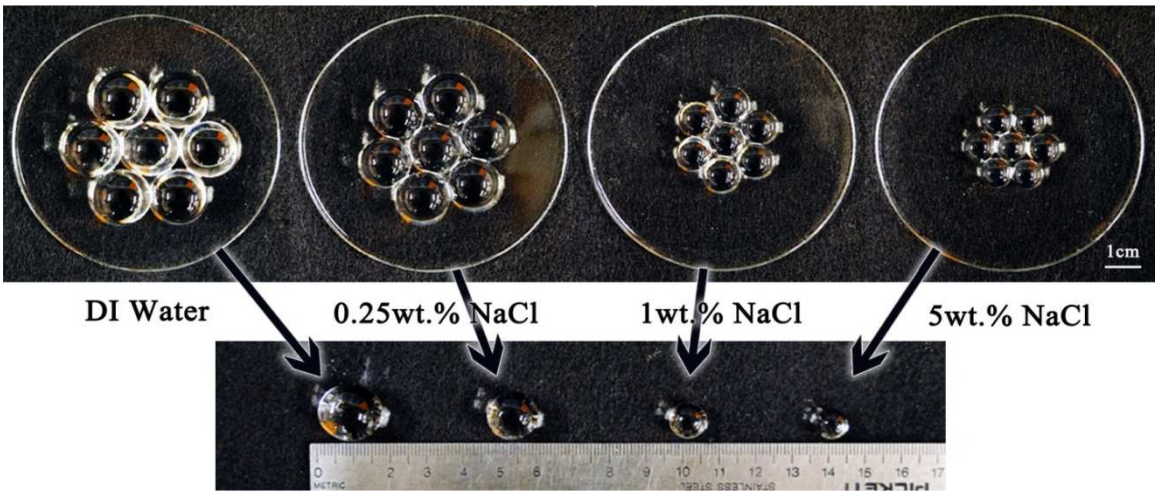

(b)

Figure 4-6. Uniform sphere gel particles (a) the swelling ratio (b) the shape of the particles in different brine concentration.

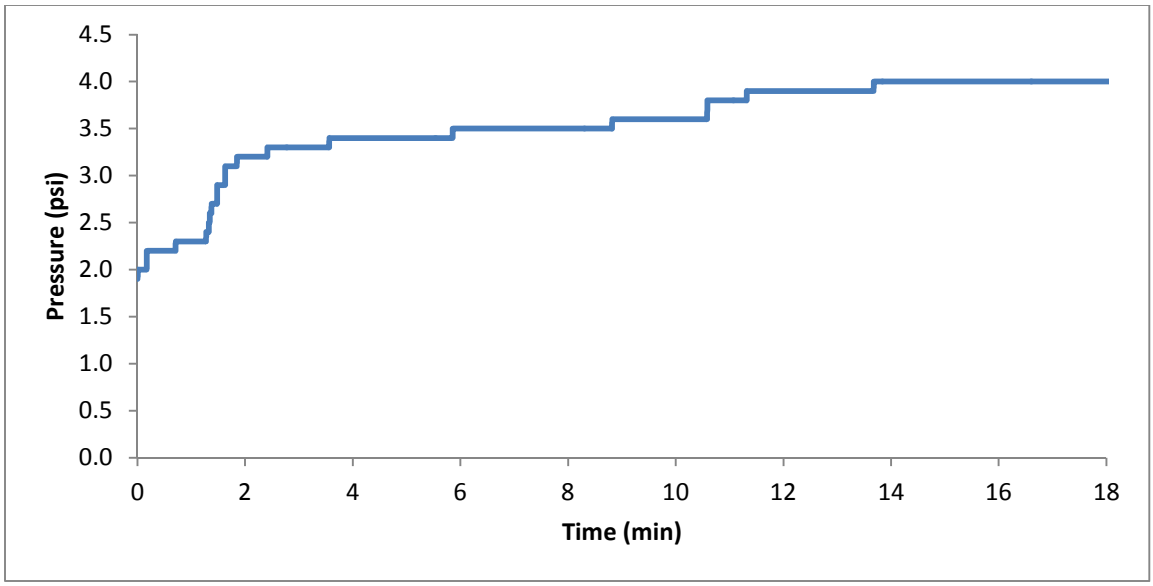

Figure 4-7. Uniform sphere gel particles injection pressure DI water.

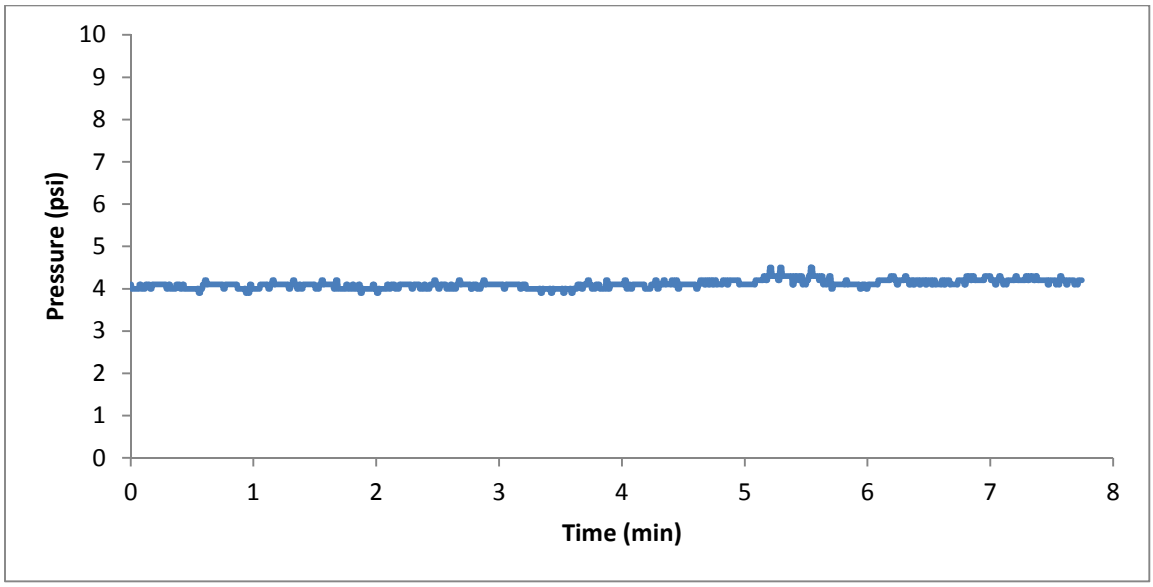

Figure 4-8. Uniform sphere gel particles injection pressure 5.0 wt. % NaCl.

4.5.2.2 Interpretation of the injection pressure in terms of PPGs heterogeneity. The experiment was run using constant flow rate. At the beginning**,** the pressure will start to build up causing the piston to move. As the piston moves, the gel particles will be accumulated and adhering to each other on the surface of the fracture leading to a further increase in the injecting pressure. Later, the gel particles will start to deform or break depending on the injection pressure and the fracture width and then the gel particles will be extruded through the open fracture yielding a sudden decrease in the injecting pressure response. Such phenomenon was repeated throughout the injection time. Generally, the deformations of the gel particles depend on the elasticity of the particles. Larger gel particles or fully swollen particles are weaker, which makes them more deformable and to be easily extruded through the open fracture.

4.5.2.3 Developing a criterion to obtain the PPGs injection pressure. After confirming that the heterogeneity of the PPGs tends to cause some fluctuation in the pressure response, a criterion was developed to diminish the errors that might be encountered in the study of examining the transportation of the PPGs injection pressure through various open fracture plates. The criterion can be summarized as the following:

- A large sample was prepared for each PPG that was swollen in a certain brine concentration.
- For each swollen PPGs and a certain fracture width, for example 5.0 wt. % NaCl through 0.50 mm fracture, three sets of injection experiments were conducted.
- As mentioned previously, inconsistent pressure response was perceived during the constant flow rate injection; therefore, sufficient test duration of 20 minutes was

allowed for each constant flow rate to acquire long-term data in order to reduce uncertainty in the pressure data interpretation.

- The average injection pressure was taken for each of three runs and the total average of all the runs was obtained after confirming that there is no significant variance change in the values.
- After the acquisition of the pressure data, SAS software was used to generate boxplots. The boxplots can assist in determining the range of the pressure response for each constant flow rate. As stated above, for each set up of brine concentration and fracture width, three PPG injections experiments were conducted and consequently three box plots were attained. Figures 4-9 through 4-20 present the boxplots that were generated using SAS software. For a certain brine concentration and fracture width, there is an effect in the mean data of the injection pressure with respect to changing the injection flow rate. Therefore, the mean values of the injection pressure data were considered to examine the various effects that were mentioned above.

Therefore, for the rest of this chapter, PPGs injection pressure is referred to an average pressure of a total of three sets of experiments that were performed using either the same flow rate or the same brine concentration.

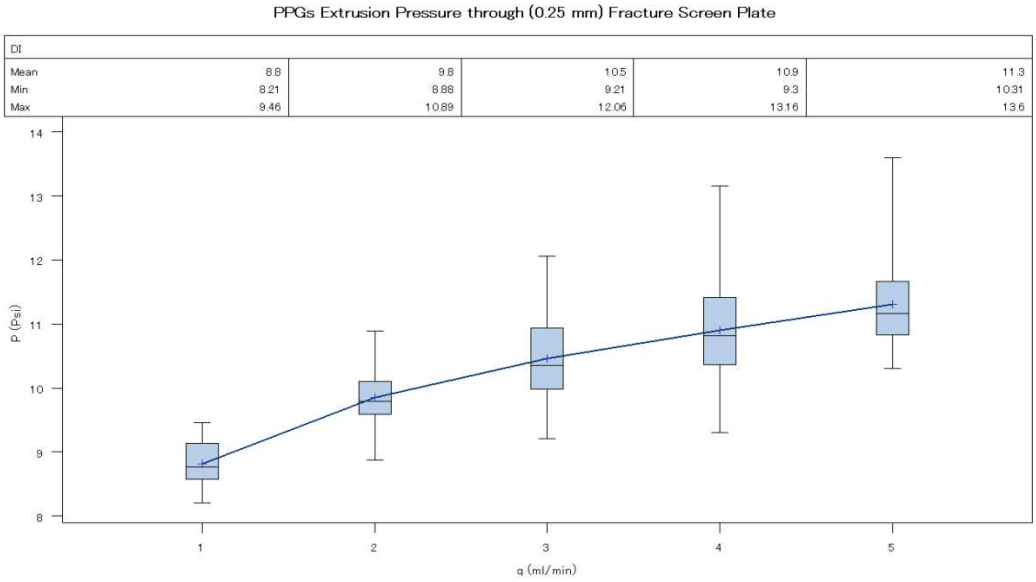

Figure 4-9. Boxplot of DI water PPG extrusion pressure through 0.25 mm fracture.

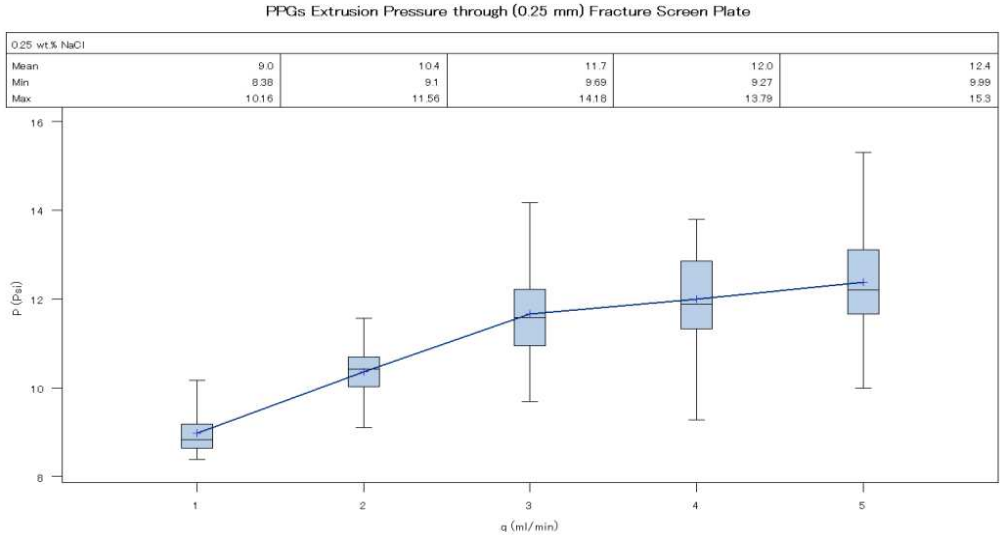

Figure 4-10. Boxplot of 0.25 wt. % NaCl PPG extrusion pressure through 0.25 mm fracture.

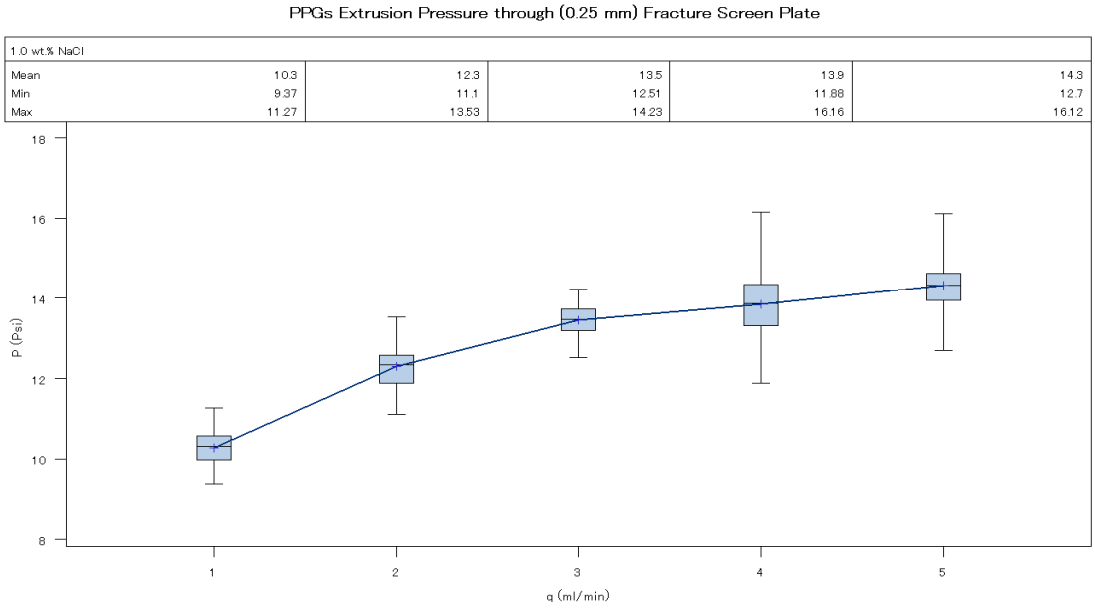

Figure 4-11. Boxplot of 1.0 wt. % NaCl PPG extrusion pressure through 0.25 mm fracture.

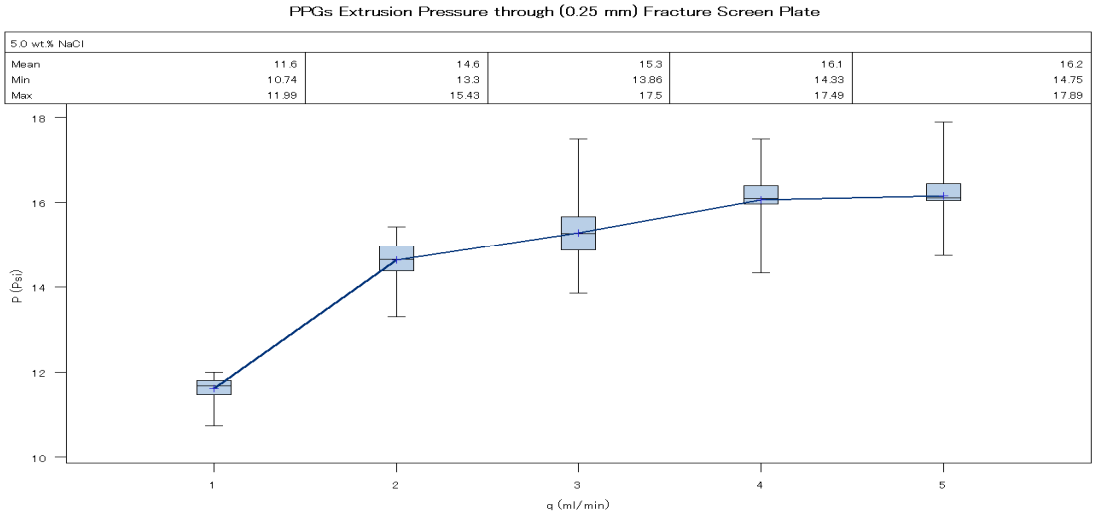

Figure 4-12. Boxplot of 5.0 wt. % NaCl PPG extrusion pressure through 0.25 mm fracture.

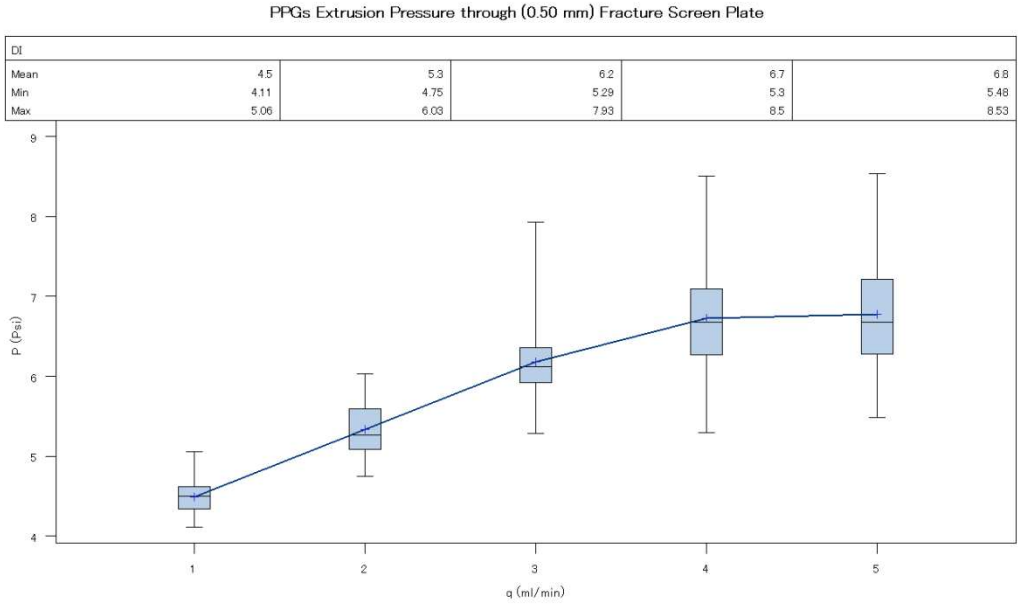

Figure 4-13. Boxplot of DI Water PPG extrusion pressure through 0.5 mm fracture.

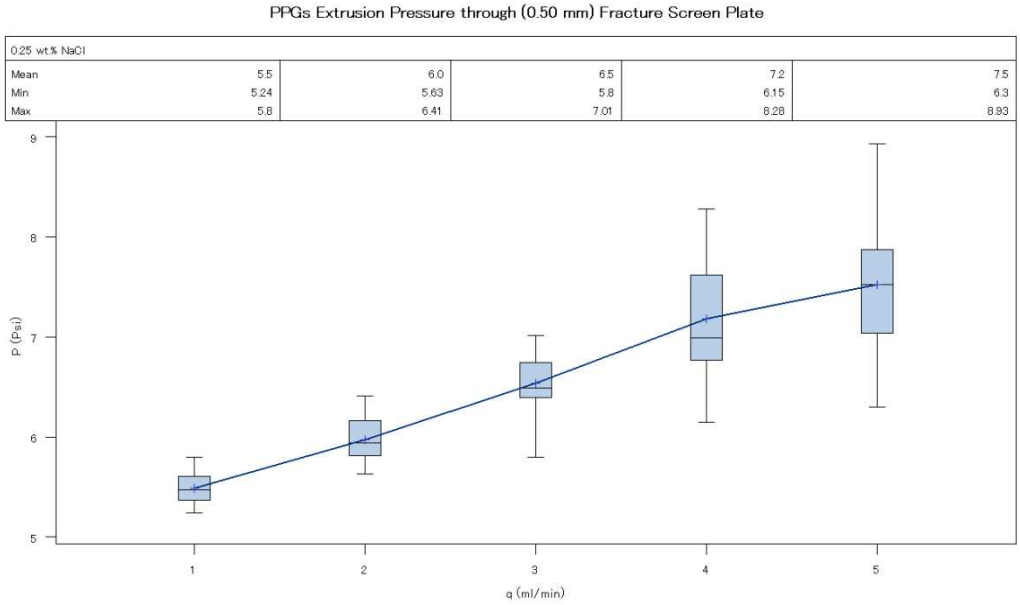

Figure 4-14. Boxplot of 0.25 wt. % NaCl PPG extrusion pressure through 0.5 mm fracture.

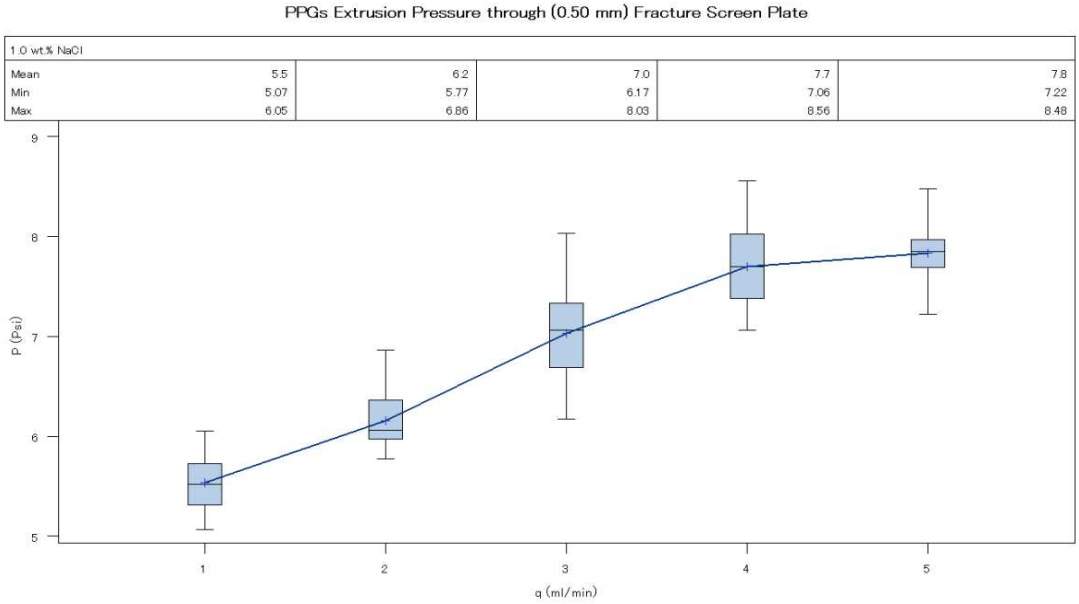

Figure 4-15. Boxplot of 1.0 wt. % NaCl PPG extrusion pressure through 0.5 mm fracture.

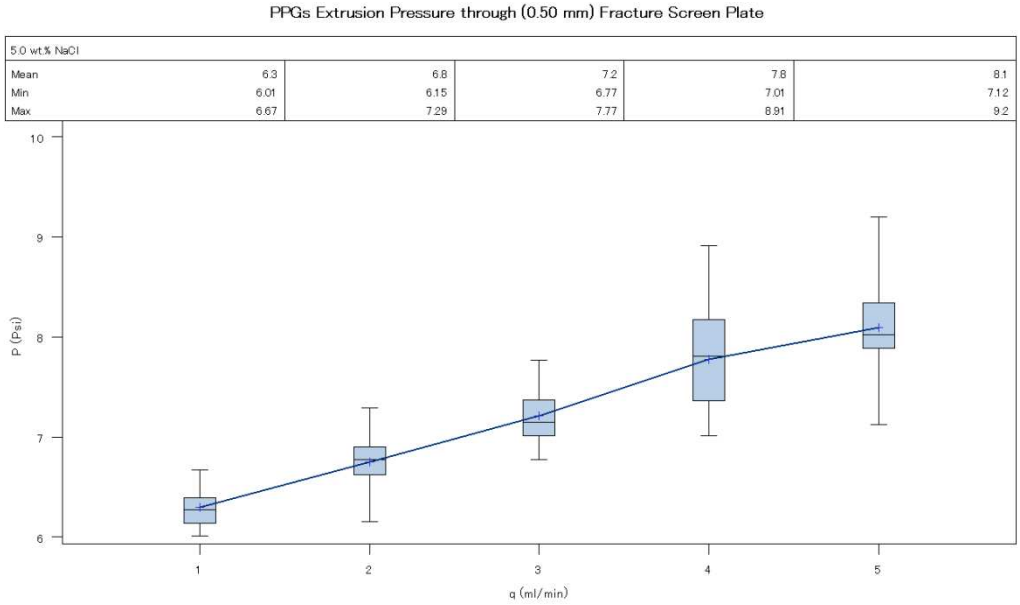

Figure 4-16. Boxplot of 5.0 wt. % NaCl PPG extrusion pressure through 0.5 mm fracture.

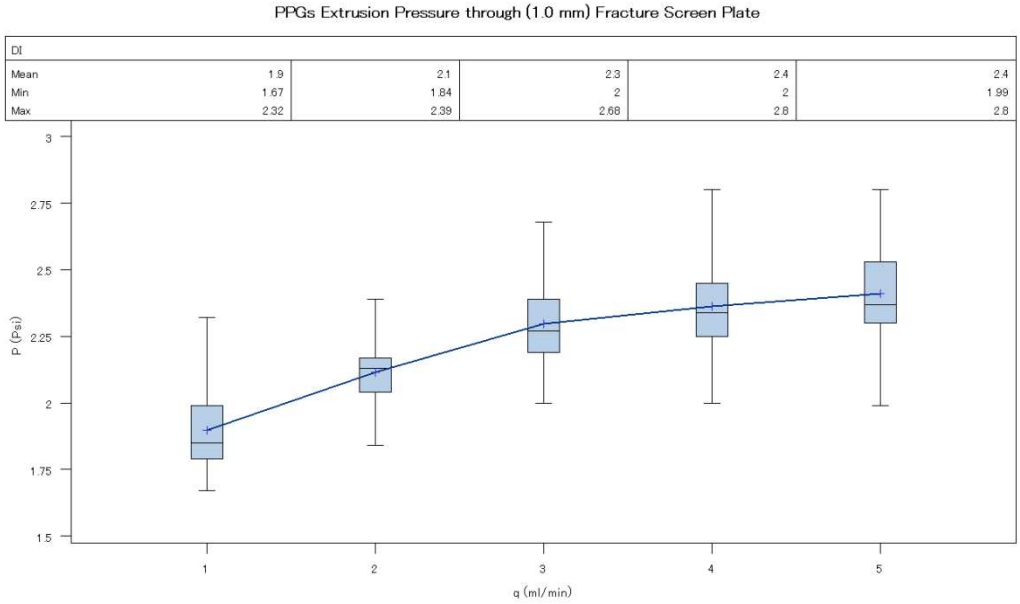

Figure 4-17. Boxplot of DI Water PPG extrusion pressure through 1.0 mm fracture.

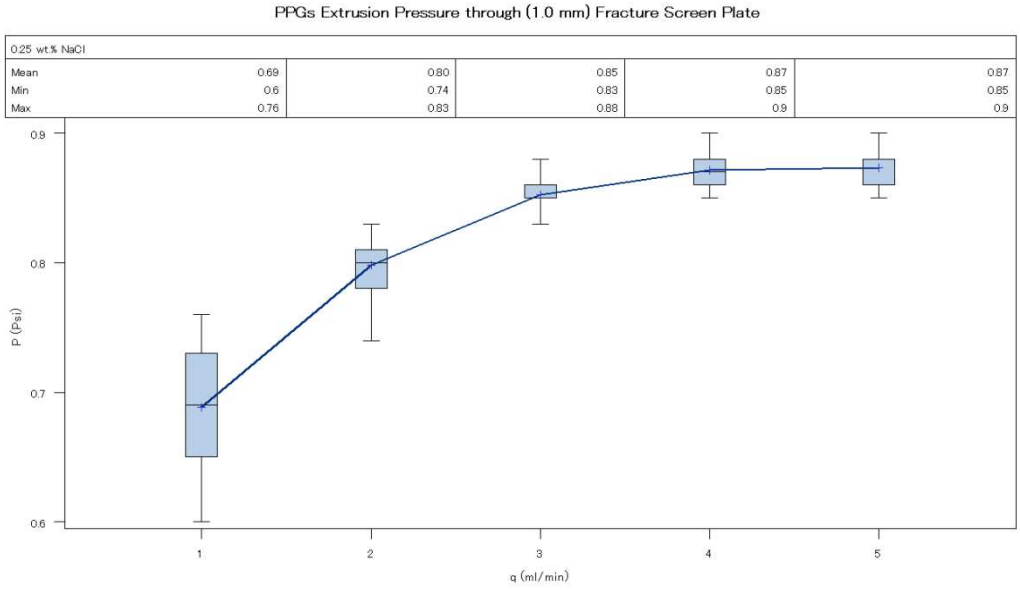

Figure 4-18. Boxplot of 0.25 wt. % NaCl PPG extrusion pressure through 1.0 mm fracture.

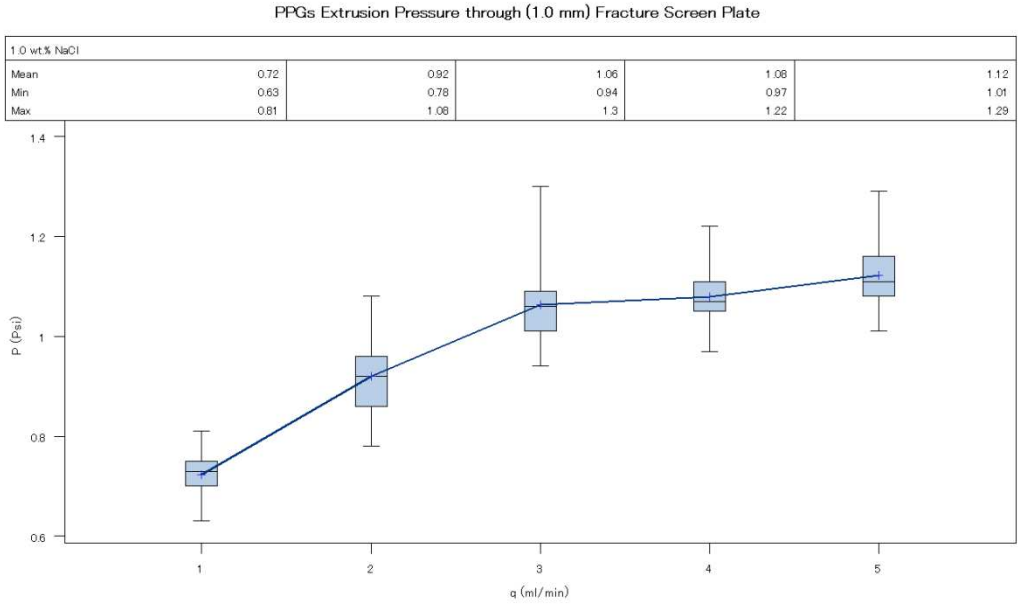

Figure 4-19. Boxplot of 1.0 wt. % NaCl PPG extrusion pressure through 1.0 mm fracture.

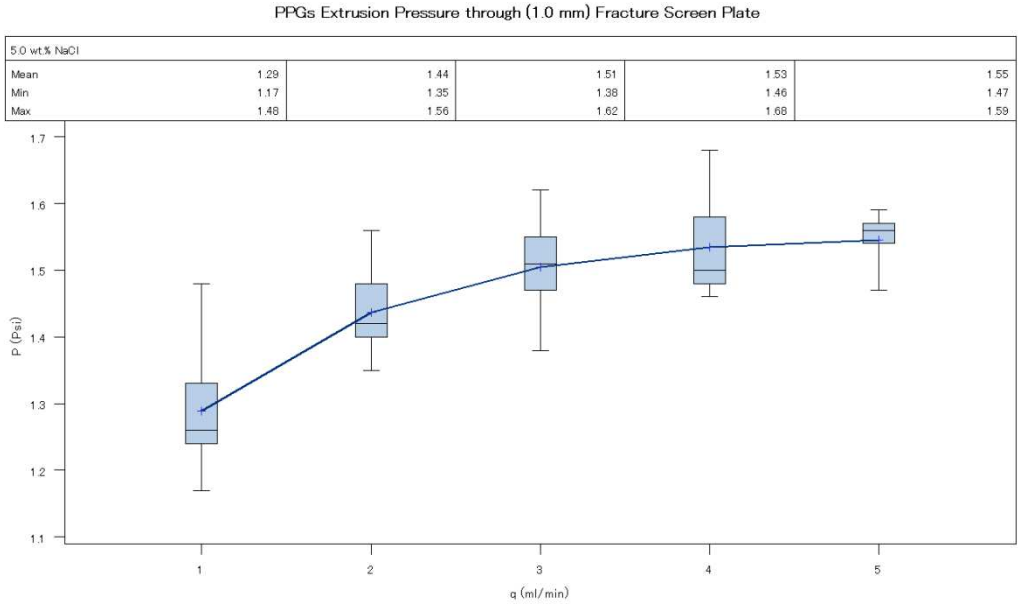

Figure 4-20. Boxplot of 5.0 wt. % NaCl PPG extrusion pressure through 1.0 mm fracture.

4.5.3 Effect of Injection Flow Rate on PPGs Injection Pressure. After obtaining the threshold pressure for each set of brine concentration and width of the open fracture plate, five different constant injection flow rates were used to examine the effect of changing the flow rate on the PPGs injection pressure. Figures 4-21 through 4-23 show the effect of changing the flow rate on the PPGs injection pressure. From the figures, it is evident that increasing the flow rate will yield an increase in the PPGs injection pressure for all the brine concentrations and for all the different open fracture plates. However, the increase is not significant especially at high flow rates. The injection pressure of PPGs will increase slightly at the beginning and then reach a plateau.

For the PPGs that was swollen at 5.0 wt. % NaCl and extruded through 0.25 mm open fracture screen plate, the injection pressure increased from 11.8 to 14.5 psi when the injection flow rate increased from 1.0 to 2.0 ml/m. Then, the injection pressure only increased 0.1 psi when the injection flow rate was increased from 4.0 to 5.0 ml/m. Seright (1999) attributed such a trend to a strong slip effect that is exhibited by the gel where is little or no viscous dissipation of energy occurred within the moving gel plug. Thus, the hydrodynamic lift force that is acting on the particle to transport through the pore will increase with flow rate resulting in an increase in the particles mobilizations (Baghdkian et al, 1989). Moreover, this trend is consistent with the findings from the PPGs injections in the oil fields where it was observed that the injection pressure of the PPGs did not increase significantly in accordance with the increase in the injection pumping rate (Bai et al, 2007a).

4.5.4 Effect of Brine Concentration on PPGs Injection Pressure. The dry gel particles were swollen in four different brine concentrations (0, 0.25, 1.0 and 5.0 wt. % NaCl) to obtain fully swollen PPGs that vary in their strength and swelling ratio. Then, the swollen PPGs were loaded in the model to examine how the brine concentration can impact the injection pressure of PPGs through the different open fracture plates. Figures 4-21 through 4-23 show the effect of the brine concentration on the injection pressure of the PPGs. The results reveal that at a constant flow rate, increasing the brine concentration will result in increase in the PPGs injection pressure regardless the size of the fracture.

For instance, at a constant flow rate of 5.0 ml/m for PPG prepared with DI, 0.25, 1.0 and 5.0 wt. % NaCl and extruded through 0.25 mm open fracture screen plate, the injection pressures were 11.4, 12.6, 14.2 and 16.2 psi, respectively. Whereas, at 5.0 ml/m injection flow rate for the same brine concentrations, the PPGs injection pressures increase slightly 6.5 , 6.8, 7.8 and 8.2 psi when the PPGs extruded through 0.50 mm open fracture screen plate. The results clearly show that the PPGs that were swollen at low brine concentrations are softer and more deformable compared to the PPGs that were swollen in high brine concentration.

However, in the case where the PPGs was swollen in DI water and propagated through 1.0 mm open fracture plate, the injection pressure was higher than the rest of different swollen PPGs particles. For example at 5.0 ml/m constant injection flow rate, the PPGs injection pressures for 0.25, 1.0 and 5.0 wt. % NaCl PPGs were 0.87, 1.05 and 1.56 psi, respectively. Whereas, for DI water PPG, the injection pressure was 2.3 psi. This can be explained by the low injection pressures that were observed in general for all

the different swollen gel particles where the pressure only ranged from 0.80 psi to 2.2 psi. The later might indicate that since the DI PPGs are bigger in size and the injection pressure was low, the effect of brine concentration might be insignificant compared to the other open fracture 0.25 and 0.50 mm. More studies need to be conducted to examine the nature of PPGs propagation and extrusion behavior through 1.0 mm open fracture plate.

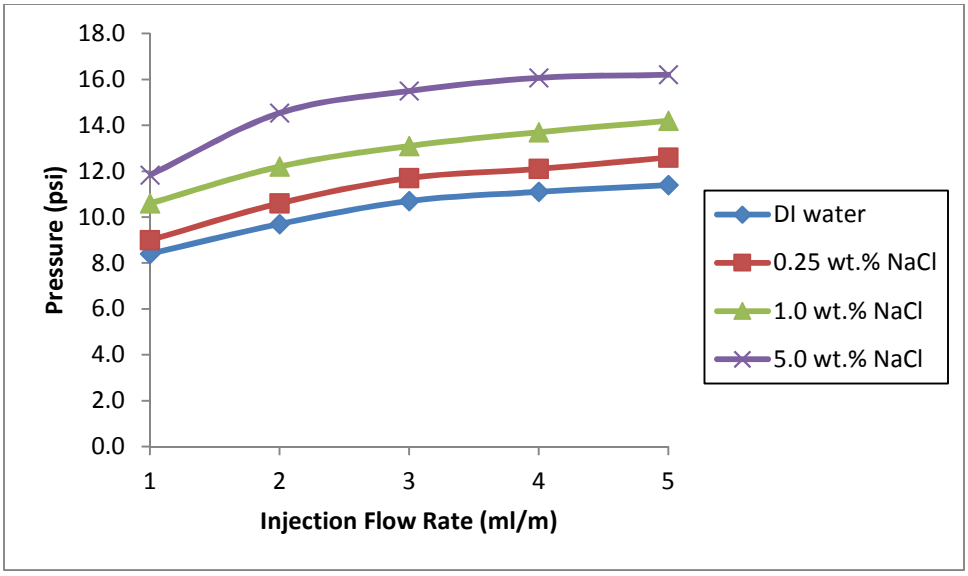

Figure 4-21. PPGs injection pressure through 0.25 mm fracture as a function of injection flow rate and brine concentration.

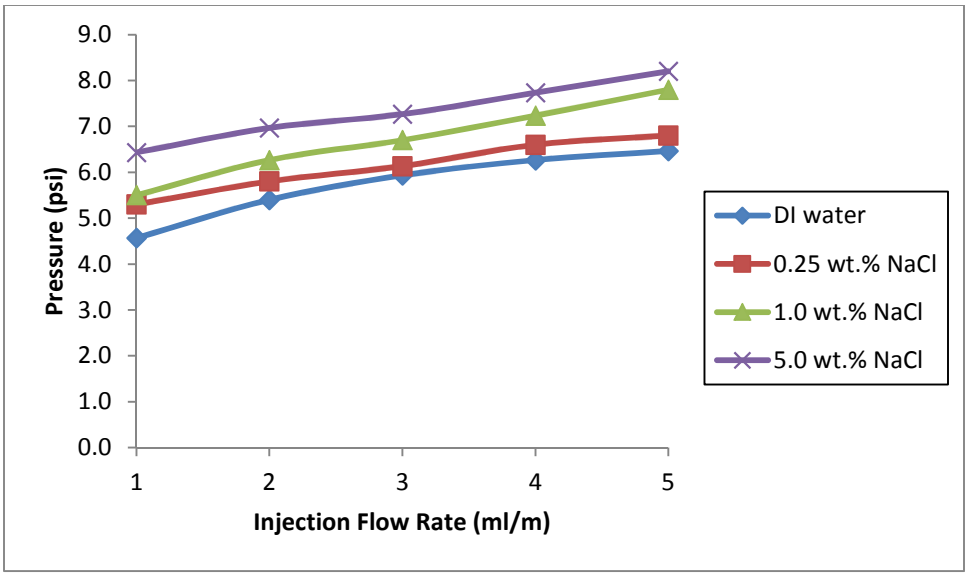

Figure 4-22. PPGs injection pressure through 0.50 mm fracture as a function of injection flow rate and brine concentration.

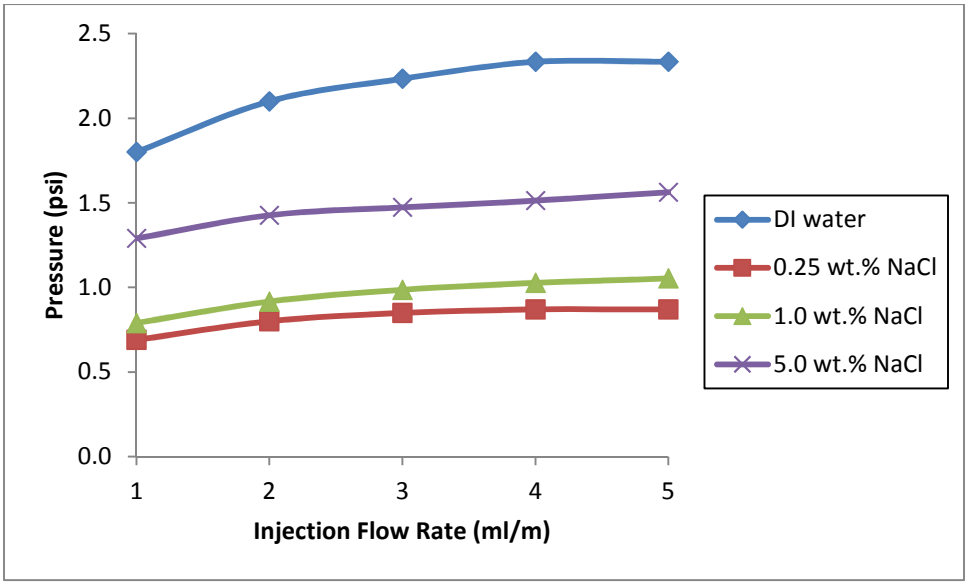

Figure 4-23. PPGs injection pressure through 1.0 mm fracture as a function of injection flow Rate and brine concentration.

4.5.5 Effect of Fracture Width on PPGs Injection Pressure. Three different open fracture plates with widths of 0.25, 0.50 and 1.0 mm were used to investigate how the PPGs injection pressure changes with respect to varying the width of the open fracture plate. Figures 4-24 through 4-26 indicate that for a given flow rate and brine concentration, PPGs injection pressure decreased as the fracture width increased. For example, for the PPG that was swollen in 1.0 wt. % NaCl and at a constant injection flow rate of 1.0 ml/m, the injection pressure was 10.6 psi at 0.25 mm fracture size. However, when the 1.0 wt. % PPGs got extruded through 0.50 mm fracture, the injection pressure was almost reduced to half to be 5.5 psi, and sequentially the injection pressure was pretty low around 0.79 psi when the same composition, at the same flow rate got transported through the largest fracture width which is 1.0 mm. the same trend was observed in the all the different PPGs that was swollen in different brine concentration.

For the PPGs that was prepared with 5.0 wt. % NaCl and at constant injection flow rate of 5.0 ml/m, the PPGs injection pressures were 16.2, 8.2, and 1.56 psi for the open fracture plate with width of 0.25, 0.50 and 1.0 mm, respectively. The results imply that the bigger the size of the open fracture, the more conductive it is and thus less injection pressure is required for the PPGs to be transported. Furthermore, these results indicate that at a certain brine concentration and flow rate, the PPGs injection pressure is inversely proportional to the size of the fracture. This finding is consistent with (Zhang and Bai, 2011) and (Seright, 1988) when they concluded that the gel extrusion pressure is inversely proportional to the open fracture width size.

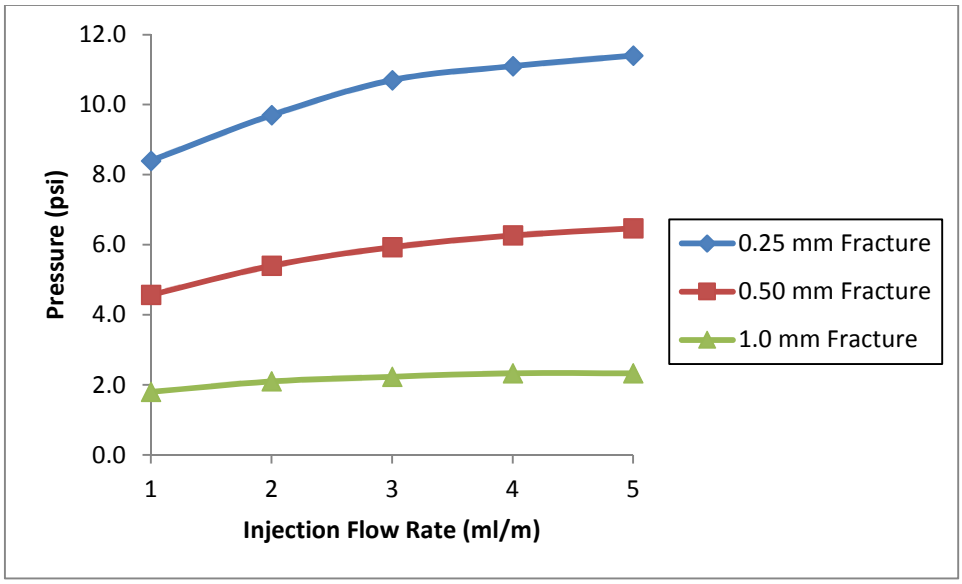

Figure 4-24. DI water PPGs injection pressure through various open fracture plates.

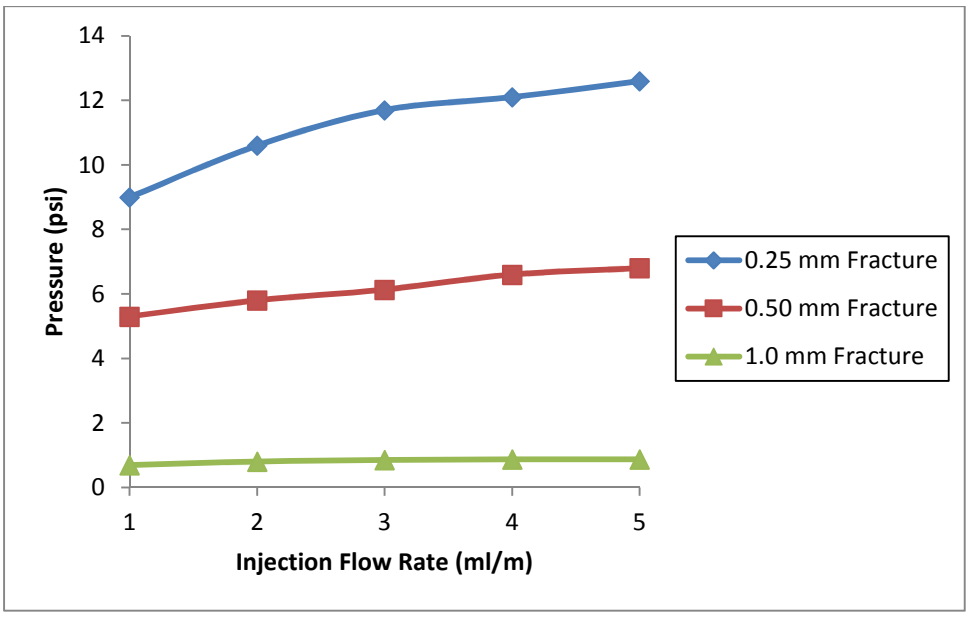

Figure 4-25. 0.25 wt. % PPGs injection pressure through various open fracture plates.

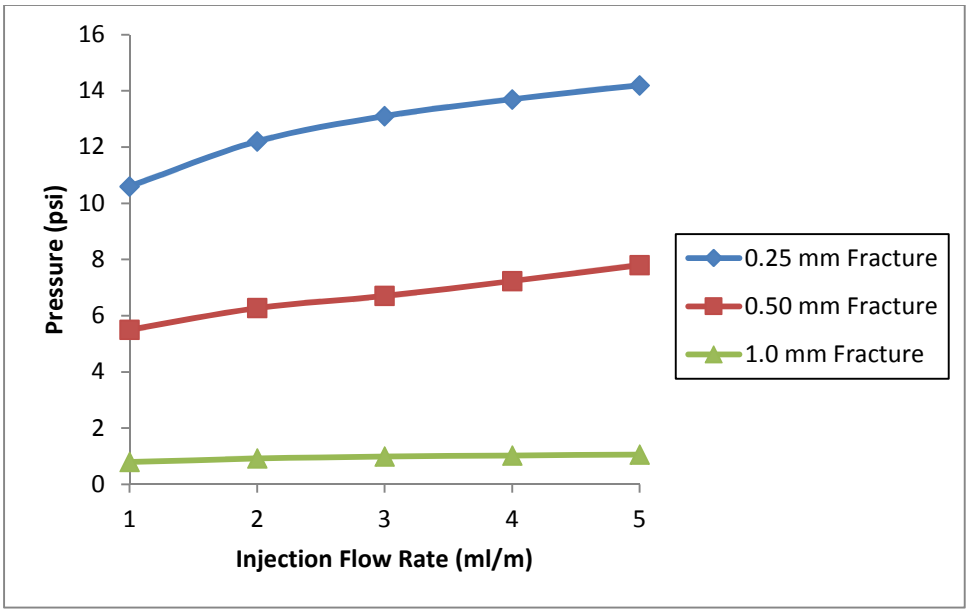

Figure 4-26. 1.0 wt. % PPGs injection pressure through various open fracture plates.

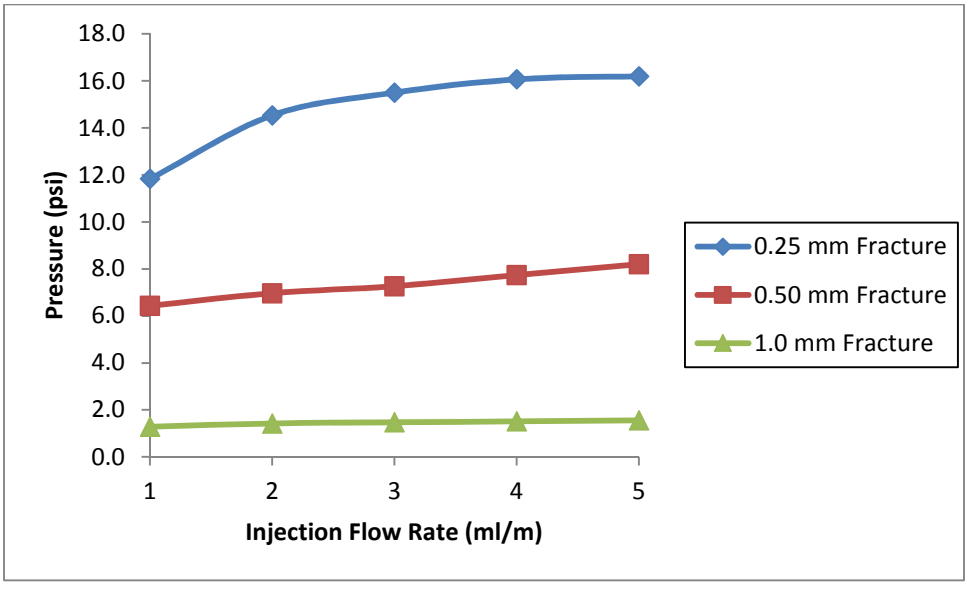

Figure 4-27. 5.0 wt. % PPGs injection pressure through various open fracture plates.

4.5.6 Rheological Model of PPGs through Open Fracture Plate Model. PPGs injection pressure vs. the injection flow rate can be fitted using the power-law model which indicates that the PPGs are shear-thinning materials. Table 4-2 summarizes the fitting equations for the stable injection pressure of the PPGs with respect to the constant injection flow rate for all the brine concentrations and through the different open fracture. The apparent consistency constant and the flow index can be referred to the brine concentration and the fracture width, respectively.

Table 4-2. Fitting equations for PPGs injection pressure as a function of injection flow rate.

Fracture width (mm)	Brine Concentration. (%)	Fitting Equations	R^2
0.25	DI	$P = 8.463q^{0.1948}$	0.9883
	0.25%	$P = 9.0918q^{0.2105}$	0.9891
	1.0%	$P = 10.668q^{0.1816}$	0.9965
	5.0%	$P = 12.189q^{0.1979}$	0.9396
0.50	DI	$P = 4.6046q^{0.2198}$	0.994
	0.25%	$P = 5.2515q^{0.1568}$	0.9845
	1.0%	$P = 5.4428q^{0.2096}$	0.9837
	5.0%	$P = 6.3527q^{0.1444}$	0.9617
1.0	DI	$P = 1.8321q^{0.1672}$	0.962
	0.25%	$P = 0.7048q^{0.1491}$	0.9367
	1.0%	$P = 0.7988q^{0.1807}$	0.988
	5.0%	$P = 1.2989q^{0.1151}$	0.9866

4.5.7 Resistance Factor Calculations for PPGs through Open Fracture Plate.

The resistance factor can be defined as the ratio of PPGs injection pressure drop to the water injection pressure at the same injection flow rate. It can be referred to as the apparent viscosity which describes the macroscopic rheology of the gel in porous media relative to that of water. The water injection pressure could not be measured experimentally due to the fact that the PPGs were injected through open fractures plates. Therefore, the following equation was used to calculate the water injection pressure drop through the fracture screen plate as it is described by Buckingham's equation for flow through slots of fine clearance (Engler, 2010).

$$\Delta P_w = \frac{(12)(14.7)}{9.86\times10^9}\frac{q_f\ l_f \mu}{(n_f A)h_f {w_f}^3} \tag{7}$$

Where**:**

ΔP_w is the water pressure drop across the fracture screen plate in (psi)

q_f is the injection flow rate in (cc/s)

l_f is the total fracture length in (cm)

μ is the water viscosity in (cp)

n_f is the number of fractures per unit area

A is the cross sectional area of the fracture screen plate in (cm^2)

h_f is the fracture height in (cm)

w_f is the width of the fracture in (cm)

4.5.7.1 Effect of injection flow rate on resistance factor. Figures 4-28 through 4-30 plot the resistance factor against the injection flow rate in log-log scale. It is clear that the resistance factor decreases with the increase in the injection flow rate. Thus, the relationship demonstrates that the apparent viscosity of PPGs decreases with an increase in the injection flow rate. This behavior occurs due to the elasticity nature of PPGs which exhibits a shear-thinning fluid during their transportation through the open fractures in porous media. The relationship between the resistance factor and the flow rate can be fitted with a high accuracy using the power-law equation in the following format:

$$Fr = Kq^n \tag{8}$$

Where F_r is the resistance factor, q is the flow rate in ml/m, and K and n are constant coefficients. Table 4-3 lists the fitting equations and their correlations coefficients.

4.5.7.2 Effect of brine concentration on resistance factor. Figures 4-28 through 4-30 indicate that the resistance factor for PPGs transportation through the open fracture screen plate increases with the increase in the brine concentration. The relationship indicates that for the PPGs that were swollen in high brine concentration have a higher apparent viscosity to the PPGs that were swollen in a low brine concentration.

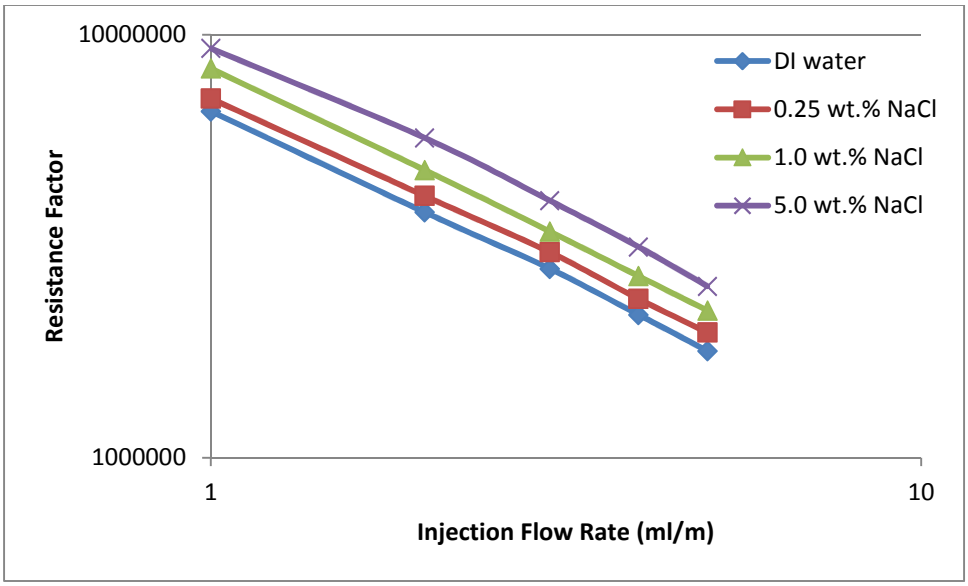

Figure 4-28. Resistance factor through 0.25 mm fracture as a function of injection flow rate and brine concentration.

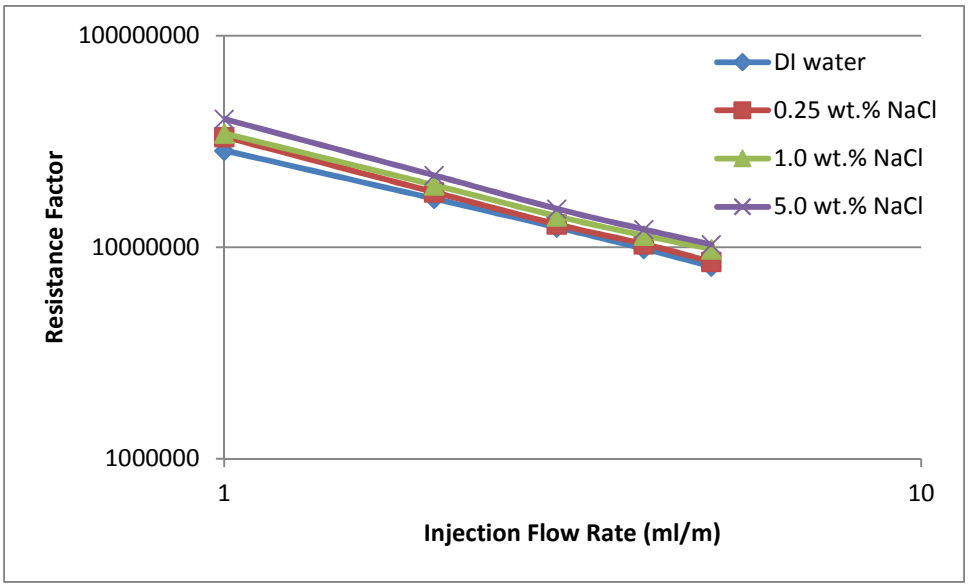

Figure 4-29. Resistance factor through 0.50 mm fracture as a function of injection flow rate and brine concentration.

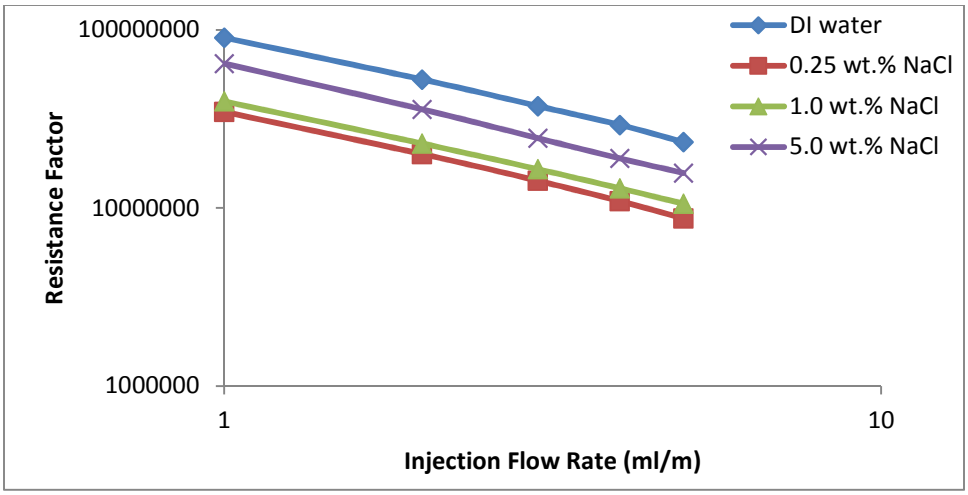

Figure 4-30. Resistance factor through 1.0 mm fracture as a function of injection flow rate and brine concentration.

4.5.7.3 Fracture width effect on resistance factor. It can be seen from Figures 4-31 through 4-34 that the resistance factor of PPGs increases with the increase in the fracture width. This trend is consistent with the behavior of bulk gel in fractures and porous media (Seright 2001) and the transportation of PPGs through open fracture model (Zhang and Bai, 2011) and PPGs extrusion through open conduits (Imqam et al., 2014). The results might be in contradiction with the common assumption that the narrower the fracture the more resistance force will be exerted on PPGs to pass through the fracture. However, since the resistance factor is defined as the PPGs pressure drop to that pressure drop of water in the same fracture that implies that water pressure drop decreases significantly with the increase in the fracture width, such a decrease in the water pressure drop will be leading to a high resistance factor. Moreover, from the results it can be conclude that the apparent viscosity of PPGs increase with the increase in the fracture width.

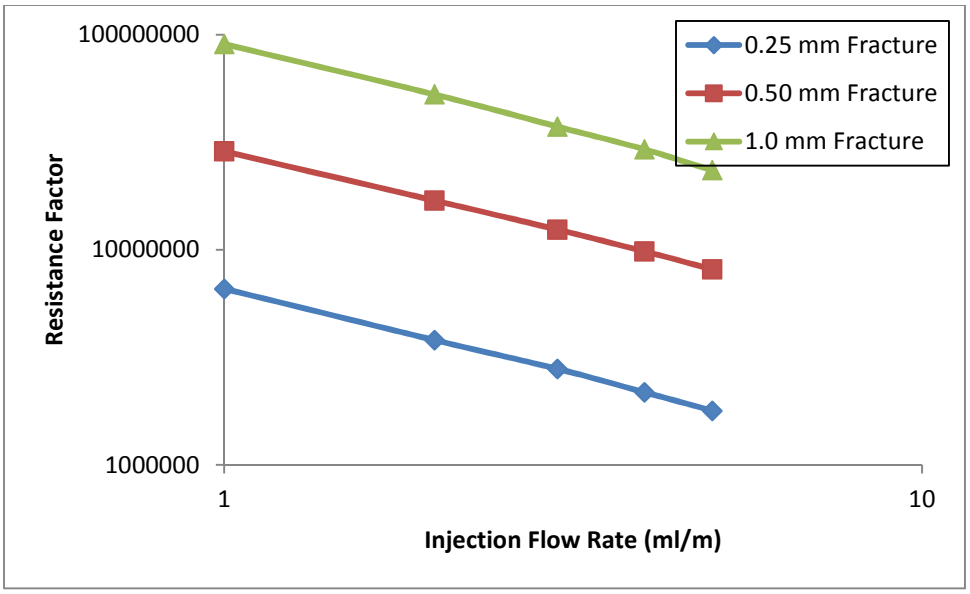

Figure 4-31. DI water PPGs resistance factor through various open fracture plate model.

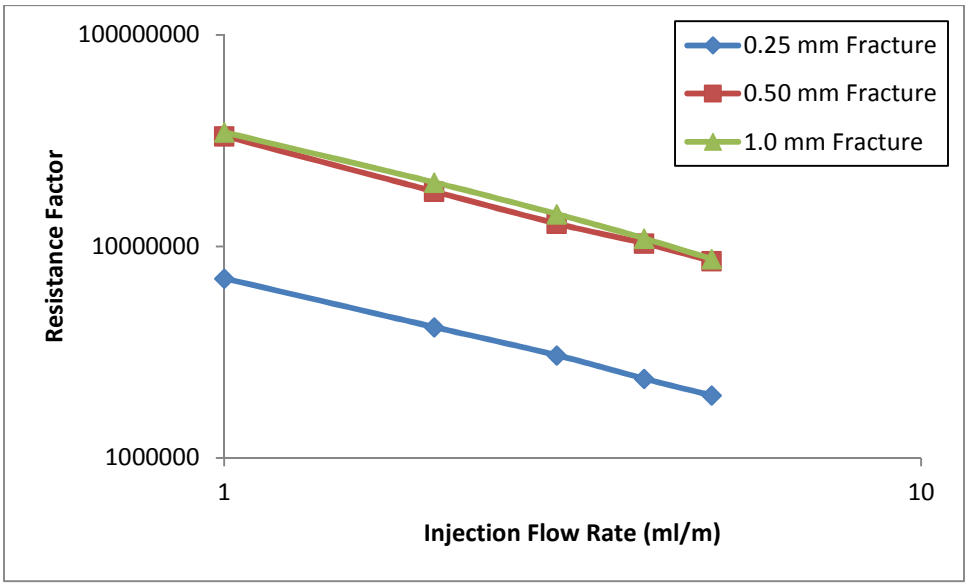

Figure 4-32. 0.25 wt. % PPGs resistance factor through various open fracture plate model.

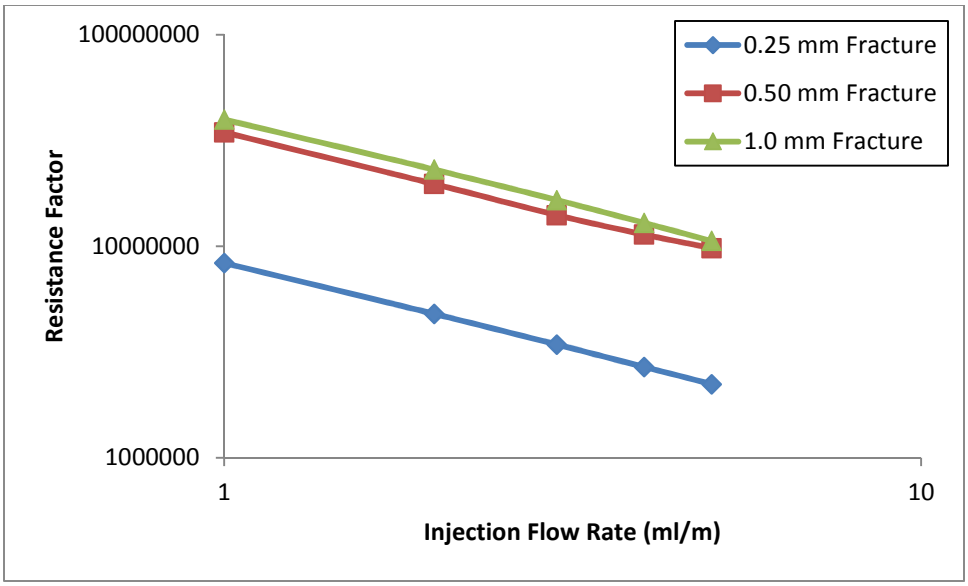

Figure 4-33. 1.0 wt. % PPGs resistance factor through various open fracture plate model.

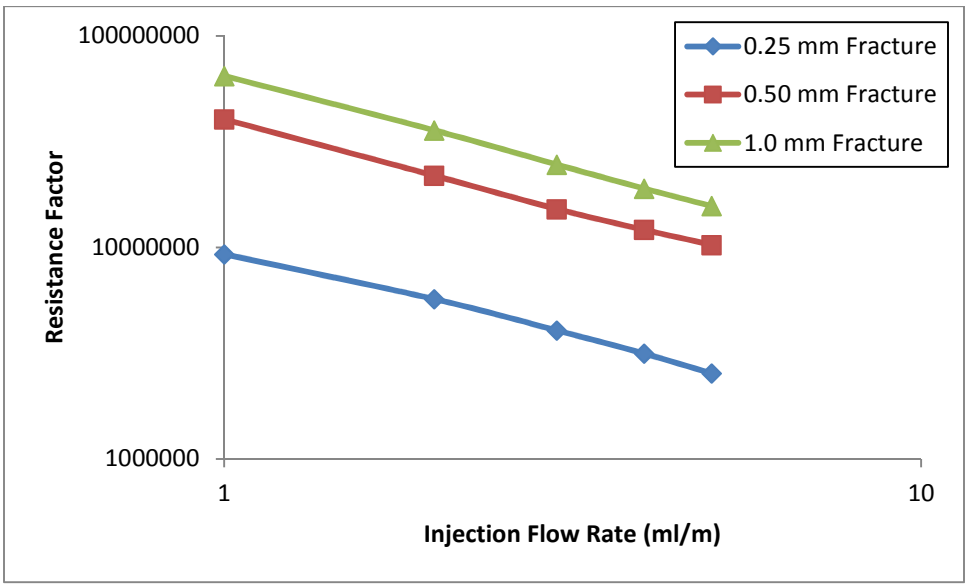

Figure 4-34. 5.0 wt. % PPGs resistance factor through various open fracture plate model.

Table 4-3. Fitting equations for resistance factor.

Fracture width (mm)	Brine Concentration. (%)	Fitting Equations	R^2
0.25	DI	$F_r = 6.64E+06q^{-0.805}$	0.9993
	0.25%	$F_r = 7.13E+06q^{-0.79}$	0.9992
	1.0%	$F_r = 8.37E+06q^{-0.818}$	0.9998
	5.0%	$F_r = 9.56E+06q^{-0.802}$	0.9961
0.50	DI	$F_r = 2.89E+07q^{-0.78}$	0.9995
	0.25%	$F_r = 3.30E+07q^{-0.843}$	0.9995
	1.0%	$F_r = 3.42E+07q^{-0.79}$	0.9988
	5.0%	$F_r = 3.99E+07q^{-0.856}$	0.9989
1.0	DI	$F_r = 9.20E+07q^{-0.833}$	0.9984
	0.25%	$F_r = 3.54E+07q^{-0.851}$	0.9979
	1.0%	$F_r = 4.01E+07q^{-0.819}$	0.9994
	5.0%	$F_r = 6.52E+07q^{-0.885}$	0.9998

4.5.8 PPGs Injectivity through Open Fracture Plates. Injectivity is defined as the flow rate divided by the injection pressure. It is a fundamental parameter that measures the difficulty of injecting PPGs. High values of injectivity indicates that the injection is easier.

4.5.8.1 Effect of injection flow rate in PPGs injectivity. Figures 4-35 through 4-37 show that the PPGs injectivity is highly dependent on the injection pressure and it increases linearly with the increase in the constant injection flow rate.

4.5.8.2 Effect of brine concentration on PPGs injectivity. The effect of the brine concentration on the PPGs injectivity can be seen in Figures 4-35 through 4-37. It is evident at a constant injection flow rate, PPGs injectivity decreases with the increase in in

brine concentration. For example, at an injection flow rate of 5.0 ml/m, the injectivity for PPG prepared with DI, 0.25, 1.0 and 5.0 wt. % NaCl and extruded through 0.25 mm fracture are 0.45, 0.40, 0.35 and 0.31, respectively. The results show that the PPG that was prepared with low brine concentration is easier to be injected compared with the PPG that was prepared using higher brine concentration. This is due to the fact that the fully swollen gel particles i.e. in low brine concentration are larger in size and consequently more deformable, and thus have high injectivity. However, in the case where PPG was prepared using DI water and extruded through 1.0 mm fracture, it has low injectivity compared to the rest of the brine concentrations. This could be related to the fact that PPG injection pressures were low and the size of the particle matters. However, a reverse trend in PPGs injection pressure was not observed to confirm this finding.

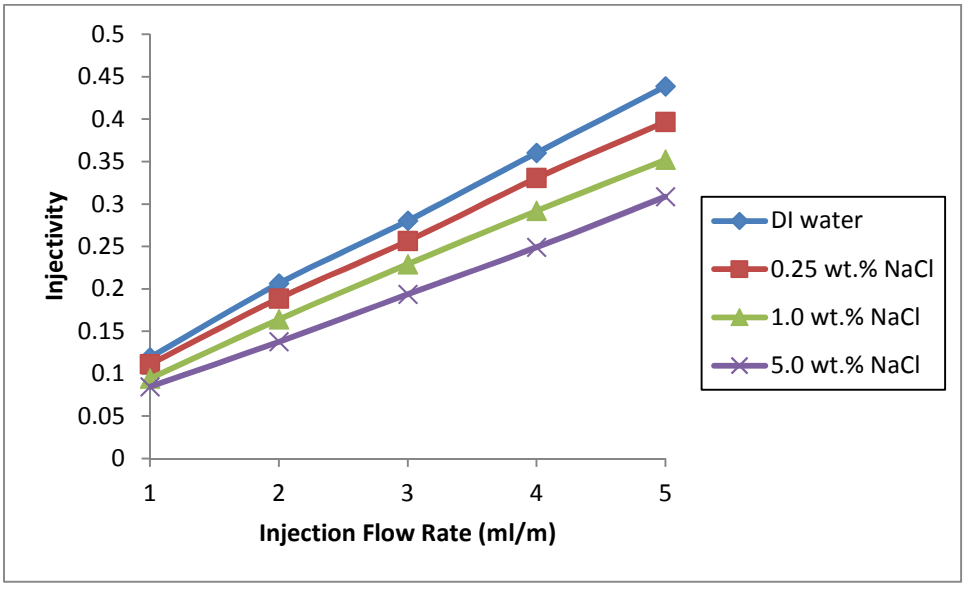

Figure 4-35. PPGs injectivity through 0.25 mm fracture as a function of injection flow rate and brine concentration.

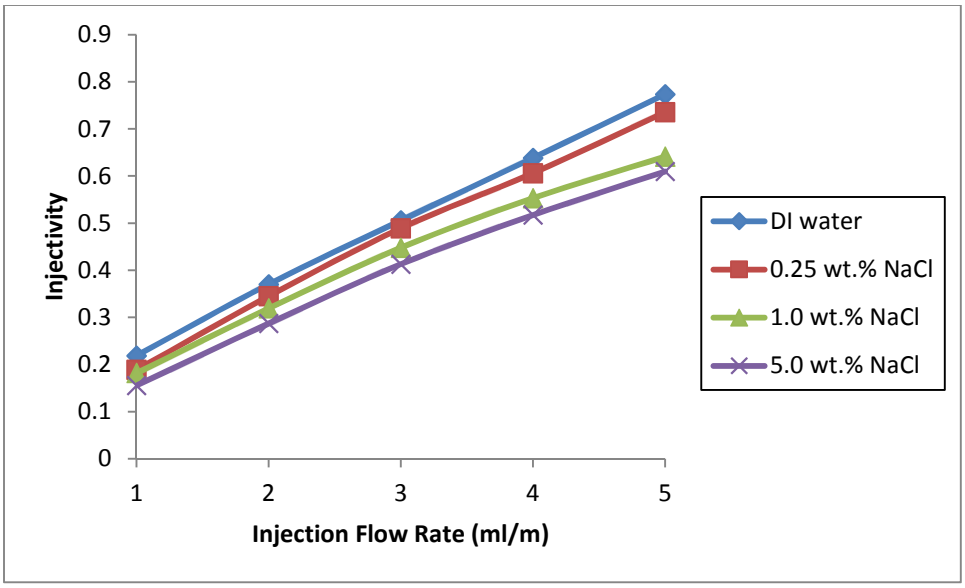

Figure 4-36. PPGs injectivity through 0.50 mm fracture as a function of injection flow rate and brine concentration.

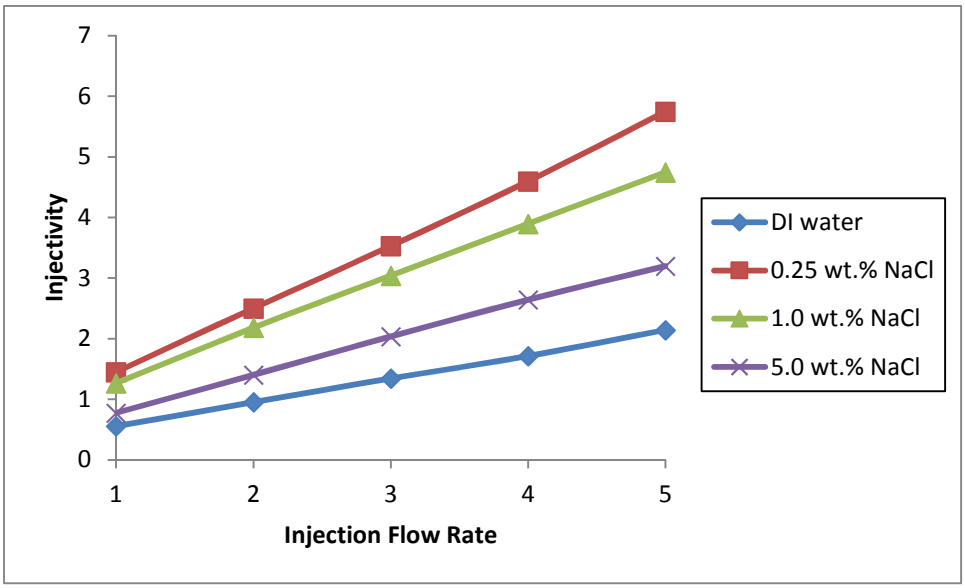

Figure 4-37. PPGs injectivity through 1.0 mm fracture as a function of injection flow rate and brine concentration.

4.5.8.3 Effect of fracture-width on PPGs injectivity. Figures 4-38 through 4-41 show the effect of fracture width on PPGs injectivity for each brine concentration. It is clear that regardless of the brine concentration, the injectivity increases as the fracture-width increases. For instance, as it is shown in Figure 4-41, for the PPGs prepared with 5.0 wt. % NaCl, at constant injection flow rate of 5.0 ml/m, PPGs injectivity for 0.25, 0.50 and 1.0 mm fractures are 0.31, 0.61 and 3.2, respectively. This indicates that the PPG injectivity increase significantly as the size of the fracture increases.

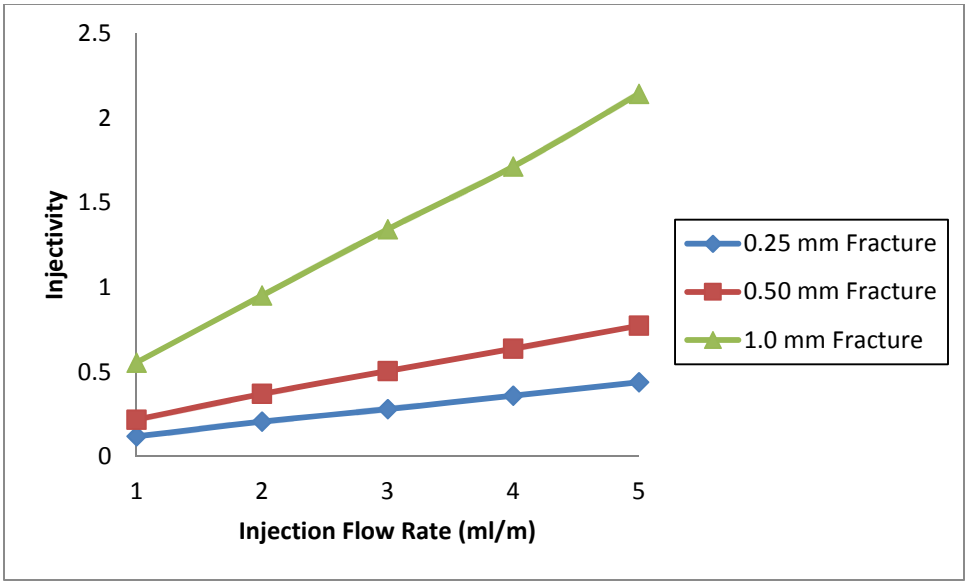

Figure 4-38. DI water PPGs injectivity through various open fracture plate model.

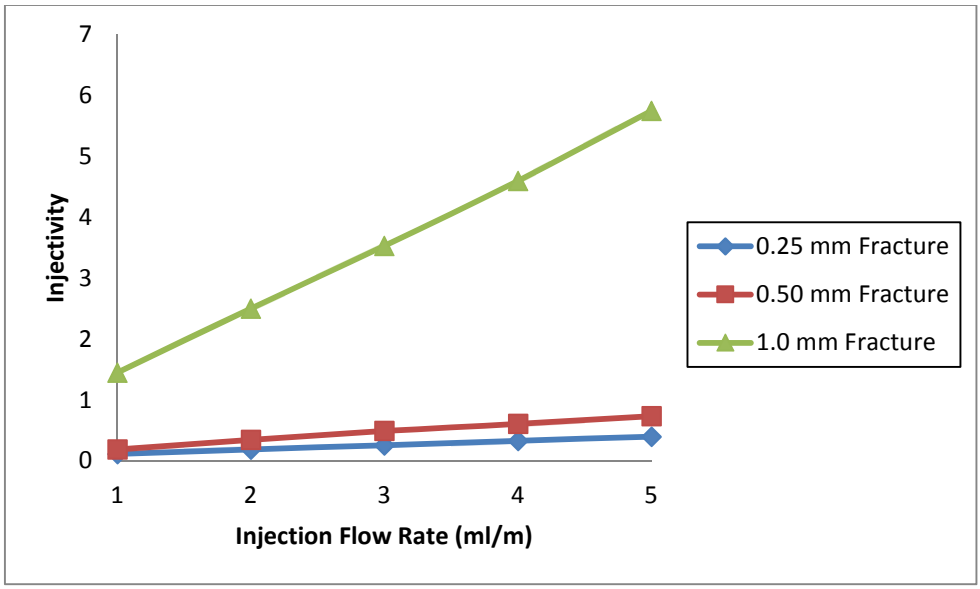

Figure 4-39. 0.25 wt. % NaCl PPGs injectivity through various open fracture plate model.

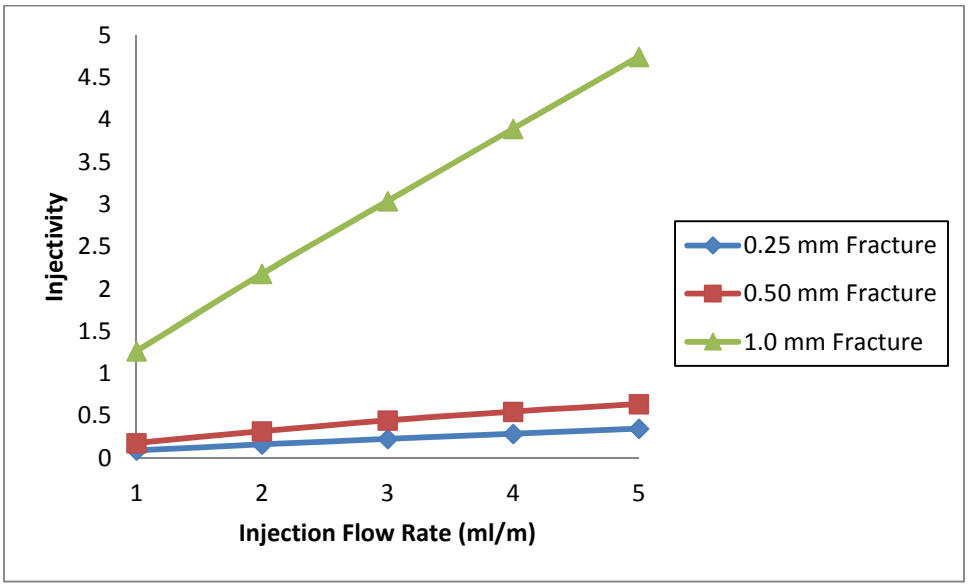

Figure 4-40. 1.0 wt. % NaCl PPGs injectivity through various open fracture plate model.

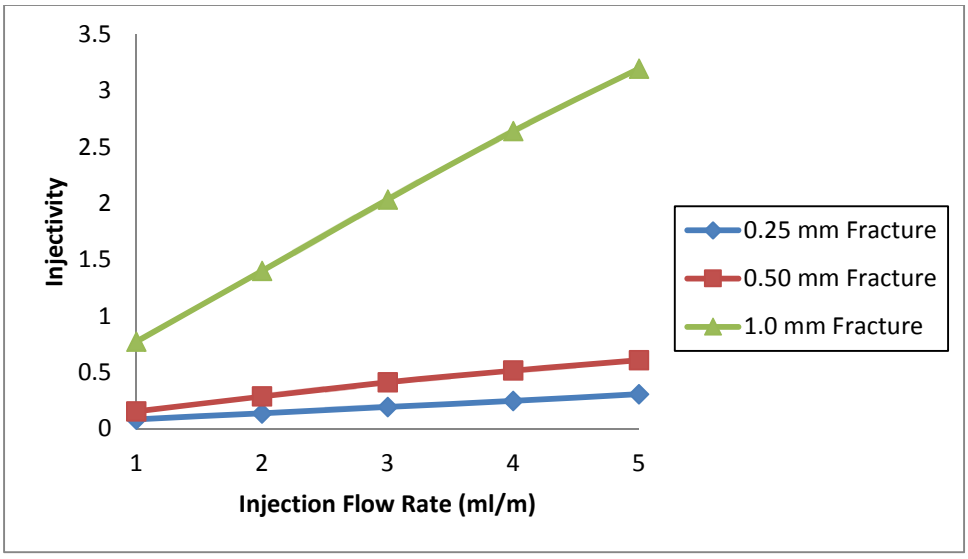

Figure 4-41. 5.0 wt. % NaCl PPGs injectivity through various open fracture plate model.

4.5.9 Particle Size Distribution of the Extruded PPGs. The PPGs that were Initially swollen in DI water and 0.25, 1.0 and 5.0 wt. % NaCl and extruded through the different open fractures plates have been considered in this study. Based on the particle evaluation index and the image analysis of the extruded gel particles, the extrusion pattern was identified.

4.5.9.1 Comparison between the PSD of DI water PPG before and after extrusion. Figure 4-42a and b present frequency and PSD comparison of DI water PPG that has an initial equivalent diameter of 5.828 mm and extruded the three different fractures sizes. From these figures along with the image observations of the extruded gel particles Figure 4-46, it is clear that the severities of the broken particles were inversely proportional to the size of the fracture because DI water PPG is considered to be a week gel. When the DI water PPG extruded through the 0.25 and 0.50 mm fractures, most of the particles were broken into small pieces and then passed through the fracture plate.

The equivalent diameters of these two extruded particles have been reduced from 5.828 to 1.917 mm (67.1 %) reduction and from 5.828 to 2.534 mm (56.5 %) reduction, which yield a particle evaluation index of 0.329 and 0.435, respectively.

When the DI water PPG extruded through 1.0 mm fracture, a few particles fall in the same particle size distribution of the initial swollen DI water PPG which is can be attributed to the injection pressure that these particles were exposed to pass through the 1.0 m fracture. As a result, the reduction in the equivalent diameter was low, from 5.828 to 4.294 (26.32 %) which gives a particle evaluation index of 0.737. Based on the evaluation index values along with the visual observation of the extruded gel particles, it can be concluded that the DI water PPG follow a brake and pass through pattern when the particles were transported through the different open fracture screen plates.

4.5.9.2 Comparison between the PSD of 0.25 wt. % NaCl PPG before and after extrusion. Figure 4-43a and b presents the frequency distribution and the PSD of the extruded 0.25 wt. % NaCl PPG, which has initial swollen equivalent diameter of 4.640 mm through the various fractures. It is evident that from these two figures along with the image observations Figure 4-47 that the particles exhibited broken and pass pattern. However, the intensity of the broken particles was less compared to the DI water PPG. When 0.25 wt. % NaCl extruded through the 0.25 , 0.50 and 1.0 mm fractures, the equivalent diameters of these extruded particles were reduced to 3.069 mm (33.9 %), 3.099 (33.2 %) and 3.934 mm (15.2 %), respectively. In the scenario where the 0.25 wt. % PPG transported the 1.0 mm fracture, the high standard deviation and broad trend of the particle size distribution is related to the low injection pressure that was observed in the experiment. The particle evaluation index for 0.25 wt. % NaCl PPG through the various

open fracture plates were measured to be (0.661, 0.668 and 0.848), which is still the range of broken and pass pattern.

4.5.9.3 Comparison between the PSD of 1.0 wt. % NaCl PPG before and after extrusion. Figure 4-44a and b demonstrates the frequency and the normal particle size distribution of the 1.0 wt. % NaCl PPG through the various fractures. The initial swollen equivalent diameter of 1.0 wt. % PPG is 3.764 mm, and when this particle transported though the 0.25 mm fracture, some particles were broken and that can be seen in the deflection of the particle size distribution to the left through the 0.25 mm fracture compared to the initial swollen particle size distribution. The equivalent diameter was reduced from 3.764 to 3.093 (17.8 %) which gives a particle evaluation index of 0.822. On the contrary, when 1.0 wt. % NaCl PPG extruded through 0.50 and 1.00 mm fractures, there were no pronounced reduction in the equivalent diameters. In fact, the equivalent diameter only reduced (3.8 %) when the particles extruded through 0.50 mm fracture, and reduced to (0.88 %). The particle evaluation index was measured to be 0.961 and 0.991, respectively. Based on the particle evaluation index and the visual observation of the extruded images Figure 4-48, a conclusion can be drawn that the 1.0 wt. % PPG extruded through 0.50 and 1.0 mm fractures follow the pass pattern.

4.5.9.4 Comparison between the PSD of 5.0 wt. % NaCl PPG before and after extrusion. Figure 4-45a and b show the frequency and the PSD of the 5.0 wt. % NaCl PPG through the various fractures. The initial swollen equivalent diameter of 5.0 wt. % PPG is 3.126 mm. The extrusion behavior of these particles through the various fractures is similar to the extrusion of the 1.0 wt. % NaCl. I.e., the particles were partially broken when they extruded through the 0.25 mm fracture and the equivalent swollen diameter

reduced from 3.126 to 2.722 mm (12.9 %). The visual observation of the extruded particles Figure 4-49 along with the particle evaluation index of 0.871 reveals that the particles follows the brake and pass pattern. However, when the 5.0 wt. % NaCl PPG extruded through the 0.50 and 1.00 mm fractures, there were no significant reduction in the extruded swollen gel particles. In 0.50 mm fracture, the equivalent diameter only reduced from 3.126 to 3.108 mm (0.58 %), and in 1.0 mm fracture, the extruded equivalent diameter remain almost the same 3.118 mm (0.26 %) reduction. The particle evaluation index of 5.0 wt. % NaCl through 0.50 and 1.00 m fractures was measured to be 0.994 and 0.997, respectively. According to the particle evaluation index and the visual observation of the extruded particles, it can be concluded that 5.0 wt. % NaCl PPG follow the pass pattern through 0.50 and 1.0 mm fractures. Table 4-4 summarizes the particle evaluation index and the extrusion pattern of the PPGs through the open fracture plates model.

4.5.9.5 Relation between the particle evaluation index and threshold pressure. Figure 4-50 presents the relation between the particle evaluation index with PPGs threshold pressure as a function of brine concentration. It can be seen from the figure that weak swollen PPGs will exhibit a severe reduction in their size upon the influence of the injection pressure. Whereas, the strong swollen PPGs, i.e. 1.0 and 5.0 wt. % NaCl PPGs will almost maintain their size during their transportation through the different fractures. Therefore, it can be concluded that injecting strong PPGs particles will be more preferable through fractures. When the PPG particles maintain their size inside the fracture that can lead to develop a high resistance to the injected water and thus, ensure the stability of the gel placement into the fractures.

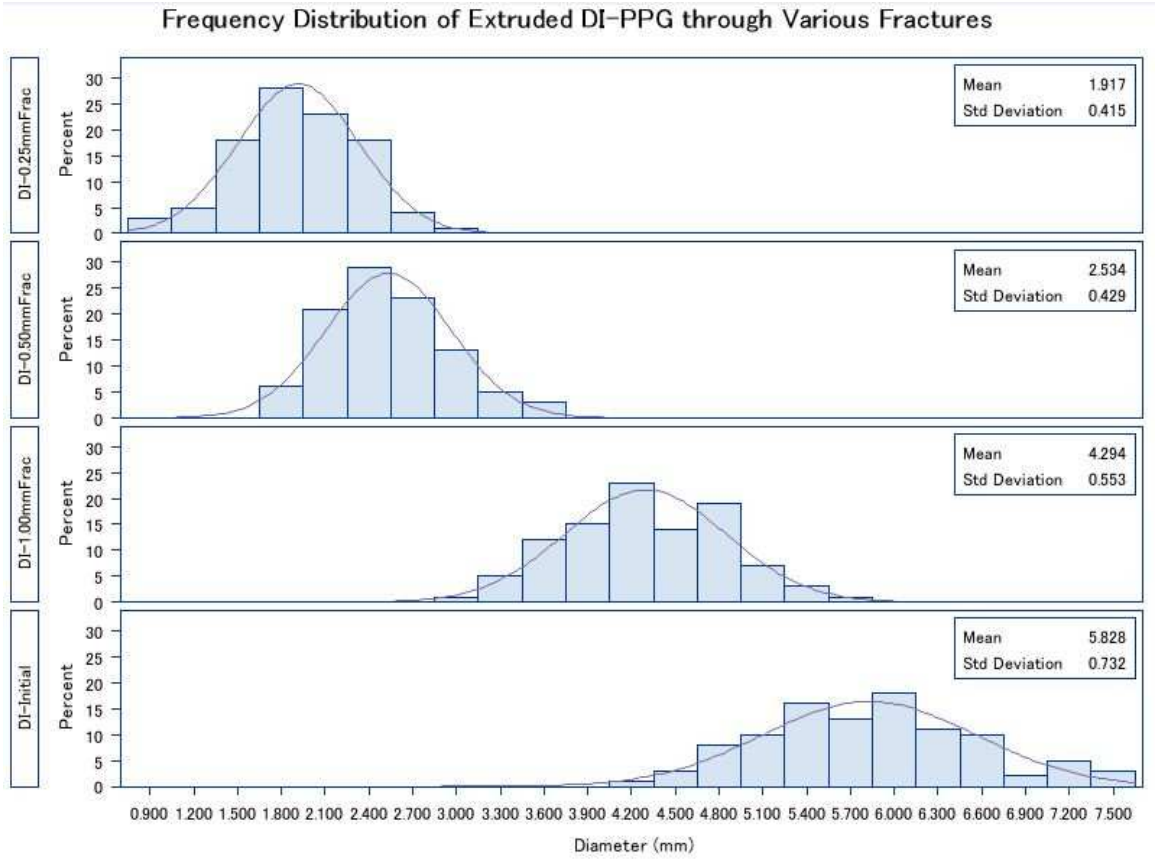

(a)

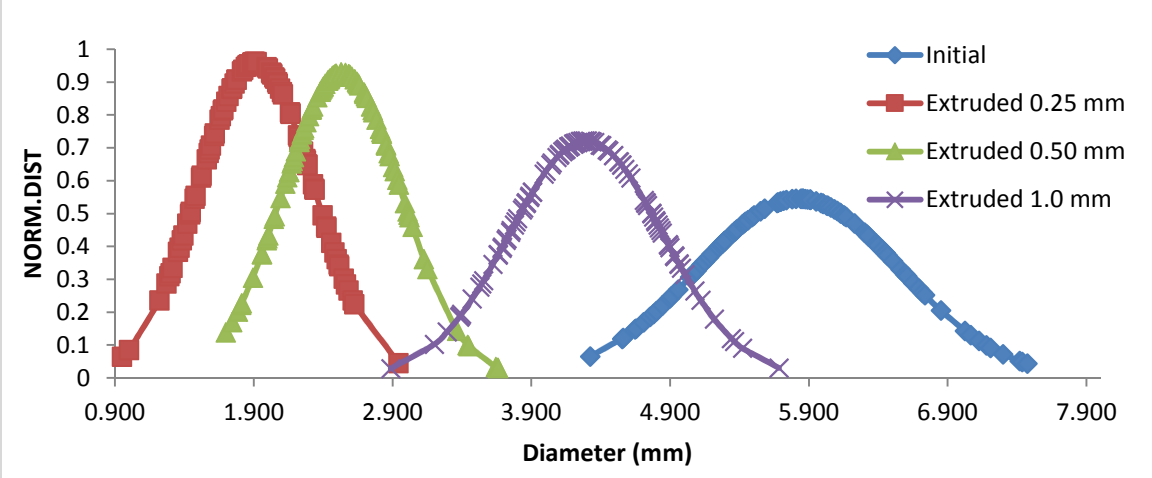

(b)

Figure 4-42. Comparisons between DI water PPG before and after extrusion through Open fracture plates model (a) frequency distribution (b) PSD.

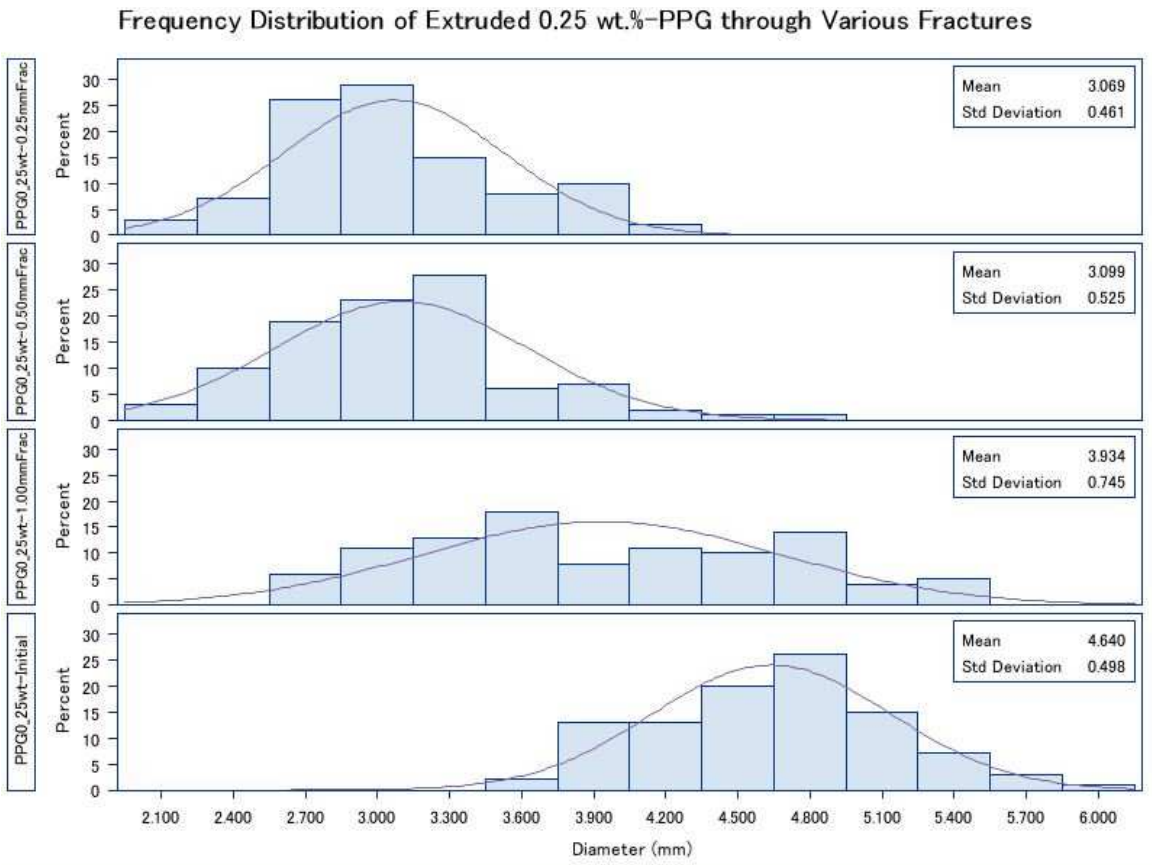

(a)

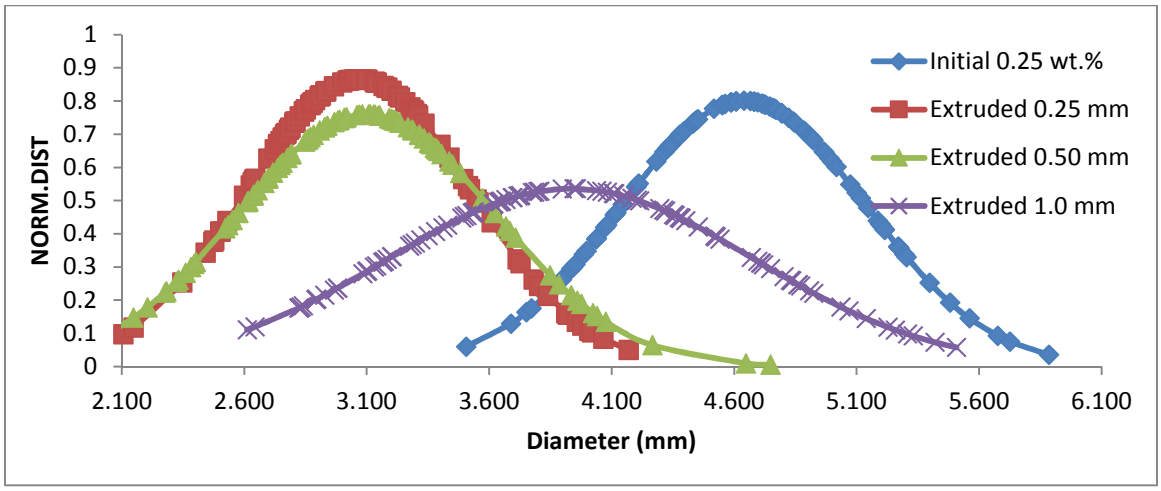

(b)

Figure 4-43. Comparisons between 0.25 wt. % NaCl PPG before and after extrusion through open fracture plates model (a) frequency distribution (b) PSD.

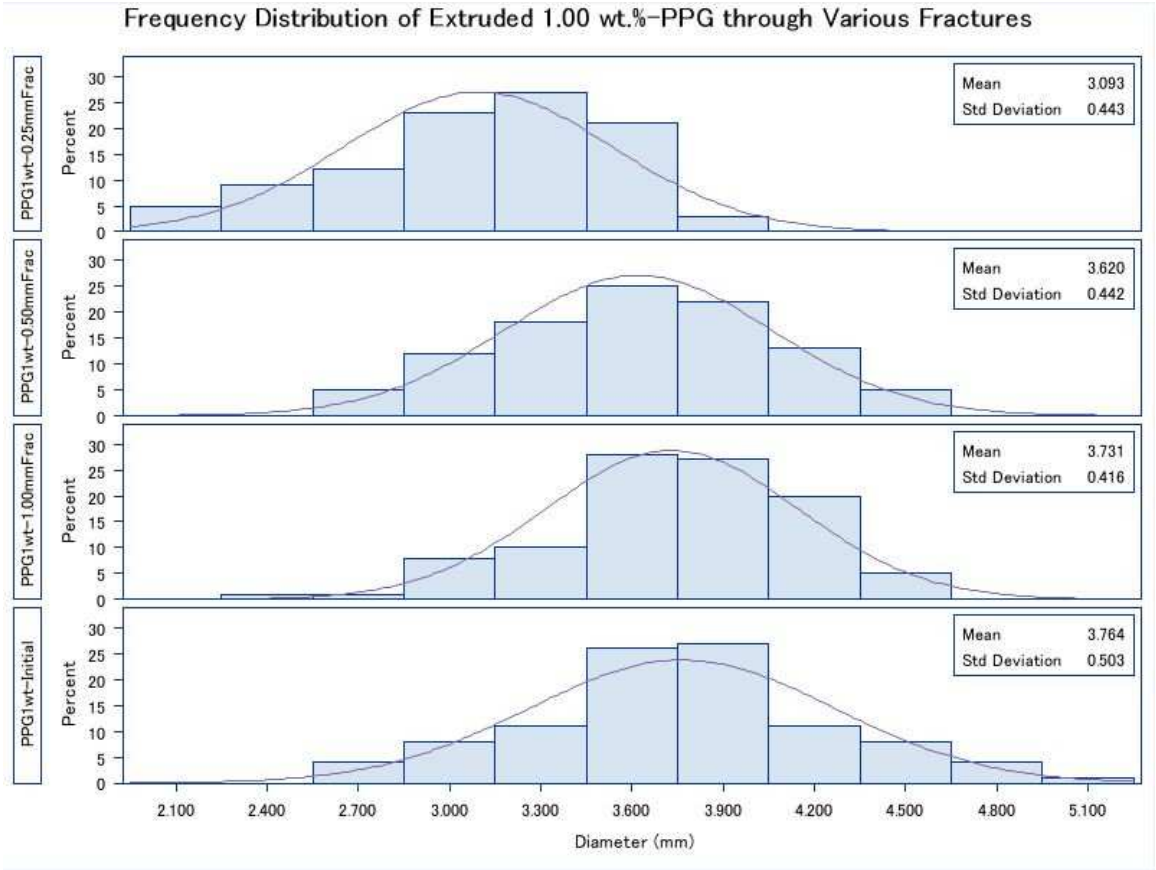

(a)

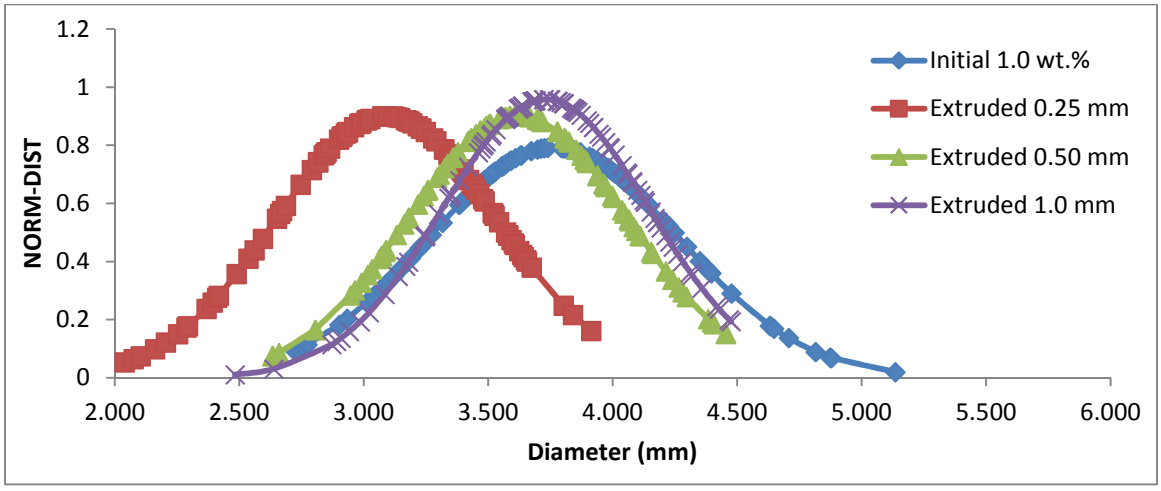

(b)

Figure 4-44. Comparisons between 1.0 wt. % NaCl PPG before and after extrusion through open fracture plates model (a) frequency distribution (b) PSD.

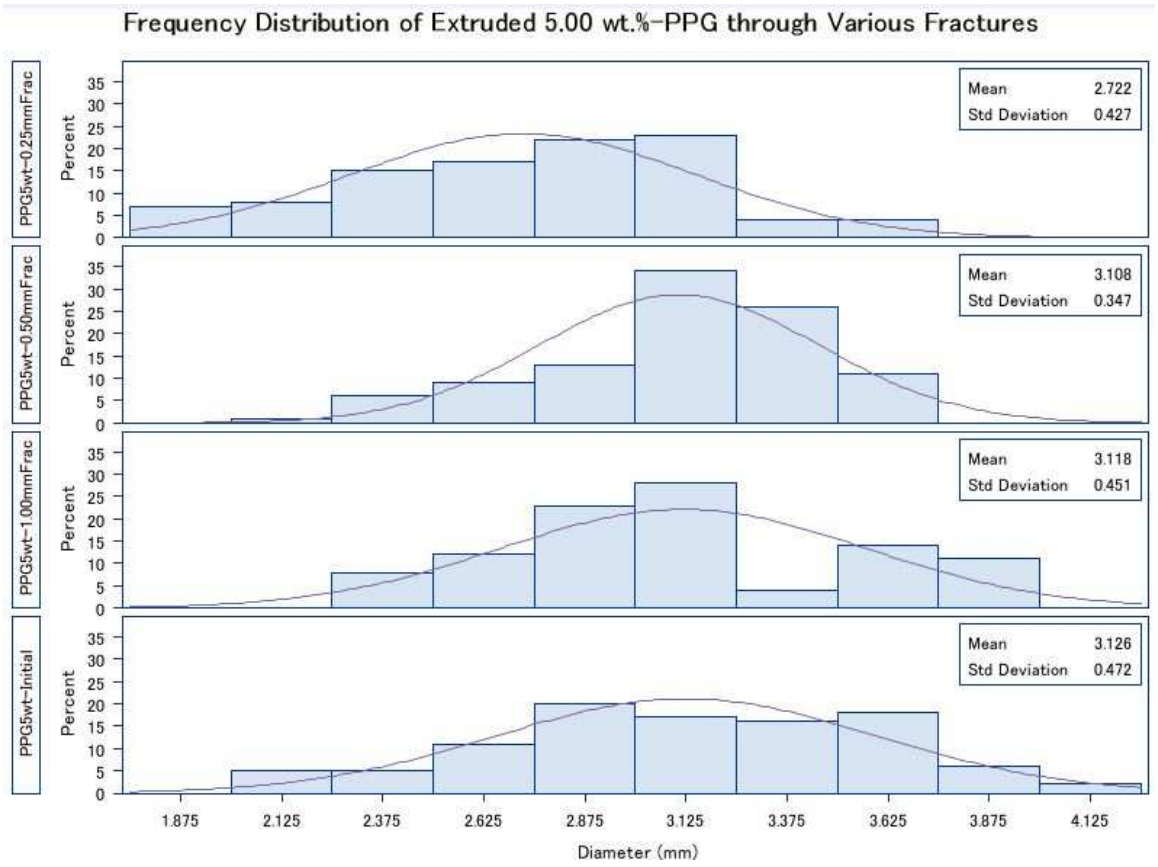

(a)

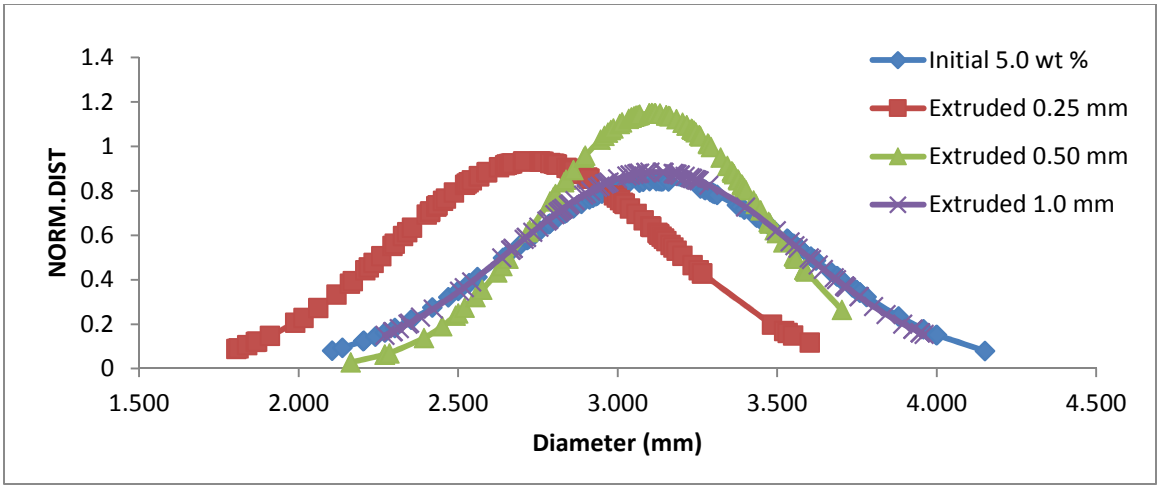

(b)

Figure 4-45. Comparisons between 5.0 wt. % NaCl PPG before and after extrusion through open fracture plates model (a) frequency distribution (b) PSD.

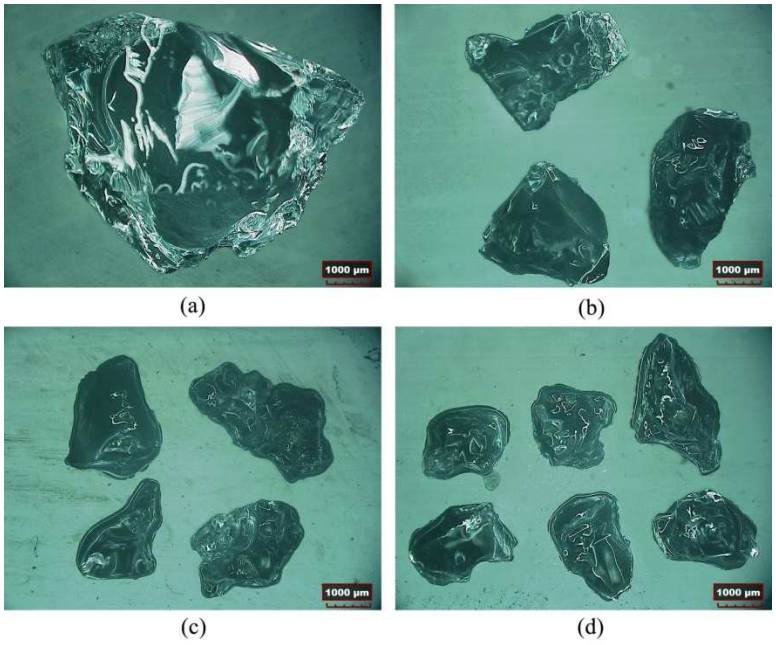

Figure 4-46. Comparison between initial and extruded DI water PPG (a) initial (b) extruded through 1.0 mm fracture (c) 0.50 mm fracture and (d) 0.25 mm fracture.

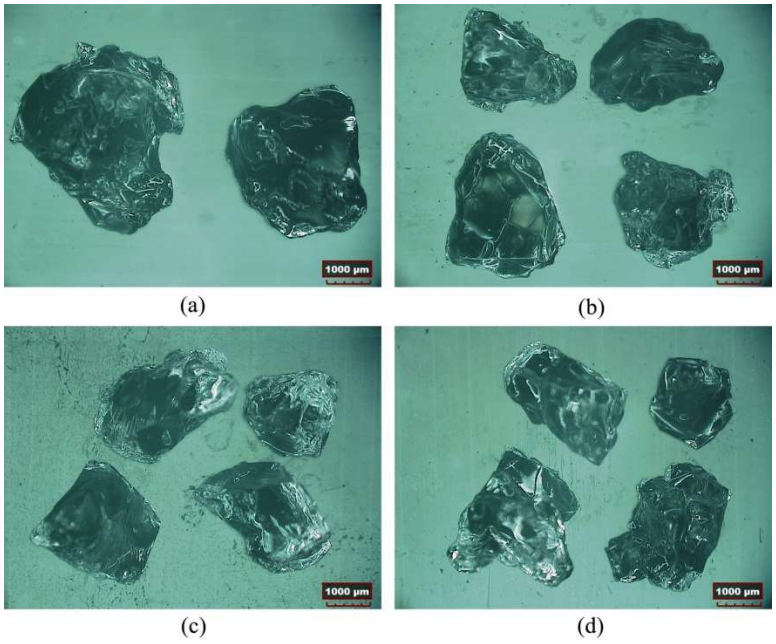

Figure 4-47. Comparison between initial and extruded 0.25 wt. % NaCl PPG (a) Initial (b) extruded through 1.0 mm fracture (c) 0.50 mm fracture and (d) 0.25 mm fracture.

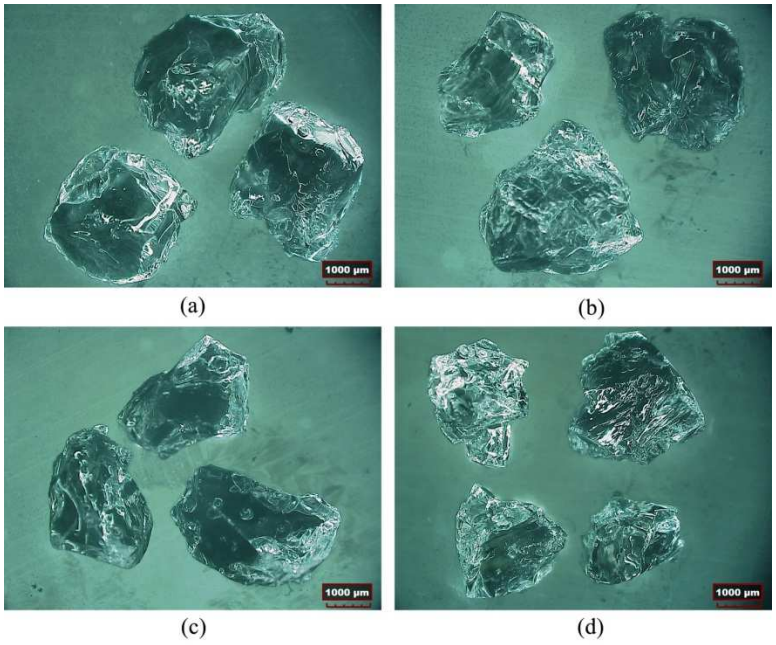

Figure 4-48. Comparison between initial and extruded 1.0 wt. % NaCl PPG (a) Initial (b) extruded through 1.0 mm fracture (c) 0.50 mm fracture and (d) 0.25 mm fracture.

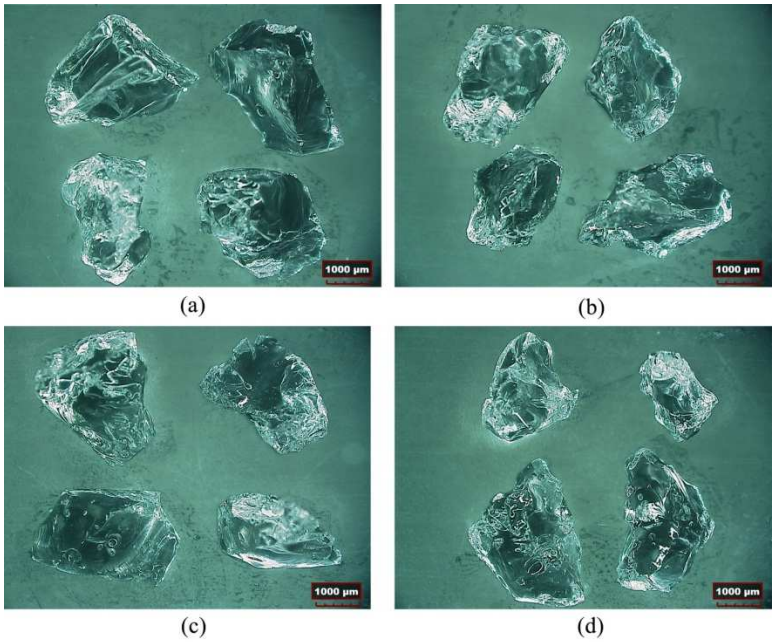

Figure 4-49. Comparison between initial and extruded 5.0 wt. % NaCl PPG (a) Initial (b) extruded through 1.0 mm fracture (c) 0.50 mm fracture and (d) 0.25 mm fracture.

Table 4-4. Particle evaluation index and extrusion pattern for PPG transport through open fracture plate model.

	Initial Equivalent Diameter (mm)	Extruded through Fracture size (mm)	Equivalent Diameter After Extrusion (mm)	Particle Evaluation Index	Extrusion Pattern
DI water PPG	5.828	0.25	1. 917	0.329	Broken and Pass
		0.50	2.534	0.661	Broken and Pass
		1.0	4.294	0.822	Broken and Pass
0.25 wt. % NaCl PPG	4.640	0.25	3.069	0.661	Broken and Pass
		0.50	3.099	0.668	Broken and Pass
		1.0	3.934	0.848	Broken and Pass
1.0 wt. % NaCl PPG	3.764	0.25	3.093	0.822	Broken and Pass
		0.50	3.62	0.962	Pass
		1.0	3.731	0.991	Pass
5.0 wt.% NaCl PPG	3.126	0.25	2.732	0.874	Broken and Pass
		0.50	3.108	0.994	Pass
		1.0	3.118	0.997	Pass

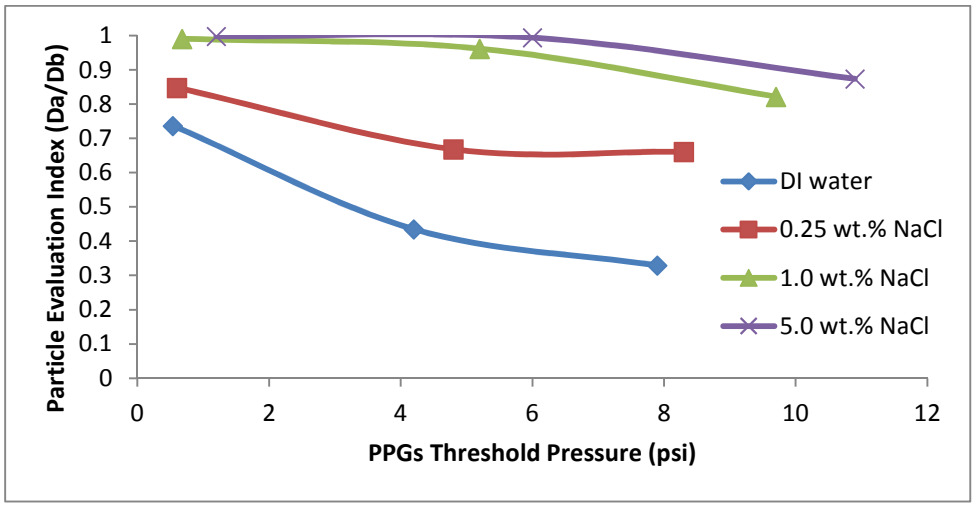

Figure 4-50. Particle evaluation index as a function of threshold pressure and brine concentration.

4.5.10 General Full-Factorial Design. Minitab statistical software was used to conduct a full-factorial design to determine the most influential factor on PPGs Injection pressure, resistance factor and injectivity. Three parameters were considered in thus study; fracture width, swelling ratio which is related to the brine concentration and the PPGs injection flow rate. Figure 4-51 demonstrates Pareto Chart of the standardized effects considering the PPGs injection pressure as a response. The factorial design results show that the fracture width of the open fracture screen plates had the most influential effect on the PPGs injection pressure. The swelling ration ranked second and the injection flow rate has the least influential effect on the PPGs injection pressure.

For the resistance factor, the Pareto Chart in Figure 4-52 reveals that the injection flow rate is the factor that mostly influenced the resistance factor. However, the fracture width effect was close to the effect of the injection flow rate. Additionally, the figure shows that the swelling ratio had the least effect on the resistance factor calculations. Figure 4-53 show the ranking of the three parameters on the injectivity as a response. Similar to the PPGs injection pressure, the fracture width had the most predominant effect on the injectivity. Swelling ratio is the least influential factor between the three parameters.

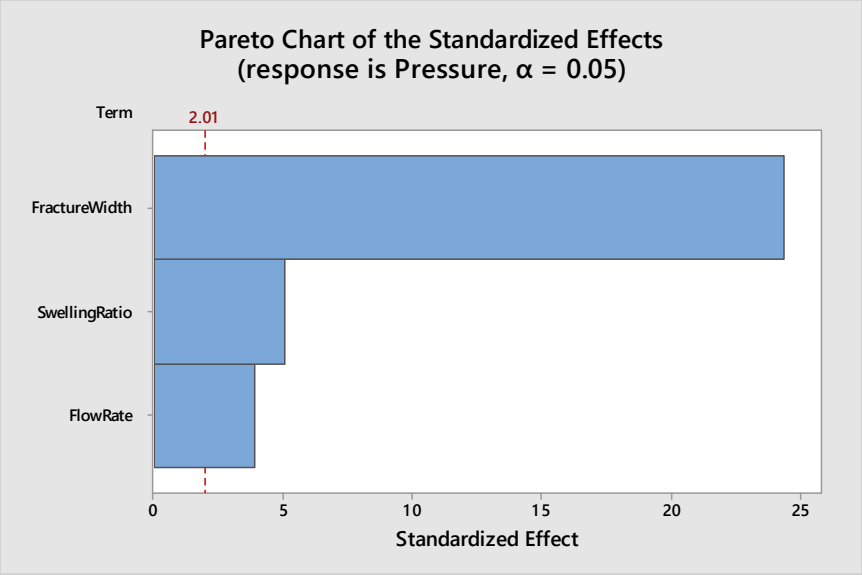

Figure 4-51. Pareto chart of the injection pressure as a response.

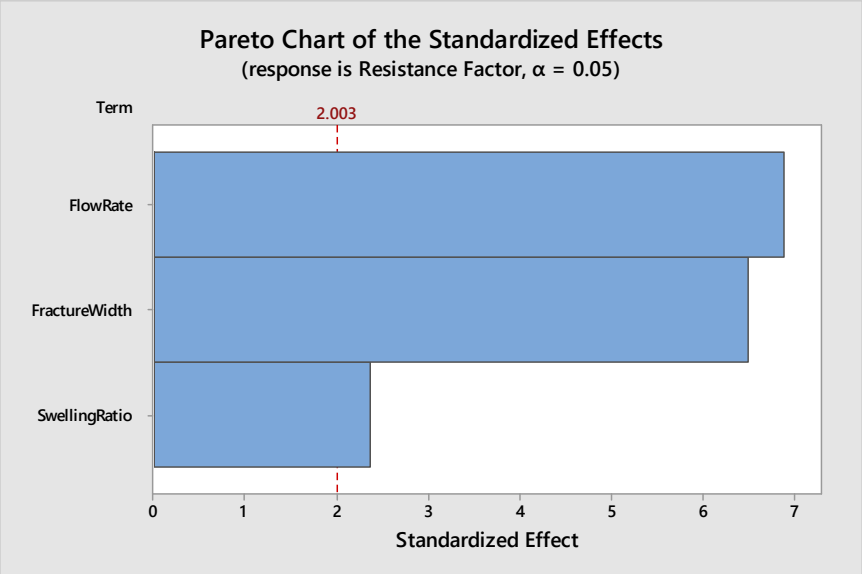

Figure 4-52. Pareto chart of the resistance factor as a response.

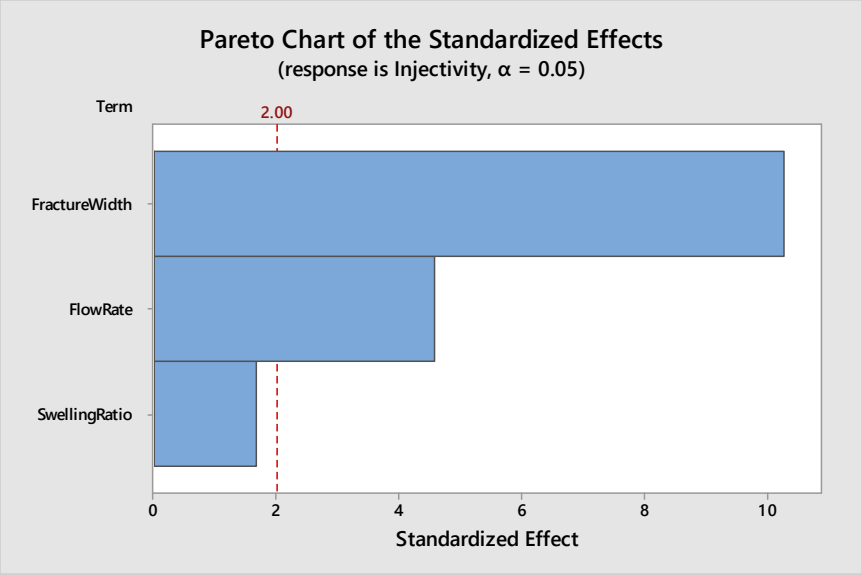

Figure 4-53. Pareto chart of the injectivity as a response.

4.6 CONCLUSION

This chapter examined the evaluation of millimeter-sized PPGs through open fracture plate model the major outcomes of this study can be summarized in the following points:

- The PPGs injections pressure increases as both the brine concentration and the injection flow rate increase. However, the increase is not significant due to the high fluid conductivity within the fractures.
- As demonstrated by the power law model, PPGs exhibit shear-thinning or pseudoplastic behavior.
- The PPGs resistance factor increases as the injection flow rate decreases.
- The PPGs resistance factor increases with the increase in the fracture- width size.

- The PPGs threshold pressure increases as the brine concentration increases regardless the size of the fracture.
- Evaluation of the extruded PPGs particle size distribution from the various fractures can facilitate in understanding the extrusion pattern of PPGs through fractures.
- Gel injectivity decreases as brine concentration increases.
- The full-factorial design show that the fracture width is the most influential factor on both the PPGs injection pressure and injectivity, whereas the flow rate affects the resistance factor the most.

5. FILTRATION TEST USING POROUS CERAMIC DISKS

5.1 SUMMARY

This chapter presents the experimental work that was performed to utilize the experimental apparatus to conduct filtration test using viscous gel. Two types of ceramic disks from OFITE with different permeability were used in order to simulate the porous media. Different concentrations of the viscous gel were used. Consequently, the plugging efficiency, the water residual resistance factor, and the total fluid loss of the viscous gel were measured. The results showed that the viscous gel with high concentrations reduced the permeability of the ceramic disk dramatically by forming a permeable gel cake on the disk surface. Additionally, the result of this study has shown that the use of the simple experimental apparatus can assist in conducting a filtration test for a certain viscous gel.

Four experiments were performed to examine the viscous gel plugging efficiency and transformation mechanism through the use of porous ceramic disks. The viscous gel was injected through 170-53 ceramic disk using three concentrations of 5000, 2500 and 1000 ppm. One experiment was conducted using 170-53-3 ceramic disk to examine the difference in the plugging efficiency with respect to changing the permeability of the porous ceramic disk. The total fluid loss, the plugging efficiency and the residual resistance factor were measured for each.

5.2 EXPERIMENTAL MATERIALS

5.2.1 Viscous Gel. A viscous gel with a mesh size of (100/150) was used in this study. Firstly, the brine solution was prepared by adding 7373 mg/L total salinity to DI water. Then, the viscous gel with the desired concentration was mixed with the brine solution using the magnetic stirrer. The sample was left for one day to ensure the gel was fully absorbed in the solution and to avoid any gel precipitations in the solution.

5.2.2 Porous Ceramic Disks. Two types of porous ceramic disks that were provided by the OFITE used in this study. According to OFITE, these porous ceramic disks have specification numbers of 170-53 and 170-53-3 and the permeability is 15 and 3 Darcy, respectively. The porous ceramic disks have a diameter of 2.5 in and a height of 0.25 in. The porosity for each ceramic disk was measured using the saturation method. Table 5-1 summarizes the specifications of the porous ceramic disks that were deployed in this study.

Table 5-1. Specification of the porous ceramic disks.

Ceramic Disk Part #	Permeability (Darcy)	Diameter (inches)	Height (inches)	Porosity (%)
170-53	15	2.5	0.25	41.27
170-53-3	3	2.5	0.25	40.88

5.3 EXPERIMENTAL SETUP AND PROCEDURE

5.3.1 Experimental Setup. In this study, the experimental apparatus was utilized to run the filtration test. Some adjustments were made to the outlet of the accumulator by placing a spacer between the ceramic disk and the effluent to ensure that the viscous gel will be exposed to the entire surface area of the porous ceramic disk.

5.3.2 Experimental Procedure. The experimental procedure was as follows:

- The porosity of the porous ceramic disks was measured using the saturation method.
- The viscous gel sample of the desired concentration was taken from the magnetic stirrer and placed directly into the accumulator.
- The viscosity of each sample was measured using the Brookfield viscometer.
- The porous ceramic disk was attached to the bottom of the accumulator.
- Then, the experiment was run using constant injection pressure that was provided from ISCO pump.
- The fluid loss flow rate was measured continuously during the experiment.
- Once both the fluid loss flow rate and the pressure reading form the gauge that was mounted at the bottom of the accumulator got stabilized, the constant pressure from the ISCO pump was increased.
- When the fluid loss flow rate remained constant with increasing the constant pressure from the pump, the experiment got stopped.
- The height of the gel cake buildup was measured.
- The viscosity off the extruded gel was measure and compared to the initial viscosity.

- Brine injection was then conducted using constant injection flow rate to find the permeability reduction.
- After obtaining the reduced permeability, both the plugging efficiency and the residual resistance factor were measured.

5.4 EXPERIMENTAL RESULTS AND DISCUSSIONS

5.4.1 Filtration Test (5000 PPM-170-53 Ceramic Disk). Figure 5-1 shows the cumulative volume loss in ml with respect to the cumulative time in minutes as a function of the stabilized injection pressure. The filtration test was conducted using 5000 ppm viscous gel with 170-53 porous ceramic disk that has an initial permeability of 15 Darcy. Figure 5-2 presents the fluid loss stabilized flow rate as a function of the stabilized injection pressure which demonstrates a sudden decline in the fluid loss flow rate. From these figures, it is clear that the 5000 ppm viscous gel formed a strong permeable gel cake on the surface of the ceramic disk. Figure 5-3 shows the viscosity measurements of 5000 ppm viscous gel before and after the filtration test. The significant decrease in the gel viscosity after extrusion indicates that most of the gel particles were gathered on the surface of porous ceramic disk. Figure 5-4 shows a comparison between the initial after the filtration test.

5.4.2 Filtration Test (2500 PPM-170-53 Ceramic Disk). Figures 5-5 through 5-8 present the results of the filtration test that was conducted using 2500 ppm viscous gel. The results show a similar trend as in the filtration test was conducted using 5000 ppm viscous gel. The results show that the 2500 ppm viscous gel formed a gel cake on the surface of the ceramic disk.

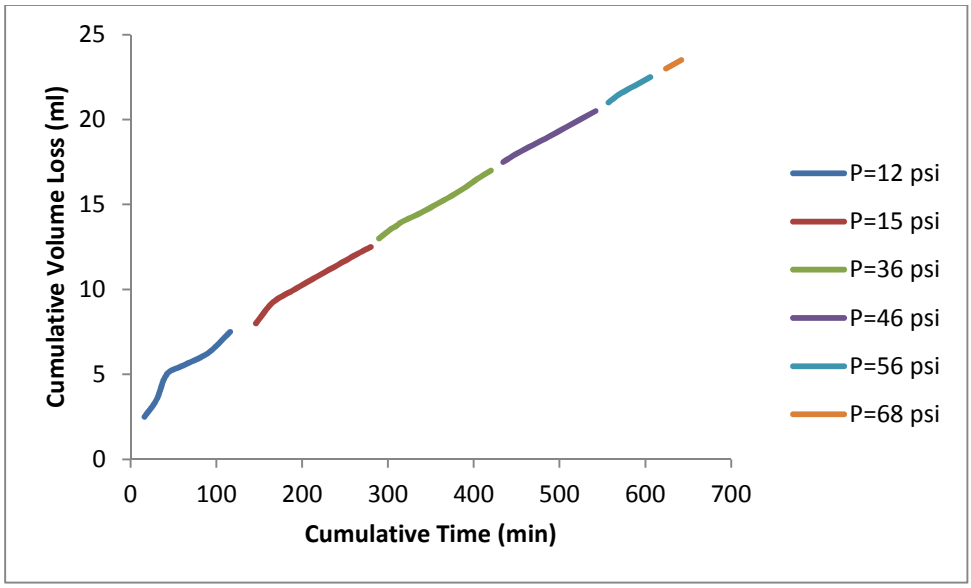

Figure 5-1. Cumulative volume loss vs. cumulative time for 5000 ppm viscous gel as a function of constant injection pressure.

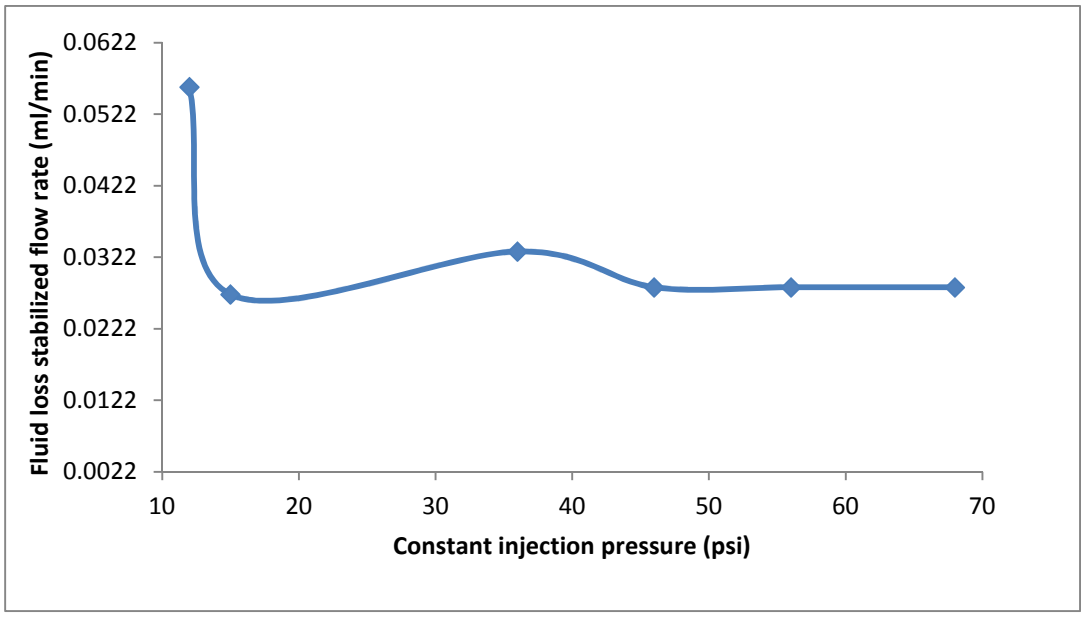

Figure 5-2. Fluid loss stabilized flow rate vs. constant injection pressure for 5000 ppm viscous gel.

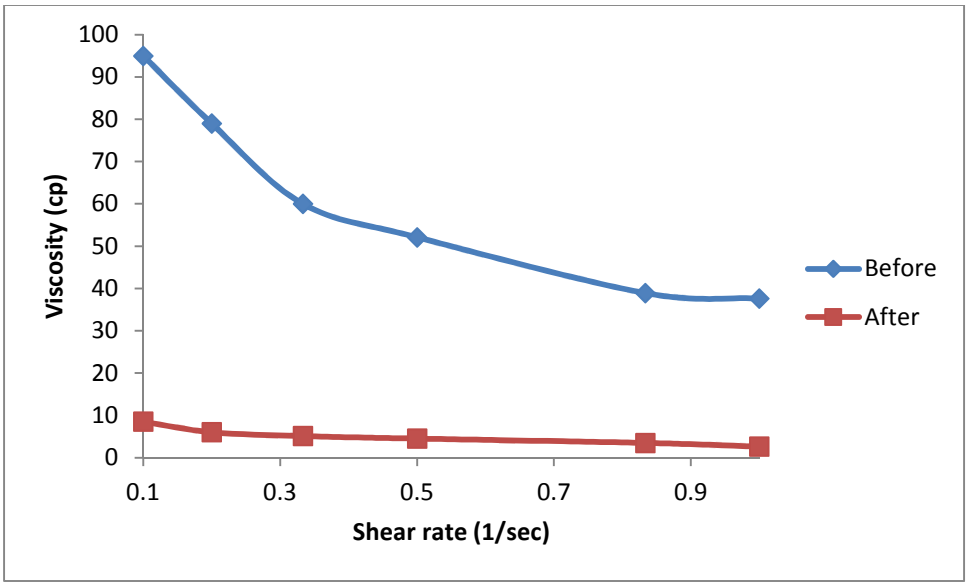

Figure 5-3. Viscosity measurements before and after filtration test for 5000 ppm viscous gel.

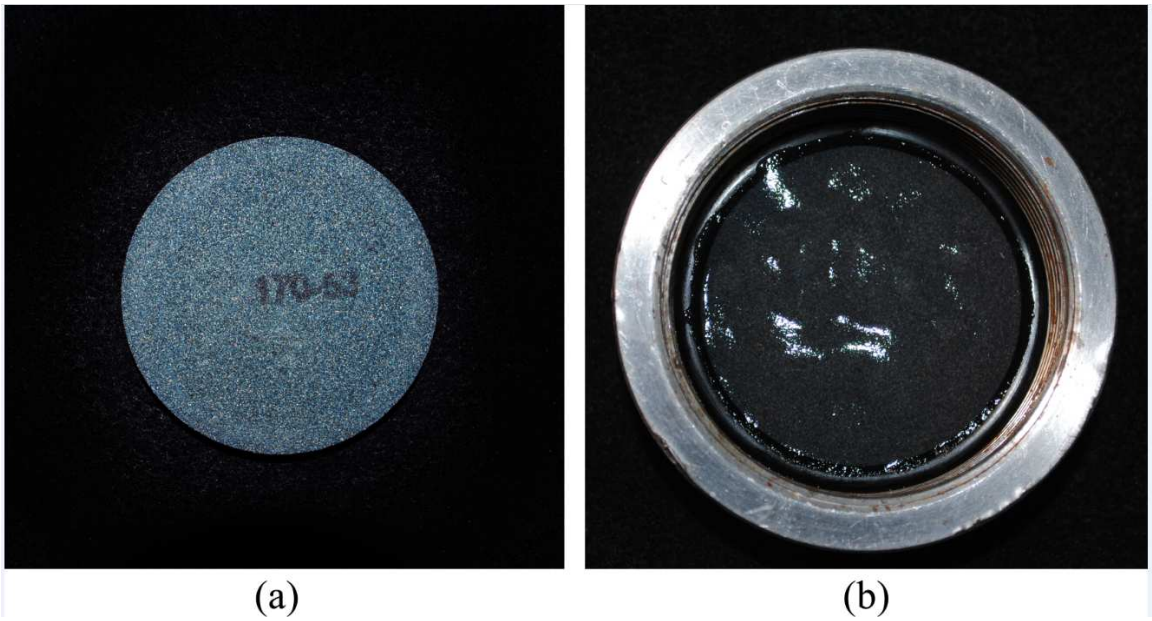

Figure 5-4. Comparison between initial surface of the ceramic disk and after filtration test for 5000 ppm viscous gel. (a) initial (b) after filtration test.

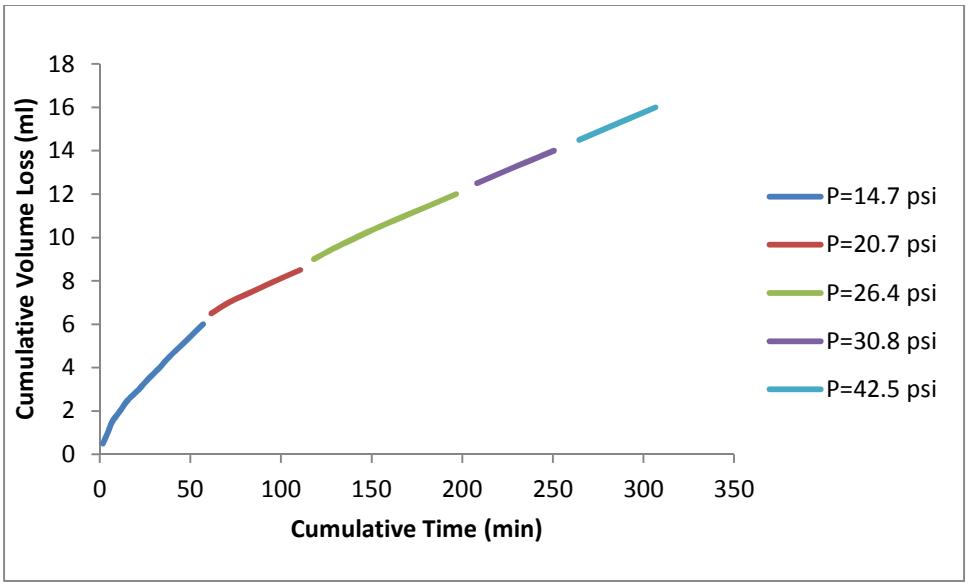

Figure 5-5. Cumulative volume loss vs. cumulative time for 2500 ppm viscous gel as a function of constant injection pressure.

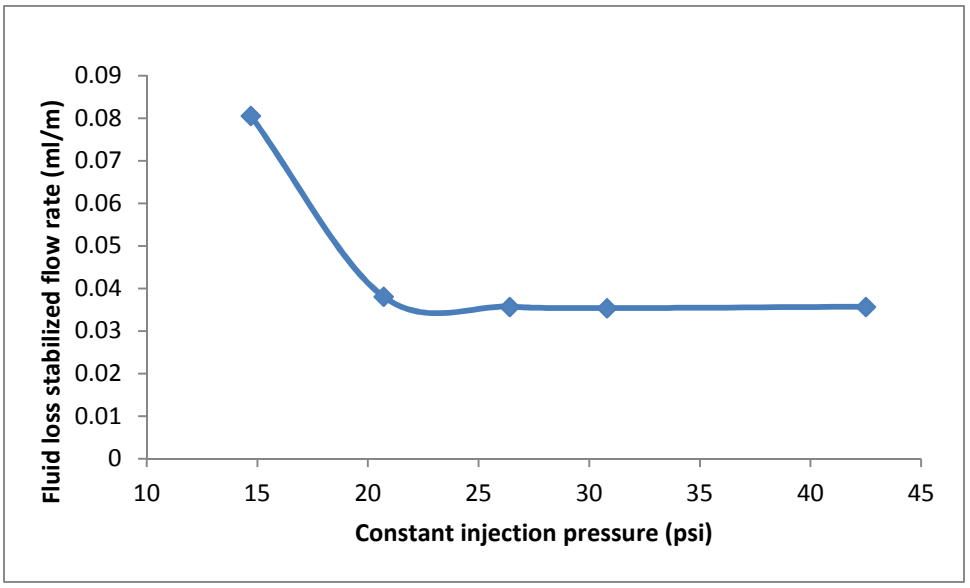

Figure 5-6. Fluid loss stabilized flow rate vs. constant injection pressure for 2500 ppm viscous gel.

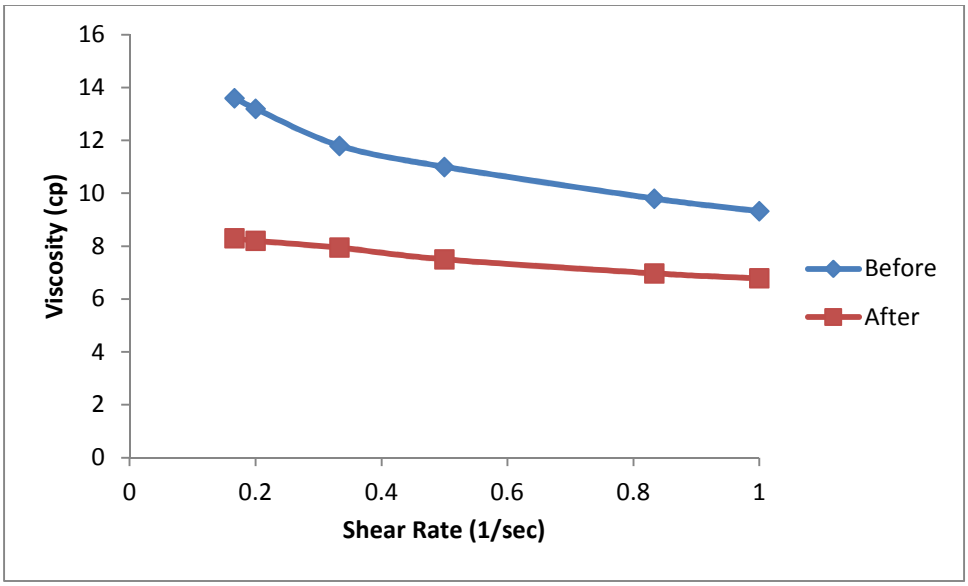

Figure 5-7. Viscosity measurements before and after filtration test for 2500 ppm viscous gel.

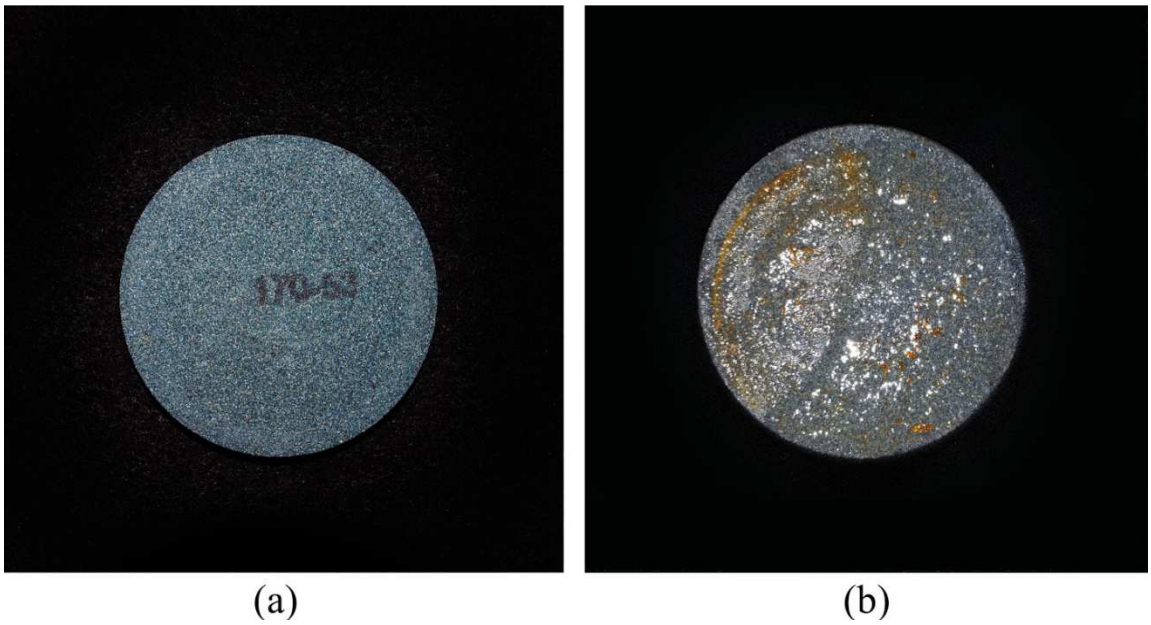

Figure 5-8. Comparison between initial surface of the ceramic disk and after filtration test for 2500 ppm viscous gel. (a) initial (b) after filtration test.

5.4.3 Filtration Test (1000 PPM-170-53 Ceramic Disk). Figures 5-9 through 5-12 show the results of the filtration test that was conducted using 1000 ppm viscous gel. The sudden increase in the cumulative volume loss with respect to the cumulative time is an indication that the 1000 ppm viscous gel did not plug the porous ceramic disk. Figure 5-12 shows that there is no significant gel cake build up on the surface of the ceramic disk and that can be confirmed by the constant pressure flow rate relation, where the flow rate remains constant at the beginning of the injection due to the precipitation of gel particles on the surface of the ceramic disk. Then, increasing the constant pressure caused the gel particles to transport easily through the ceramic disk leading to a rapid increase in the fluid loss.

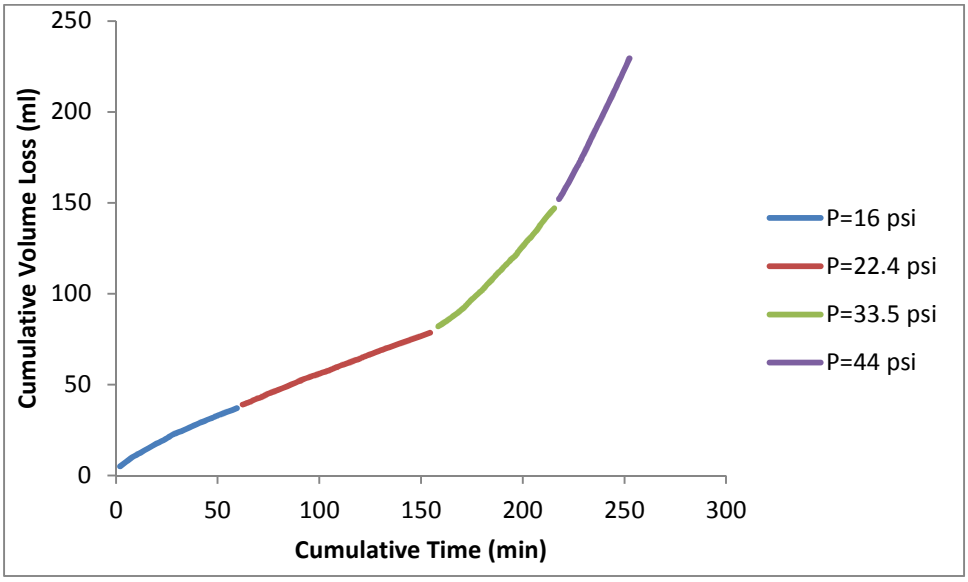

Figure 5-9. Cumulative volume loss vs. cumulative time for 1000 ppm viscous gel as a function of constant injection pressure.

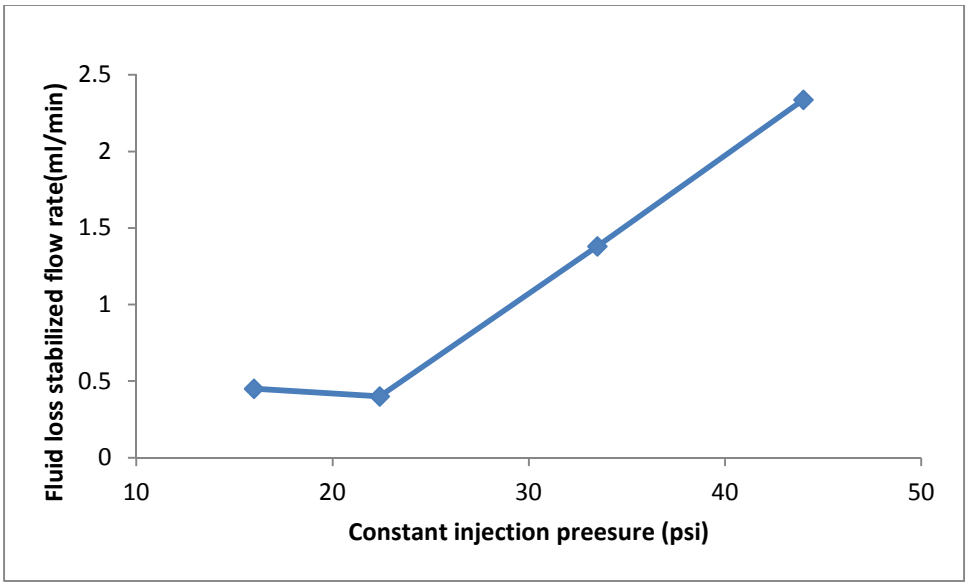

Figure 5-10. Fluid loss stabilized flow rate vs. constant injection pressure for 1000 ppm viscous gel.

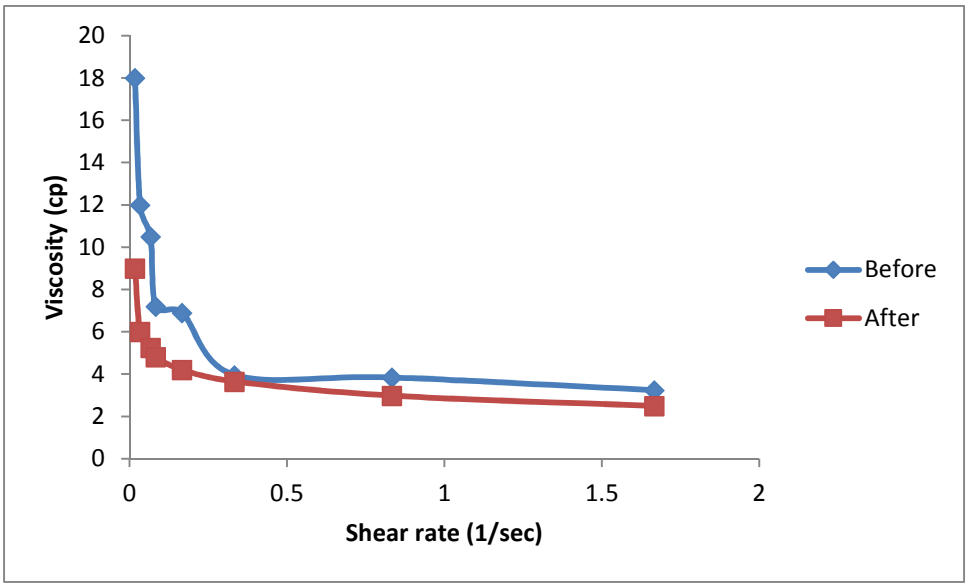

Figure 5-11. Viscosity measurements before and after filtration test for 1000 ppm viscous gel.

Figure 5-12. Comparison between initial surface of the ceramic disk and after filtration test for 1000 ppm viscous gel. (a) initial (b) after filtration test.

5.4.4 Filtration Test (1000 PPM-170-53-3 Ceramic Disk). One filtration test was conducted using 1000 ppm viscous gel with a porous ceramic disk that has an initial permeability of 3 Darcy. Figures 5-13 through 5-15 present the results of the filtration test. It is clear that the fluid loss stabilized flow rate decreases rapidly reaching a constant flow rate due to the buildup of the gel on the surface of the ceramic disk as it is seen in Figure 5-16. Table 5-2 summarizes the reduced permeability measurements that were done after the injection of brine, gel cake thickness and the water residual resistance factor.

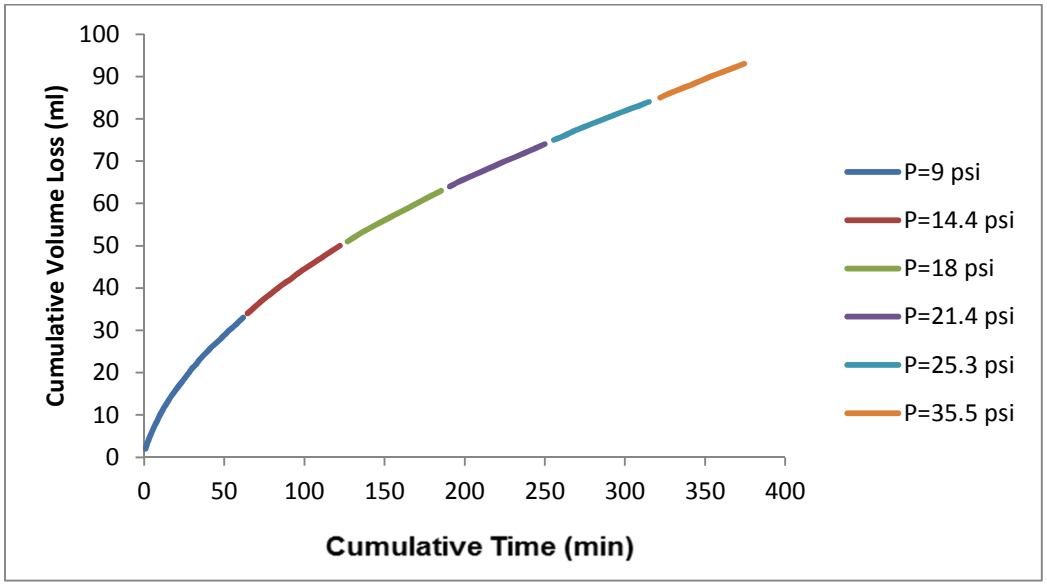

Figure 5-13. Cumulative volume loss vs. cumulative time for 1000 ppm viscous gel through (170-53-3) ceramic disk as a function of constant injection pressure.

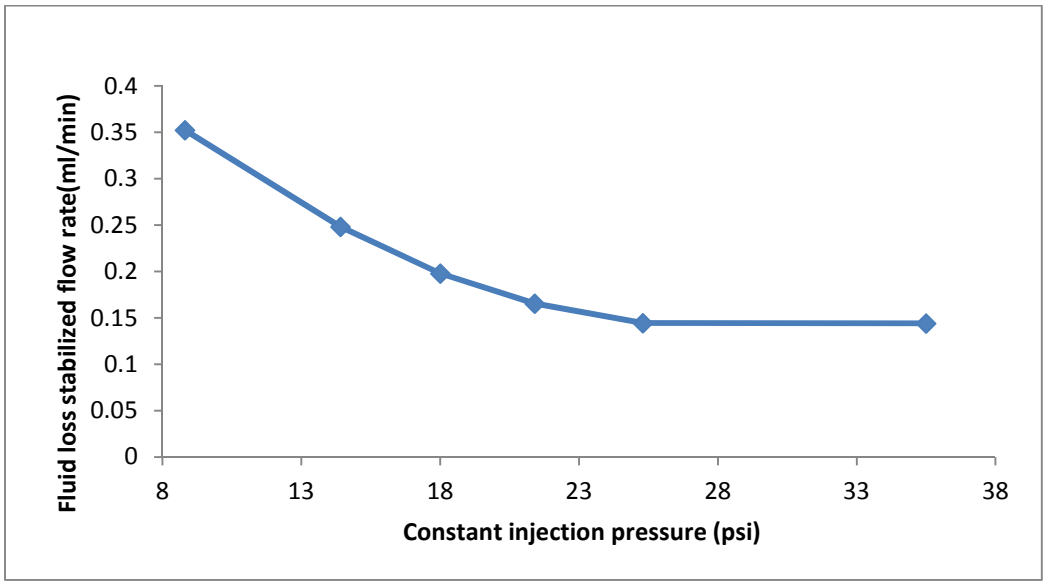

Figure 5-14. Fluid loss stabilized flow rate vs. constant injection pressure for 1000 ppm viscous gel through (170-53-3) ceramic disk.

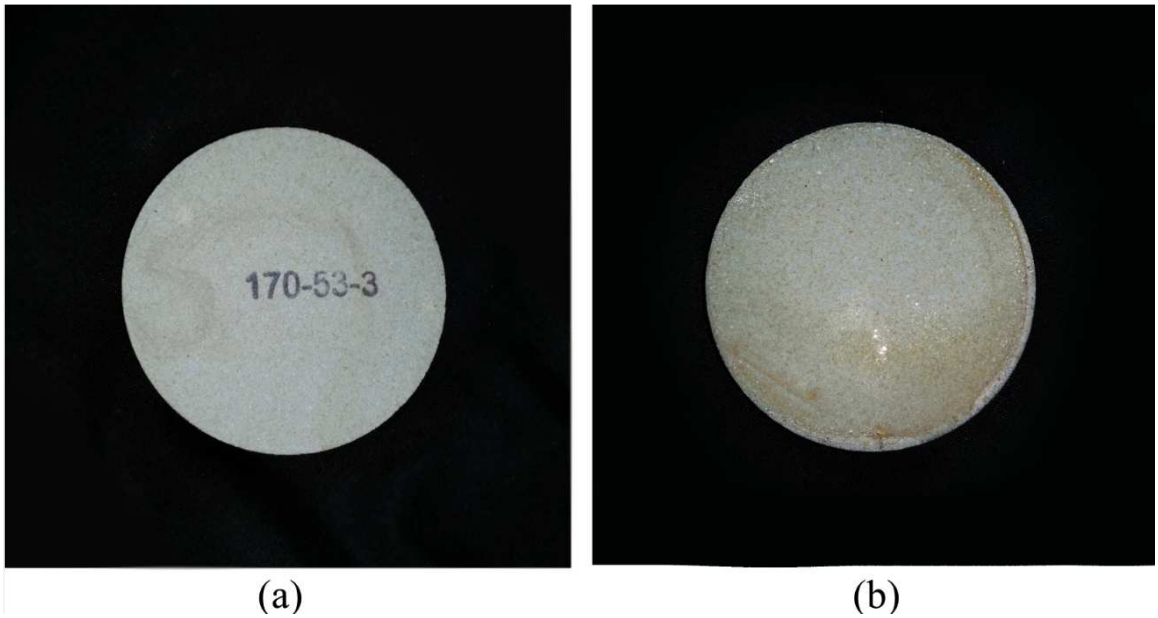

Figure 5-15. Comparison between initial surface of the ceramic disk and after filtration test for 1000 ppm viscous gel through (170-53-3) ceramic disk. (a) initial (b) after filtration test.

Table 5-2. Peremability reduction and gel cake buildup height (H).

Part #	**Con (ppm)**	**K Reduction (md)**	**H (in)**	**Residual resistance factor**
170-53	5000	0.5	0.4	30000
	2500	1.4	0.324	10714
	1000	102.8	0.3	146
170-53-3	1000	53.3	0.35	56

6. SUGGESTED FUTURE WORK

The major findings from this study should be combined with the previous experimental results that were conducted using the PPGs by Dr. Bai's group. The combined results should be analyzed both statistically and numerically. As a result, the existed correlations can be validated and new correlations can be generated in order to enhance and optimize the PPGs treatment.

Some work should be performed to investigate the feasibility of using the millimeter-sized PPGs as lost circulation materials (LCM).

A full-experimental design should be conducted before running a new set of experiments for PPGs evaluation. That can be beneficial to build a comprehension of the major outcomes of the experiments and the interaction among them.

In this study, an accumulator with a fluid capacity of 500 ml was used. However, an accumulator with a higher capacity should be used in the future work in order to obtain more data points for a better evaluation of the rheological properties of the PPGs.

G' measurements should be performed on the extruded PPGs samples from the models and they should be related to the PPGs threshold pressure and the extrusion pattern.

A new set of models should be designed that have different plate thicknesses. That can be beneficial in examining how the thickness impacts the experimental results.

BIBLIOGRAPHY

Al-Anazi, H. A., & Sharma, M. M. (2002, January 1). Use of a pH Sensitive Polymer for Conformance Control. Society of Petroleum Engineers. doi:10.2118/73782-MS.

Al-Ibadi, A., & Civan, F. (2012, January 1). Experimental Study of Gel Particles Transport Through Porous Media. Society of Petroleum Engineers. doi:10.2118/153557-MS.

Awang, M., & Seng, G. M. (2003, January 1). Development of a Correlation for Estimating Gelation in Porous Media Using Bottle Test Measurements. Society of Petroleum Engineers. doi:10.2118/84862-MS.

Azari, M., & Soliman, M. (1996, January 1). Review of Reservoir Engineering Aspects of Conformance Control Technology. Society of Petroleum Engineers. doi:10.2118/35171-MS

Bai, B., Huang, F., Liu, Y., Seright, R. S., & Wang, Y. (2008, January 1). Case Study on Prefromed Particle Gel for In-Depth Fluid Diversion. Society of Petroleum Engineers. doi:10.2118/113997-MS

Bai, B., Li, L., Liu, Y., Liu, L., Wang, Z., and You, C. 2007a. Conformance Control by Preformed Particle Gel: Factors Affecting It Properties and Applications, SPE Reservoir Evaluation & Engineering. Journal. 10 (4), 415-421.

Bai, B., Liu Y., Coste, J.P., and Li, L, C. 2007b. Preformed particle gel for conformance control: transport mechanism through Porous media. SPE Reservoir Evaluation & Engineering. Journal. 10 (02): 176–184.

Bai, B., Wei, M., & Liu, Y. (2013, March 23). Field and Lab Experience With a Successful Preformed Particle Gel Conformance Control Technology. Society of Petroleum Engineers. doi:10.2118/164511-MS.

Chauveteau, G., et al.: "Method for Preparing Microgels of Controlled Size," US Patent 6579909, 2000.

Chauveteau, G., Omari, A., Tabary, R., Renard, M., Veerapen, J., & Rose, J. (2001, January 1). New Size-Controlled Microgels for Oil Production. Society of Petroleum Engineers. doi:10.2118/64988-MS.

Chauveteau, G., Tabary, R., Le Bon, C., Renard, M., Feng, Y., & Omari, A. (2003, January 1). In-Depth Permeability Control by Adsorption of Soft Size-Controlled Microgels. Society of Petroleum Engineers. doi:10.2118/82228-MS

Chauveteau, G., Tabary, R., Le Bon, C., Renard, M., Feng, Y., & Omari, A. (2003, January 1). In-Depth Permeability Control by Adsorption of Soft Size-Controlled Microgels. Society of Petroleum Engineers. doi:10.2118/82228-MS.

Cheung, S. et al.: "A Swelling Polymer for In-depth Profile Modification: Update on Field Applications," presented at SPE Applied Technology Workshop of Chemical Methods of Reducing Water Production, San Antonia, Texas, USA, March 4-6, 2007.

Coste, J.-P., Liu, Y., Bai, B., LI, Y., Shen, P., Wang, Z., & Zhu, G. (2000, January 1). In-Depth Fluid Diversion by Pre-Gelled Particles. Laboratory Study and Pilot Testing. Society of Petroleum Engineers. doi:10.2118/59362-MS.

Frampton, H., Morgan, J. C., Cheung, S. K., Munson, L., Chang, K. T., & Williams, D. (2004, January 1). Development Of A Novel Waterflood Conformance Control System. Society of Petroleum Engineers. doi:10.2118/89391-MS.

Ganguly, S., Willhite, G. P., Green, D. W., & McCool, C. S. (2001, January 1). The Effect of Fluid Leakoff on Gel Placement and Gel Stability in Fractures. Society of Petroleum Engineers. doi:10.2118/64987-MS

Gardner, D. C. (1983, January 1). Rheological Characterization of Crosslinked and Delayed Crosslinked Fracturing Fluids Using a Closed-Loop Pipe Viscometer. Society of Petroleum Engineers. doi:10.2118/12028-MS.

Huh, C., Choi, S. K., & Sharma, M. M. (2005, January 1). A Rheological Model for pH-Sensitive Ionic Polymer Solutions for Optimal Mobility Control Applications. Society of Petroleum Engineers. doi:10.2118/96914-MS.

Kakadjian, S., Rauseo, O., & Mejias, F. (1999, January 1). Dynamic Rheology as a Method for Quantify Gel Strength of Water Shutoff Systems. Society of Petroleum Engineers. doi:10.2118/50751-MS.

Liang, J., & Seright, R. S. (2000, January 1). Wall-Effect/Gel-Droplet Model of Disproportionate Permeability Reduction. Society of Petroleum Engineers. doi:10.2118/59344-MS

Liang, J.-T., Lee, R. L., & Seright, R. S. (1993, November 1). Gel Placement in Production Wells. Society of Petroleum Engineers. doi:10.2118/20211-PA.

Liu, J., & Seright, R. S. (2000, January 1). Rheology of Gels Used For Conformance Control in Fractures. Society of Petroleum Engineers. doi:10.2118/59318-MS.

Meister, J. (1985, January 1). Bulk Gel Strength Tester. Society of Petroleum Engineers. doi:10.2118/13567-MS.

Mustoni, J. L., Denyer, P., & Norman, C. (2010, January 1). Deep Conformance Control by a Novel Thermally Activated Particle System to Improve Sweep Efficiency in Mature

Waterfloods of the San Jorge Basin. Society of Petroleum Engineers. doi:10.2118/129732-MS

Parera. D. I and Shanks. R. A, Polym. Int. 39 (1996) 121-27.

Pritchett, J., Frampton, H., Brinkman, J., Cheung, S., Morgan, J., Chang, K. T., … Goodgame, J. (2003, January 1). Field Application of a New In-Depth Waterflood Conformance Improvement Tool. Society of Petroleum Engineers. doi:10.2118/84897-MS.

Ramazani-Harandi et al.: Polymer Testing 25 (2006) 470-474.

Riccardo Po, J. Macromol. Sci., Rev. Macromol. Chem. Phys, 34 (1994) 607-662.

Roger J. H., George S., Norman F. C., and Miller K.: "IOR and EOR: Effective Communication Requires A Definition of Terms," JPT, June, 2003.

Rousseau, D., Chauveteau, G., Renard, M., Tabary, R., Zaitoun, A., Mallo, P., … Omari, A. (2005, January 1). Rheology and Transport in Porous Media of New Water Shutoff / Conformance Control Microgels. Society of Petroleum Engineers. doi:10.2118/93254-MS.

Sayil. C, Okay. O, Polymer 42 (2001) 7639-7652.

Seright, R. S. (1988, January 1). Placement of Gels To Modify Injection Profiles. Society of Petroleum Engineers. doi:10.2118/17332-MS.

Seright, R. S. (1997, February 1). Use of Preformed Gels for Conformance Control in Fractured Systems. Society of Petroleum Engineers. doi:10.2118/35351-PA.

Seright, R. S. (1999, January 1). Mechanism for Gel Propagation Through Fractures. Society of Petroleum Engineers. doi:10.2118/55628-MS.

Seright, R. S., & Liang, J. (1995, January 1). A Comparison of Different Types of Blocking Agents. Society of Petroleum Engineers. doi:10.2118/30120-MS

Seright, R. S., Lane, R. H., & Sydansk, R. D. (2001, January 1). A Strategy for Attacking Excess Water Production. Society of Petroleum Engineers. doi:10.2118/70067-MS

Seright, R.S.: "Conformance Improvement Using Gels," Annual Technical Progress Report (U.S. DOE Report DOE/BC/15316-6), U.S. DOE Contract DE-FC26-01BC15316 (Sept. 2004) 72.

Seright, R.S.: "Gel Propagation through Fractures," SPE Production & Facilities, Nov 2001, 225-232.

Smith, J. E. (1989, January 1). The Transition Pressure: A Quick Method for Quantifying Polyacrylamide Gel Strength. Society of Petroleum Engineers. doi:10.2118/18739-MS.

Smith, J. E. (1995, January 1). Performance of 18 Polymers in Aluminum Citrate Colloidal Dispersion Gels. Society of Petroleum Engineers. doi:10.2118/28989-MS.

Soliman, M. Y., East, L., & Gorell, S. (1999, January 1). Reservoir Conformance Approach and Management Practices for Improved Recovery Opportunities: Process and Case History. Society of Petroleum Engineers. doi:10.2118/53918-MS.

Sydansk, R. D. (1990, August 1). A Newly Developed Chromium(III) Gel Technology. Society of Petroleum Engineers. doi:10.2118/19308-PA.

Sydansk, R.D. et al.: "Polymer Gels Formulated With a Combination of High- and Low-Molecular-Weight Polymers Provide Improved Performance for Water-Shutoff Treatments of Fractured Production Wells," SPE Production & Facilities, Vol.19 (4), 229-236, 2004.

Sydansk, R.D., and Moore, P.E., 1992, "Gel Conformance Treatments Increase Oil Production in Wyoming," Oil and Gas Journal 40-45.

Sydansk, R.D.: "A New Conformance-Improvement-Treatment Chromium(III) Gel Technology" Presented at SPE/DOE EOR Symposium, April 17-20, 1988, Tulsa, Oklahoma.

U.S. DOE, Marginal & Stripper Well Revitalization, http://www.fossil.energy.gov/programs/oilgas/marginalwells.

U.S. DOE, Novel Technology Boosts Oil and Gas Production and Efficiency at 200 Sites Nationwide, http://www.fossil.energy.gov/news/techlines/2006/06056-Vortex_Technology_Success.html.

Veil, J.A., et al.: "A White Paper Describing Produced Water from Production of Crude oil, Natural Gas and Coal Bed Methane," prepared for National Energy Technology Laboratory, U.S DOE under contract W-31-109-Eng-38, Argonne National Laboratory, 2004.

Weideman, A.: "Regulation of Produced Water by the U.S. Environmental Protection Agency" in Produced Water 2: Environmental Issues and Mitigation Technologies, International Produced Water Symposium, M. Reed and S. Johnsen, eds., Plenum Press, New York, 1996.

Wu, Y.-S., & Bai, B. (2008, January 1). Modeling Particle Gel Propagation in Porous Media. Society of Petroleum Engineers. doi:10.2118/115678-MS.

Zaitoun, A., Tabary, R., Rousseau, D., Pichery, T. R., Nouyoux, S., Mallo, P., & Braun, O. (2007, January 1). Using Microgels to Shut Off Water in a Gas Storage Well. Society of Petroleum Engineers. doi:10.2118/106042-MS.

VITA

Ali Al Brahim was born in Al Hasa city, Saudi Arabia on April 25, 1988. He received his B.S. Degree in Petroleum Engineering from King Fahd University of Petroleum and Minerals in Saudi Arabia in June 2011. During his undergraduate Degree, he worked on internships and projects mainly focused on Reservoir Engineering areas. His interest in the Petroleum Engineering field motivated him to pursue a graduate Degree in Petroleum Engineering. He joined Dr. Bai's lab group as a full-time graduate student in June 2013 and started working towards his Master's Degree in Petroleum Engineering at Missouri University of Science & Technology. He served as a teaching assistant for one semester in the Reservoir Engineering lab. He received his Master's Degree in Petroleum Engineering from Missouri S&T.